Baltic Astronomy, vol. 15, 1–4, 2006.

THE 2ND MEETING ON HOT SUBDWARF STARS AND RELATED OBJECTS

R. H. Østensen
Isaac Newton Group, Apartado 321, E-38700 Santa Cruz de La Palma, Spain

1. INTRODUCTION

The first meeting dedicated to hot subdwarf stars was held in Keele, U.K. on 2003 June 16–20. The idea of such a meeting was conceived by Pierre Maxted, and in his report in the proceedings of that meeting the full background is given (Maxted 2004). When I went to that meeting, I had just started a new three-year contract as a PPARC research fellow at the Isaac Newton Group of Telescopes (ING) on La Palma, Canary Islands. Since it has been a tradition for the research fellows at ING to organize a conference or workshop during their contract period, the possibility of hosting a follow-up meeting to the Keele event was on my mind. When several people suggested La Palma as a good option for the next meeting, I was not slow to accept, and on the last day of the Keele meeting, the offer to hold another meeting on La Palma in 2005 was presented.

The title of the first meeting was Extreme Horizontal Branch Stars and Related Objects. After a lengthy discussion in the SOC it was decided to change that to Hot Subdwarf Stars and Related Objects instead. The terms EHB stars and sdB/sdO stars are often used interchangeably, but the EHB term implies a specific evolutionary history. Recently, evidence has accumulated that many of the stars that appear similar to EHB stars in spectroscopic studies may have completely different evolutionary histories. From the beginning, the intention of the meeting was to keep it open to all these similar stars, falling under the extension *and related objects*. The term *hot subdwarf stars*, however, has no evolutionary implications, but is a classical term used in spectral classifications of blue stars. This term encompasses the sdB, sdOB and sdO stars as well as the helium rich varieties usually referred to as He-sdB or He-sdO stars. With *hot subdwarf stars* we include all objects that appear in the HR diagram below the main sequence and above the white dwarf cooling track, regardless of how they got there. The *related objects* extension was kept in order to make sure that objects such as the extreme helium (EHe) stars were not left out. (Technically they are subluminous, but due to their low gravities they are not classified as He-sdB stars.)

2. THE MEETING

The meeting took place in Santa Cruz de La Palma between the 6th and the 10th of 2005 June. 58 participants arrived from all over the world, almost half again as many as at the first meeting. The organization of the meeting was carried out in a collaboration between the Isaac Newton Group (ING) and the

Nordic Optical Telescope (NOT), both which contributed a considerable amount toward the budget of the meeting. Support for specific social events was provided by the local government (Excmo. Cabildo Insular de La Palma) and the tourist board (Patronato de Turismo de La Palma). Additionally, the Real Club Náutico de Santa Cruz de La Palma has been extremely helpful by making their excellent locales available to us at no cost. Thanks to all this financial support we were able to keep a very reasonable registration fee, and even waive it completely for about a third of the participants who were students or without financial support at the time. On behalf of all the participants who enjoyed the hospitality of La Palma, I would like to thank all the organizations involved.

The meeting room at the Real Club Náutico provided an excellent environment for the event. The Club's restaurant also managed to provide excellent coffee breaks with delicious and varied snacks, as well as a very impressive conference dinner. Being in the center of the city allowed people to use the extended lunch break to explore the old city and find their own places to eat.

Fig. 1. At the meeting.

3. THE SESSIONS

The meeting was divided into sessions that covered a broad range of topics related to the hot subdwarf stars. They were:

- Evolutionary models and the UV-upturn phenomenon;
- Hot subdwarfs and hot HB stars in the field, clusters and galaxies;
- Atmospheric properties of hot subdwarf stars;
- Hot subdwarfs in binary systems;
- Asteroseismology of sdB stars.

Eight half-day sessions were completed during the meeting, with three sessions dedicated to asteroseismology, two sessions for atmospheric properties and the remaining topics filling one session each. The contributions in these proceedings are arranged roughly along the order of the listed sessions. All the talks were limited to 30 minutes, with 5 minutes extra for discussions. Interleaved with the talks were short oral presentations with discussions of the posters.

4. THE ISLAND

The island of La Palma is one of the smaller Canary Islands, with a surface area of 706 km^2 and a population of only 80 000. It is unusual in that it rises exceptionally steeply from the ocean floor (from a depth of 4000 m) to a volcanic crater rim at an altitude of between 2000 and 2500 meters. The Observatory is located around the highest point, the Roque de los Muchacos (2426 m).

Fig. 2. At the William Herschel Telescope.

The participants of the meeting were invited to tour the observatory area and visit the 4.2 m William Herschel Telescope (WHT, see Fig. 2), the 2.5 m Nordic Optical Telescope (NOT) and the 10 m Gran Telescopio Canarias (GTC) which is currently being assembled in its enormous dome.

Fig. 3. Exploring the volcanoes.

On Friday evening, after the end of the meeting, a farewell party was held at the swimming-pool resort of the Real Club Náutico, in the harbor of Santa Cruz de La Palma. Most of the participants also enjoyed the entertainment provided by the local observatory band *Manifold*, and some even braved the dance floor.

On Saturday after the end of the meeting, the participants who had the opportunity to stay another day were invited to a tour around the island, including a visit to some recent volcanoes (Fig. 3).

5. THE PROCEEDINGS

For the first meeting it was decided by the SOC to submit all contributions to a thorough refereeing process, and the participants were called to assist with the reviewing of the papers (Maxted 2004). For this second meeting we have even called upon experts not present at the meeting, in order to ensure that all papers have been refereed by qualified researchers. This process has gone exceptionally smoothly thanks to the prompt response of (almost) all the referees.

An issue that the SOC was not happy with from the proceedings of the first meeting was the long printing time. The SOC felt that the purpose of publishing results from work in progress was somewhat defeated if the time between the original presentation and the printed version was more than a year. For this reason we sought to find a publisher who could promise us quick printing and freely accessible on-line versions at an affordable price. Baltic Astronomy was quick to promise us the first issue of 2006 for our purposes. In addition to the regular journal issues, we could obtain special hard-back copies for the participants at a very reasonable price.

Oral presentations from the meeting have been given a page limit of eight pages (although a few participants has been allowed to exceed this), and short "poster" presentations were limited to four pages. Three contributions are published in other journals, and for this reason only an abstract version is presented at the end of the proceedings book, with reference to the journal paper.

6. OTHER REMARKS

The LOC put a lot of effort into designing useful web-pages to assist the participants with information about the meeting, registration and manuscript submission. (`http://www.ing.iac.es/conferences/subdwarf/`). All the pages are written in PHP[1] and changes dynamically according to what information is available. A registration system was made using a PHP interface to a MySQL[2] database. The on-line registration form allowed participants to enter their registration data, update information such as talk titles and abstracts, and the database allowed automatic update of the conference program. An automatic interface for submission of the proceedings which also did some basic checks on the manuscripts, was also provided. The pages will remain accessible for the foreseeable future, and anybody interested in reworking this system for other events can contact the author.

The SOC wishes to thank the members of the LOC for their work in managing the event. Special thanks goes to Javier Méndez of the Isaac Newton Group for his excellent work in managing the venue and all the social events, as well as the design of the poster and the photos for the meeting.

After the success of this second meeting, the group in Bamberg has offered to host the 3rd meeting in 2007. It is clear that a new tradition for a biennial series of meetings on hot subdwarf stars has been established.

REFERENCES

Maxted P. F. L. 2004, Ap&SS, 291, 193

[1] PHP (`www.php.net`) is a script language that generates HTML documents.
[2] MySQL (`www.mysql.com`) is an open source database system.

Baltic Astronomy, vol. 15, 5–12, 2006.

THE LOOK-BACK TIME EVOLUTION OF THE UV UPTURN PHENOMENON

C. H. Ree[1], Y.-W. Lee[1], Y.-J. Sohn[1], S. K. Yi[1,2], S.-J. Yoon[1,2]
and the GALEX Science Team

[1] *Center for Space Astrophysics and Department of Astronomy, Yonsei University, 134 Shinchon, Seoul 120-749, Korea*

[2] *Department of Physics, University of Oxford, Keble Road, Oxford OX1 3RH, U.K.*

Submitted 2005 August 1

Abstract. In order to investigate the origin of the far-UV (FUV) flux from early-type galaxies, *Galaxy Evolution Explorer* (GALEX) is collecting the UV data for the elliptical-rich clusters at moderate redshifts ($z < 0.25$) where the dominant FUV source is predicted to be hot horizontal-branch (HB) stars and their post-HB progeny. The early results show that the FUV flux of quiescent early-type galaxies *does* evolve substantially during the last 1–2 Gyr of look-back time, and the observed UV fading is consistent with the variation predicted by the population synthesis models where the mean temperature of HB stars declines rapidly with increasing look-back time.

Key words: galaxies: elliptical – galaxies: evolution – galaxies: stellar content – ultraviolet: galaxies

1. INTRODUCTION

It is now well established that the far-UV (FUV) flux ("UV upturn") of nearby early-type galaxies originates from a minority population of old hot helium-burning horizontal-branch (HB) stars (O'Connell 1999; Brown et al. 2000b). Stellar evolution models of HB predict that the mean temperature of HB distribution declines rapidly with decreasing age (e.g., Lee et al. 1994), and therefore the FUV flux from ellipticals should fade rapidly with look-back time (Greggio & Renzini 1990; Tantalo et al. 1996). Population synthesis models of Yi et al. (1999) also indicate that careful observations for the UV look-back time evolution could also discriminate two alternative HB solutions on the origin of UV flux, i.e., "metal-poor" and "metal-rich" HB models, which predict different ages for giant ellipticals.

The *Hubble Space Telescope* (HST) has obtained FUV images for several elliptical-rich clusters in the redshift range of $0.3 < z < 0.6$ (Brown et al. 2000a, 2003), but stellar evolution models (Lee et al. 1999; Yi et al. 1999) predict that hot HB stars must be absent at these relatively high redshifts, as no stars of low enough mass have yet evolved. Therefore, UV observations covering a lower redshift range ($z < 0.25$) are still required, in order to test the look-back time evolution effect of HB stars in giant ellipticals. Here we present the early results from the *Galaxy Evolution Explorer* (GALEX) UV observations for the Abell clusters in this redshift range, and also for the Fornax cluster as a local calibrator.

2. GALEX UV OBSERVATIONS

GALEX UV deep imaging survey for the UV upturn early-type galaxies aims at the elliptical-rich Abell clusters at $z < 0.25$. The first deep imaging target for this study was Abell 2670 at $z = 0.076$. Figure 1 shows the GALEX FUV and optical images of the early-type galaxies successfully identified within 25 arcmin^2 field of view centered on the brightest giant elliptical galaxy, a19 (Lee et al. 2005a). From a subsequent observation, we also successfully detected several early-type galaxies in Abell 951 at $z = 0.143$ in the GALEX UV images (see Figure 2; Ree et al. 2005). In most cases, their FUV lights are concentrated in the central region of the red galaxies without recent massive star formation, which is analogous to the smooth UV profiles of the quiescent UV upturn galaxies in the local Universe (Ohl et al. 1998; O'Connell 1999), with a few exceptions discussed below. The multi-orbit deep imaging UV observations with GALEX dedicated for more other elliptical-rich clusters at moderate redshifts are ongoing.

In order to compare the remote targets at various redshifts with the local samples without any systematic effect that may arise from the different aperture sizes used in the photometry, we should measure the total luminosities with sufficiently large, variable apertures. The total luminosities of those cross-matched early-type galaxies in remote clusters were measured by the elliptical aperture photometry (MAG_AUTO) with SExtractor image analysis package (Bertin & Arnouts 1996) in both FUV and optical passbands. The Galactic foreground extinctions were then corrected with $R_V = 3.1$, $R_{FUV} = 8.16$ (Cardelli et al. 1989). We do *not* convert the observed values into the restframe ones, as the *empirical* k-corrections may cause uncertainties in the comparison between the data samples at different redshifts. Instead, we will compare the apparent values with the model synthetic spectra redshifted to the target distances.

Nearby clusters of galaxies, e.g., Fornax, Virgo and Coma, are the best places to find the local early-type galaxies with various UV strengths, and they provide constraints to the model parameters in the local Universe. GALEX observations for the early-type galaxies in the Fornax cluster are presented in Figure 3. Their FUV magnitudes were measured from the surface photometry using ellipse fitting. The FUV surface brightness profiles extend smoothly, out to $r > 80''$ in the case of NGC 1399 and NGC 1404. In order to minimize the aperture effect induced by UV/optical radial gradient (Ohl et al. 1998), we estimated the FUV total magnitudes by integration of the radial profiles. We have also corrected for the Galactic foreground extinctions ($A_{FUV} = 0.09 - 0.14$), and their total magnitudes in V-band were adopted from the Third Reference Catalog of Bright Galaxies (RC3; de Vaucouleurs et al. 1991). Our FUV photometry for the elliptical galaxies in the Fornax cluster, when measured within the *International Ultraviolet Explorer satellite* (IUE) aperture ($20'' \times 10''$), agrees well with the IUE measurements (Burstein et al. 1988) to within 0.01–0.06 mag.

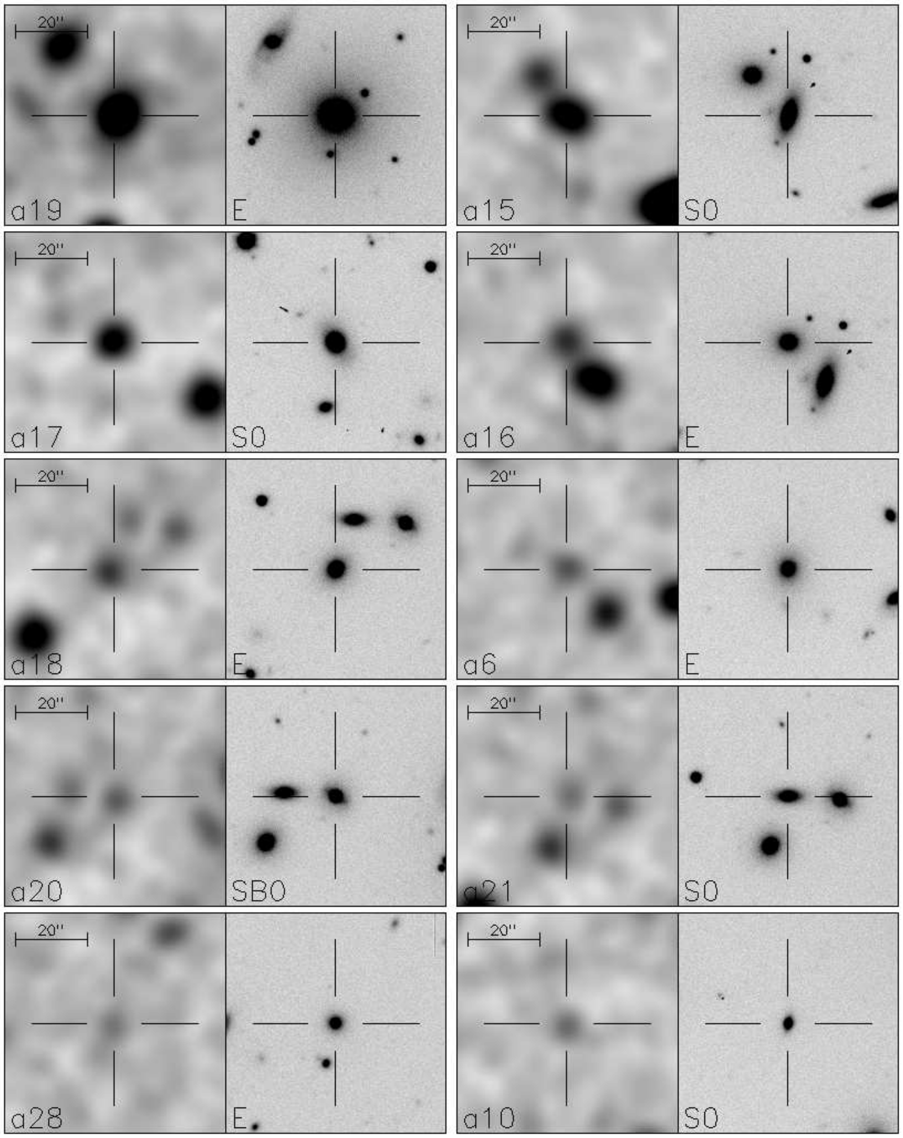

Fig. 1. GALEX FUV (*left panels*) and optical r-band (*right panels*) images ($1' \times 1'$) of the early-type galaxies in Abell 2670 ($z = 0.076$). The optical images are from Fasano et al. (2002). For some of UV-strong galaxies here, a15 and a16, there are strong evidences of young populations based on strong near-UV flux or Hα emission feature due to the residual star formation (Lee et al. 2005a).

3. MORE DISTANT CLUSTERS

Even the most massive giant elliptical galaxies ($M_V \leq -22$) should be fainter than 25th magnitude (AB) in FUV at $z > 0.3$. It would be very difficult to detect such faint *red* galaxies at high redshift with a small telescope like GALEX.

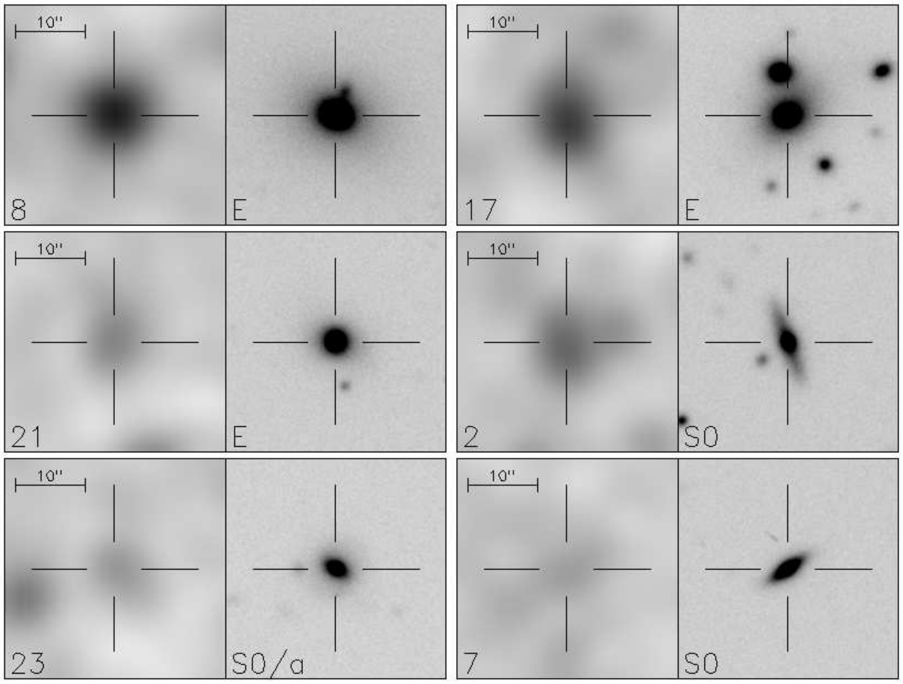

Fig. 2. GALEX FUV (*left panels*) and optical r-band (*right panels*) images ($30'' \times 30''$) of early-type galaxies in Abell 951 ($z = 0.143$). The optical images are from Fasano et al. (2000). Optical spectroscopic follow-ups are underway searching for the recent star formation signatures, if any, in these galaxies.

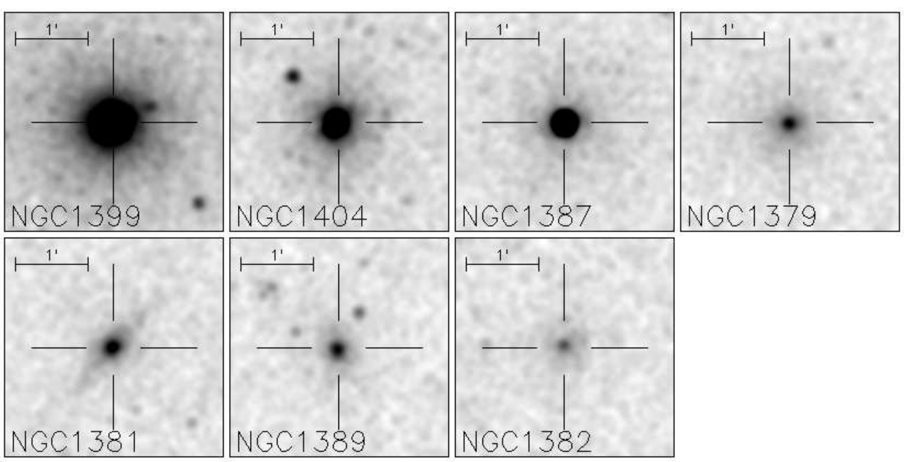

Fig. 3. GALEX FUV images ($3' \times 3'$) of the early-type galaxies in the Fornax cluster as a local calibrator. Their FUV lights are concentrated in the central region, and the radial profiles extend smoothly to $r > 1'$ for UV-strong galaxies.

However, there are several HST UV observations for the distant galaxy clusters at $0.3 < z < 0.6$ with the *Space Telescope Imaging Spectrograph* (STIS). From the literatures, we have taken the photometric measurements for the early-type galaxies in two distant clusters, Cl 1358+62 at $z = 0.33$ and Cl 0016+16 at $z = 0.55$, observed in UV by Brown et al. (2000a, 2003) and in optical passbands by van Dokkum et al. (1998) and Smail et al. (1997), respectively. The HST *Faint Object Camera* data for Abell 370 at $z = 0.375$ (Brown et al. 1998) are not included here, as they may have significant systematic errors according to Brown et al. (2003).

For the comparison with GALEX data, we converted those HST measurements to the AB magnitude system using the photometric zero-points and pivot wavelengths defined in the HST image headers ($m_{\mathrm{AB}} = m_{\mathrm{ST}} - 5\,log\,\lambda_p + 18.6921$). Model spectral energy distributions (SEDs) redshifted to $z = 0.33$ and 0.55 were then used to estimate the systematic difference between the HST and GALEX filter systems. Since the aperture radii in their analyses ($0.4''$ in FUV for both clusters, and $1.5''$ in V for CL 1358+62) are not large enough to represent total magnitudes, we applied appropriate aperture corrections, –0.32 (FUV) and –0.22 (V) for CL 1358+62. For the galaxies in CL 0016+16, we applied a correction only in FUV (–0.17 mag), as we adopted the total V magnitude from the catalog in Smail et al. (1997). The aperture correction values were obtained by utilizing the FUV (Lee et al. 2005a) and V (Marcum et al. 2001) radial profiles of NGC 1399, assuming that these clusters are at 75 (CL 1358+62) and 117 (CL 0016+16) times the distance of the Fornax cluster adopting the currently favored cosmological parameters (Ω_M, Ω_Λ, H_0) = (0.3, 0.7, 70). Finally, foreground extinction corrections are applied.

4. DISCUSSION

From the extinction-corrected apparent total magnitudes in both FUV and V passbands, we have derived the $FUV - V$ colors of the early-type galaxies in clusters, measured by GALEX (Fornax, Abell 2670 and *preliminary* analysis of Abell 951) and by HST (CL 1358+62 and CL 0016+16). The apparent redshift evolution of the observed $FUV - V$ colors is then presented in Figure 4, along with the two alternative model predictions. The "metal-poor HB model" suggests that the dominant FUV sources are very old ($t > 12$ Gyr) hot metal-poor HB stars and their post-HB progeny, and the FUV flux is expected to increase with age due to the smaller main-sequence turnoff and HB envelop masses. In the "metal-rich HB model", on the other hand, the dominant sources are old (t = 10–12 Gyr) hot super metal-rich HB and post-HB stars, and the FUV flux is predicted to increase with metallicity due to the enhanced helium enrichment and mass-loss. Even if these two alternative models are almost equally capable of reproducing the observed $FUV - V$ colors in present-epoch giant ellipticals, their evolutionary predictions are quite different from one another (see Yi et al. 1999).

The models in Figure 4 are specifically constructed to match the $FUV - V$ color of the local giant elliptical galaxy NGC 1399, the brightest galaxy in the Fornax cluster, and then passively evolved with look-back time. The model spectra and colors are then redshifted and the look-back times are converted to the equivalent redshift values, with the cosmological parameters above. Therefore, the foreground extinction-corrected observed data can be directly compared with the models. Since the NGC 1399 is a typical FUV-strong giant elliptical galaxy in the local

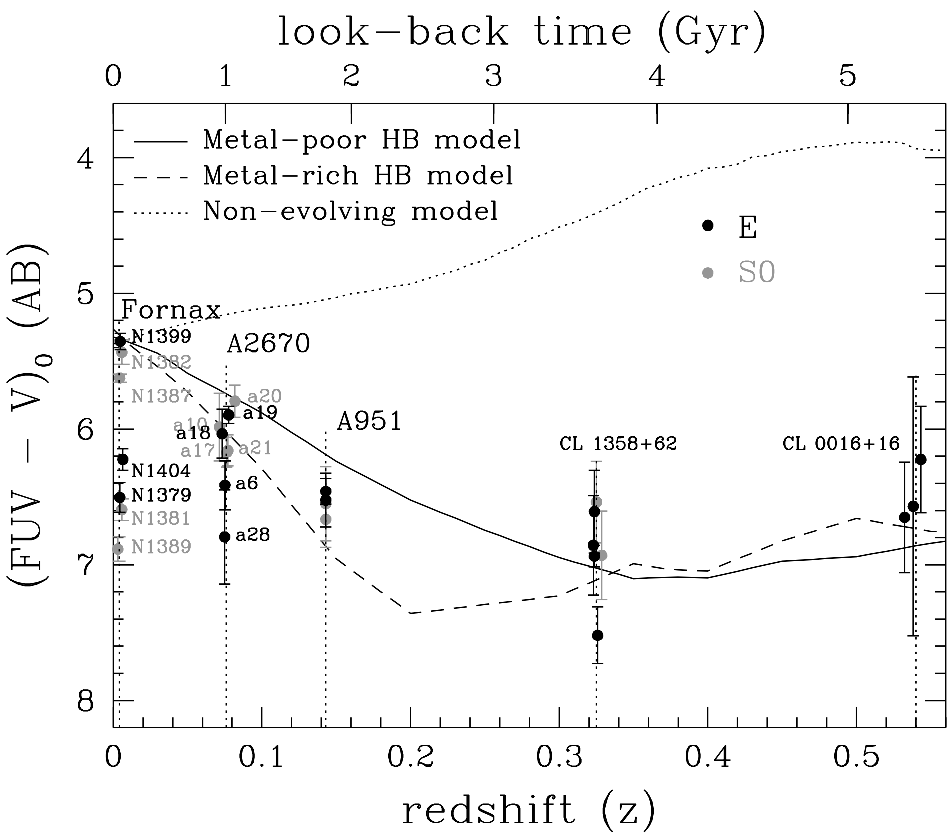

Fig. 4. Evolution of the UV upturn as a function of redshift. The observed apparent $FUV-V$ colors of the early-type galaxies in clusters at various redshifts are compared with the "metal-poor" (*solid*) and "metal-rich" (*dashed*) HB evolutionary models. The *dotted* line is for the case that the model spectrum of NGC 1399 is redshifted with no stellar evolution considered. Only the *quiescent* type of galaxy samples, without any strong star-formation signatures, are plotted (see text).

Universe, the model lines would represent the redshift (look-back time) evolution of giant ellipticals, and hence should be compared with the brightest ellipticals in each cluster. Note that there is a distinguishable amount of difference between the two alternative evolutionary models, up to ~ 1 mag. in $FUV-V$ color at $z \approx 0.2$, for the massive giant elliptical galaxies ($M_V \approx -22$).

It is clear from Figure 4 that we have detected the fading of the UV upturn expected at moderate redshifts. Compared to NGC 1399, the nearby giant elliptical galaxy in the Fornax cluster, an apparent extinction-corrected $FUV-V$ color of the giant elliptical galaxy (a19) in Abell 2670 gets redder by ~ 0.55 mag at $z = 0.076$ (look-back time ~ 1.0 Gyr). For the restframe $FUV-V$ color, this corresponds to 0.70 mag, which is consistent with the variation predicted by the models (Lee et al. 2005a). A preliminary analysis for Abell 951 ($z = 0.143$) confirms this by showing a similar amount of evolution again in the $FUV-V$ color of UV-strong giant elliptical galaxies between the look-back time of 1 and 2 Gyr. In these models, the dominant FUV source is hot HB stars for $z < 0.25$, and therefore the FUV flux fades rapidly with look-back time (redshift) as the HB temperature distribution becomes cooler with decreasing age (increasing look-back time).

For $z > 0.3$, the HST data also appear to be in reasonable agreement with our model predictions, to within the errors. Note, however, that the models become more uncertain at these relatively higher redshifts, as the dominant FUV source changes from hot HB stars to post-asymptotic giant branch (PAGB) stars for $z > 0.25$. In particular, Lee et al. (1999, see their Fig. 1) predict that the HB contribution to the total FUV flux becomes almost negligible for $z > 0.4$. At relatively higher redshifts, the total FUV flux would therefore increase as the mass of PAGB stars decreases because their lifetimes correlate inversely with their mass. Consequently, the available HST data may provide no direct test of HB evolution effect. Nevertheless, they provide a useful test on the adopted mass (0.565 $M_{\odot}$) of PAGB stars in our models.

Although we are witnessing the growing body of evidence indicating the FUV flux of quiescent early-type galaxies evolves substantially at moderate redshifts ($z < 0.25$) as the deep imaging survey with GALEX UV telescope continues, there are some issues to be solved. On the observational side of this study, UV blending and contamination by young stars are serious issues. With the given spatial resolution of GALEX (1.5 $''$/pixel), it becomes difficult to de-blend properly the UV lights purely from the old stellar population in elliptical galaxies and the possible UV contaminations by neighboring dwarf galaxies, as we reach out to $z \sim 0.2$. Furthermore, some early-type galaxies show contamination from the residual star formation in their UV spectra (Burstein et al. 1988; Yi et al. 2005), and therefore it is important to check whether our sample galaxies are not affected by a minority population of young stars. As described in Lee et al. (2005a), we found two of the UV-strong early-type galaxies in Abell 2670, a15 (S0) and a16 (E), show the evidence of young populations inferred by unusually strong near-UV flux or by strong Hα emission. Some of HST data samples also show unexpectedly strong UV flux. All of these abnormal galaxies with recent star-forming signatures are excluded in Figure 4. The optical follow-up spectroscopy continues for the other GALEX target clusters in order to discriminate such star-forming red galaxies.

On the theoretical side, the nature of extreme HB (EHB) stars and their contribution to the UV flux should be understood. The effect of EHB stars are *not* fully included in the current population synthesis models presented here. Particularly, the excessively large age (up to 30 % older than the Galactic globular clusters) required for the local giant ellipticals in the "metal-poor" HB model would be reduced significantly, if the EHB stars are explained as the minority population of super helium-rich stars (Lee et al. 2005b). In any case, the observed rapid evolution of FUV flux with look-back time at moderate redshifts, if confirmed by further observations, would infer the strong age dependency in the evolution of UV sources in old stellar systems (Lee et al. 1994; Yi et al. 1999).

ACKNOWLEDGMENTS. GALEX is a NASA Small Explorer, launched in April of 2003. We gratefully acknowledge NASA's support for construction, operation and science analysis for the GALEX mission, developed in cooperation with the Centre National d'Etudes Spatiales of France and th e Korean Ministry of Science and Technology. Yonsei University participation is funded by the Korean Ministry of Science & Technology, for which we are grateful.

REFERENCES

Bertin E., Arnouts S. 1996, A&A, 117, 393

Brown T. M., Ferguson H. C., Deharveng J.-M., Jedrzejewski R. I. 1998, ApJ, 508, L139

Brown T. M., Bowers C. W., Kimble R. A., Ferguson H. C. 2000a, ApJ, 529, L89

Brown T. M., Bowers C. W., Kimble R. A., Sweigart A. V., Ferguson H. C. 2000b, ApJ, 532, 308

Brown T. M., Ferguson H. C., Smith E., Bowers C. W., Kimble R. A., Renzini A., Rich R. M. 2003, ApJ, 584, L69

Burstein D., Bertola F., Buson L. M., Faber S. M., Lauer T. R. 1988, ApJ, 328, 440

Cardelli J. A., Calyton G. C., Mathis J. S. 1989, ApJ, 345, 245

de Vaucouleurs G., de Vaucouleurs A., Corwin H. G., Buta R. J., Paturel G., Fouque P. 1991, *Third Reference Catalog of Bright Galaxies*, Springer (RC3)

Fasano G., Bettoni D., D'Onofrio M., Kjærgaard P., Moles M. 2002, A&A, 387, 26

Fasano G., Poggianti B. M., Couch W. J., Betoni D., Kjærgaard P., Moles M. 2000, ApJ, 542, 673

Greggio L., Renzini A. 1990, ApJ, 364, 35

Lee Y.-W., Demarque P., Zinn R. 1994, ApJ, 423, 248

Lee Y.-W. et al. 2005a, ApJ, 619, L103

Lee Y.-W. et al. 2005b, ApJ, 621, L57

Lee Y.-W., Woo J.-H., Yi S., Park J.-H. 1999, in *Spectrophotometric Dating of Stars and Galaxies*, eds. I. Hubeny, S. Heap & R. Cornett, ASP Conf. Ser., 192, 307

O'Connell R. W. 1999, ARA&A, 37, 603

Ohl R. G. et al. 1998, ApJ, 505, L11

Ree C. H. et al. 2005, in preparation

Smail I., Dressler A., Couch W. J., Ellis R. S., Oemler A. 1997, ApJS, 110, 213

Tantalo R., Chiosi C., Bressan A., Fagotto F. 1996, A&A, 311, 361

van Dokkum P. G., Franx M., Kelson D. D., Illingworth G. D., Fisher D., Fabricant D. 1998, ApJ, 500, 714

Yi S., Lee Y.-W., Woo J.-H., Park J.-H., Demarque P., Oemler A. 1999, ApJ, 513, 128

Yi S. et al. 2005, ApJ, 619, L111

Baltic Astronomy, vol. 15, 13–16, 2006.

BINARY POPULATION SYNTHESIS, SDB STARS AND THE UV UPTURN

D. Brown[1], S. Yi[2], Z. Han[3] and S.-J. Yoon[2]

[1] *Department of Physics and Astrophysics, University of Oxford, Oxford, OX1 3RH, U.K.*

[2] *Department of Astronomy, Yonsei University, Sinchon 134, Seoul 120-749, Korea*

[3] *Yunnan Observatory, National Astronomical Observatories, Chinese Academy of Sciences, P.O. Box 110, Kunming, 650011, China*

Received 2005 September 19

Abstract. We aim to use the methods of binary population synthesis (BPS) to study the ultraviolet upturn (UVX) in the spectra of giant elliptical galaxies with emphasis being placed on those binary channels which could lead to the formation of stars that can account for it. This project will combine Sukyoung Yi's single star population synthesis methodology with that of Zhanwen Han's binary population synthesis methods in order to provide a more coherent study of the origin of the UV upturn, the focus being on sdB stars as the possible source of the UV upturn. The primary approach of the project will be to explore the UV upturn, with sdBs included, for several different metallicities in order to examine the UVX in composite populations.

Key words: stars: hot subdwarfs – stars: binaries: general – galaxies: elliptical – galaxies: stellar content

1. THE UV UPTURN (UVX)

At present, a moderate consensus suggests that low-mass core helium burning stars, which are in the HB phase of their evolution, serve as the strongest candidates for sources of the UVX in stellar populations. The UVX is characterized by a high increase in rest-frame UV flux (in the range of $\lambda \sim 1000$–2500 Å) in the spectra of elliptical (E) galaxies, S0 galaxies and in the bulges of spiral galaxies.

2. UVX HYPOTHESES

Most population synthesis studies of the UVX, including those of Yi (1997, 1998), assume that it arises from the evolution of single HB stars. However, others, such as Han and Podsiadlowski (HP), having conducted an extensive binary population synthesis study of the origin of sdB stars (Han et al. 2002, 2003) formed via binary channels, note that sdB stars could help account for a significant portion of UV radiation in galaxies; in fact, HP have also conducted an extensive study of the UVX at solar metallicity. In the single star scenario, two hypotheses make contradictory claims as to how the UVX originates from low-mass HB stars. The metal-rich hypothesis (Yi et al. 1997, 1998) claims that the UVX originates in metal-rich stars characterized by a high He abundance, and, hence, high mass-loss. In contrast, the metal-poor hypothesis (Park & Lee 1997) claims that the UVX is the natural consequence of the oldest, metal-poor stars in a GE having evolved into the HB phase of their lives. In the binary scenario, the UVX originates from EHB stars in the form of sdBs which result from several different types of binary evolution channels: (1) common envelope (CE) ejection; (2) RLOF in one binary component and (3) merger of two WDs.

3. INPUT MODELS

EPS models for single star evolution are here combined with the products of binary population synthesis models to produce a combined population synthesis. The EPS models and methods employed are those of Sukyoung Yi and Seok-Jin Yoon. In these, data from the Y^2 isochrones and realistic synthetic HB constructions have been reduced and processed into synthetic CMD and SED models by Seok-Jin Yoon. The sdB models are products of Han (1995) binary population synthesis code, which uses an input grid generated by an updated version of Eggleton's original stellar evolution code (Eggleton 1971, 1972, 1973). The spectral library employed is that assembled by Lejeune et al. (1997). Tables 1 and 2 list the model input parameters.

Table 1. General input parameters.

Stellar population:	10^7 single stars; 10^7 binaries
IMF:	Miller-Scalo
Age range:	1 − 20 Gyr
Metallicity:	$Z = 0.02$ (single abundance population)
Stellar mass range:	$0.1\,M_\odot < m < 100\,M_\odot$
Binary input parameters:	
Binary fraction:	67%
Flat distribution in q:	$n(q) = 1$
Critical mass ratio:	$q_{\rm crit} = 1.5$
Reimers mass-loss coefficient:	$\eta = 0.25$
Common ejection frequency:	$\alpha_{\rm CE} = 0.75$
Thermal energy conversion efficiency:	$\alpha_{\rm TH} = 0.75$

Table 2. Model input parameters.

Parameter	Yi	Han
Convective core overshoot:	$0.20H_p$	$0.25H_p$
Mixing length parameter (l/H_p)	1.7431	2.0
Helium abundance (Y):	0.27	0.28
He enrichment parameter ($\Delta Y/\Delta Z$):	2.0	2.0

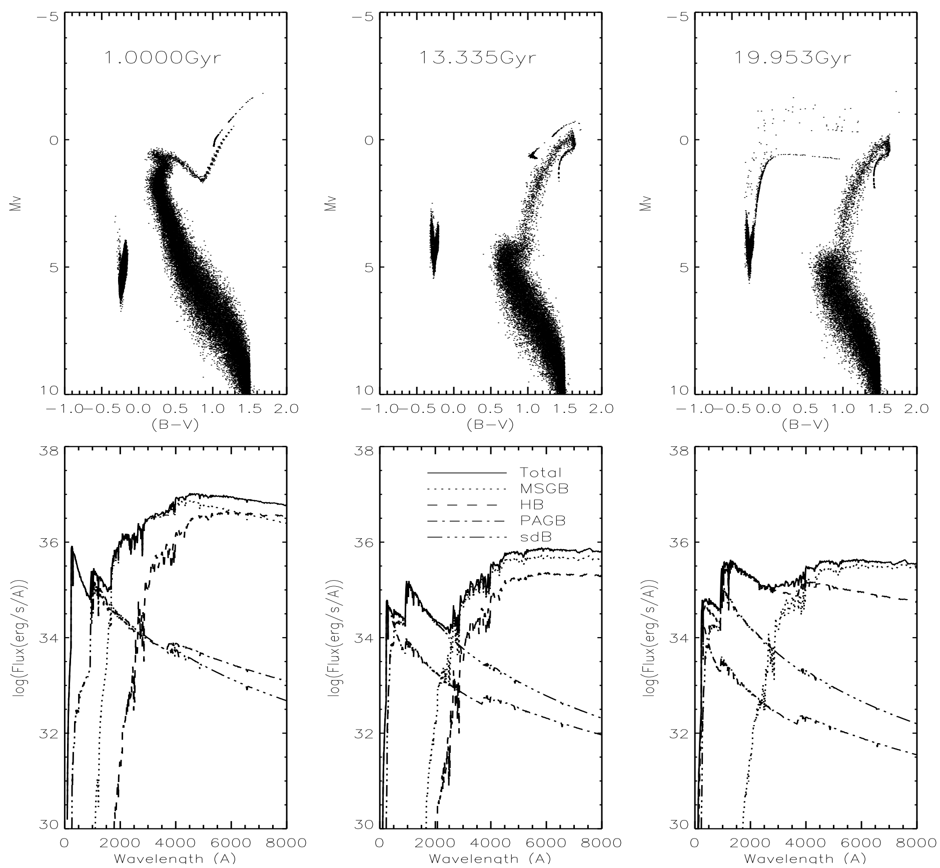

Fig. 1. Time evolution of the SSP as shown in the given CMDs and SEDs.

4. PRELIMINARY RESULTS

As a prelude to studying the UVX in composite systems (GEs), the first step of this inquiry has been to examine the UVX in a simple stellar population (SSP) for a single abundance of $Z = 0.02$. Both single and binary stars have been included in the population synthesis study. Figure 1 shows the CMD and SED time evolution of the population, respectively, for the given ages. With sdBs included, the total FUV flux decreases with increasing age until the trend is reversed by a contribution from single HB stars for late ages. The corresponding color evolution of *1500–V* with redshift z is given in Figure 2 (the solid line) along with two other models for composite systems obtained by Yi et Yoon (Lee et al. 2005). As seen, there is an increase of *1500–V* for the redshift range $0.0 < z < 0.2$ in contrast to that suggested by the other two models and empirical data points of NGC 1399 and Abell 2670. Incidentally, the cosmological parameters are $\Omega = 0.15$, $\Lambda = 0.85$, $z_F = 4.9$ and $H_o = 64.0$.

5. SUMMARY AND FUTURE PROSPECTS

Since the parameter space over which this study has been conducted is very limited ($Z = 0.02$ and $\eta = 0.25$), the results presented here are inconclusive in regard to the UVX hypotheses discussed earlier. Interestingly though, the given SSP does exhibit a UVX due to the presence of sdBs at early ages and later. However, the downward trend in *1500–V* for lower redshifts is not reversed, which differs from an increase in *1500–V* near low redshifts in GEs. The difference in results can stem from the fact that the SSP is a single abundance population whereas giant elliptical galaxies are composite metal-rich systems. Much is still to be learned from a study of Population II and super-solar stellar populations. Both abundance domains are the primary aims of this project in the future through an adaptation of Han's BPS code for different metallicities, mass-loss prescriptions and binary input parameters to see how the UV contribution from sdBs is affected.

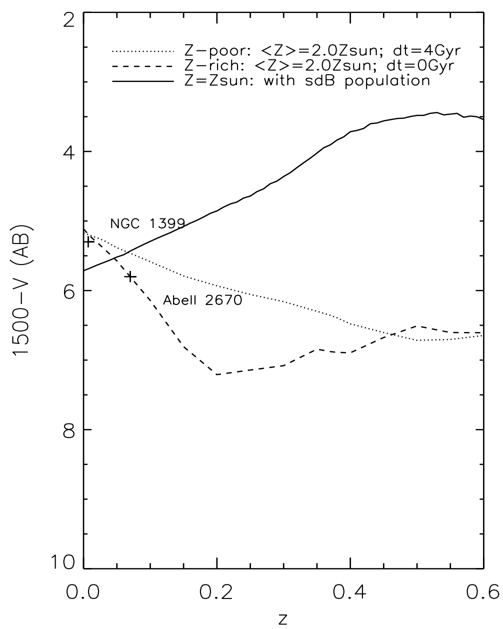

Fig. 2. Evolution of *1500–V* with z. Data points for NGC 1399 and Abell 2670 are from the GALEX survey (Lee et al. 2005).

REFERENCES

Eggleton P. P. 1971, MNRAS, 151, 351

Eggleton P. P. 1972, MNRAS, 156, 361

Eggleton P. P. 1973, MNRAS, 163, 179

Han Z. 1995, PhD thesis, Cambridge University

Han Z., Podsiadlowski P., Maxted P. F. L., Marsh T. R., Ivanova N. 2002, MNRAS, 336, 449

Han Z., Podsiadlowski P., Maxted P. F. L., Marsh T. R., Ivanova N. 2003, MNRAS, 341, 669

Lee Y. W., Ree C. H. et al. 2005, ApJ, 619, L103

Lejeune T., Cuisinier F., Buser R. 1997, A&AS, 125, 229

Park J. H., Lee Y. W. L. 1997, ApJ, 476, 28

Yi S., Demarque P., Oemler A. 1997, ApJ, 486, 201

Yi S., Demarque P., Oemler A. 1998, ApJ, 492, 480

Yi S., Lee Y. W., Woo J. H., Park J. H., Demarque P., Oemler A. 1999, ApJ, 513, 128

Baltic Astronomy, vol. 15, 17–24, 2006.

UV UPTURN OF ELLIPTICAL GALAXIES

Z. Han[1], Ph. Podsiadlowski[2] and A. Lynas-Gray[2]

[1] *National Astronomical Observatories, Yunnan Observatory, Chinese Academy of Sciences, PO Box 110, Kunming 650011, China*

[2] *University of Oxford, Department of Astrophysics, Keble Road, Oxford OX1 3RH, U.K.*

Received 2005 August 1

Abstract. We investigate the UV upturn phenomenon of elliptical galaxies by applying the binary model of hot subdwarfs of Han et al. (2002, 2003). Preliminary results show that the model provides a natural explanation for the UV upturn phenomenon and that the model could be used to detect low level recent star formation.

Key words: galaxies: elliptical – ultraviolet: galaxies – stars: binaries: close – stars: subdwarfs

1. INTRODUCTION

For old stellar populations, such as giant elliptical galaxies, far-UV radiation was expected to be almost completely dark. However, this is not the case. As surprisingly discovered by *Orbiting Astronomical Observatory 2* (OAO-2) mission in 1969, there exists a flux increase in spectral energy distributions of early-type galaxies from 2000 to 1200 Å, known as UV upturn (also referred as UV excess, UV rising-branch, UV rising flux, UVX) (see the review by O'Connell 1999). The origin of the UV upturn remained a mystery for many years ever since (see, e.g., Kjærgaard 1987). Ferguson et al. (1991), Dorman et al. (1995) and Brown et al. (1995, 1997) identified that UV upturn is mainly from extreme horizontal branch (EHB) stars. Brown et al. (2000) resolved hot HB stars for the first time in an elliptical galaxy (the core of M 32).

EHB stars are core-helium burning stars with very thin hydrogen envelopes ($M_{\rm env} \le 0.02 M_\odot$). They are the major source of far UV radiation in the evolutionary population synthesis study of giant elliptical galaxies. There are two schools of thought about the UV upturn, metal-poor school (Lee 1994; Park & Lee 1997) and metal-rich school (Bressan et al. 1994, 1996; Tantalo et al. 1996; Yi et al. 1995, 1997a, 1997b, 1998). Both schools adopt the formation channel of EHB stars from single stellar evolution, in which stellar wind mass-loss near the tip of the first giant branch (FGB) may strip off a giant's envelope and leave an almost bare helium core (e.g., D'Cruz et al. 1996).

The metal-poor school ascribes the UV-upturn to an old metal-poor population (the metal-poor tail of the wide metallicity distribution). An uncomfortably large age (~ 20 Gyr) is required to explain observations. In the metal-rich school, the UV-upturn results from the metal-rich population of giant elliptical galaxies. In order to fit observations, some assumptions need to be made, i.e., helium enrichment parameter $\Delta Y/\Delta Z > 2.5$, a fine-tuning of Reimer's mass-loss coefficient and its dependence on metallicity, a metallicity of 1–3 $Z_\odot$ and an age usually larger than 10 Gyr. Some of the assumptions are not justified.

In both schools, the formation of EHB stars is due to stellar wind mass-loss near the tip of the FGB, and therefore there is a sudden onset of the formation of EHB stars when a stellar population evolves. In other words, the UV upturn of elliptical galaxies declines rapidly with redshift. However, this is not the case, as shown by HST observations of Brown et al. (1998, 2000, 2003).

However, more than half of hot subdwarfs are found in binaries observationally (e.g., Maxted et al. 2001). Han et al. (2002, 2003) therefore proposed a binary model for the formation of EHB stars (or hot subdwarfs). In the model, there are three channels for the formation of hot subdwarfs, i.e., common envelope ejection for hot subdwarf binaries with short orbital periods, stable Roche lobe overflow for hot subdwarfs with long orbital periods, and merger of helium white dwarfs to form single hot subdwarfs. The model can explain the main observational characteristics of hot subdwarfs, in particular their distributions in the orbital period vs. minimum companion mass diagram and in the effective temperature vs. surface gravity diagram, their distributions of orbital period and mass function, their binary fraction and the fraction of hot subdwarf binaries with white dwarf (WD) companions, their birth rates and their space density.

In this paper we apply the binary model of Han et al. (2002, 2003) to the study of UV upturn and give the preliminary results. A more systematic and comprehensive study will be published elsewhere.

2. THE APPROACH

Han et al. (1994, 1995a, 1995b, 1998, 2003) developed a binary population synthesis (BPS) code, with which millions of stars (including binaries) can be evolved simultaneously from the zero-age main sequence (ZAMS) to white dwarfs or supernova explosion. The code can simulate in a Monte Carlo way the formation of many interesting stellar objects, such as type Ia supernovae, cataclysmic variables, double degenerates, barium stars, etc.

We incorporate the binary hot subdwarf model of Han et al. (2002, 2003) into the BPS code so that we can carry out Monte Carlo simulations and obtain the hot subdwarf population and its evolution. In the simulations, we adopt a metallicity of $Z = 0.02$, the critical mass ratio $q_{\rm crit} = 1.5$ for stable Roche lobe overflow on first giant branch (FGB) or asymptotic giant branch (AGB), common envelope ejection efficiency $\alpha_{\rm CE} = 0.75$ and thermal contribution to the ejection $\alpha_{\rm th} = 0.75$ (see section 7.4 of Han et al. 2003 for details). In addition, the simulations also require as input the star formation rate (SFR), the initial mass function (IMF) of the primary, the initial mass-ratio distribution and the distribution of initial orbital separations as follows.

(1) The SFR is taken to be a single burst.

(2) A simple approximation to the IMF of Miller & Scalo (1979) is used; the primary mass is generated with the formula of Eggleton, Fitchett & Tout (1989)

$$M_1 = \frac{0.19X}{(1-X)^{0.75} + 0.032(1-X)^{0.25}}, \tag{1}$$

where X is a random number uniformly distributed between 0 and 1. The adopted ranges of primary masses are 0.8 to $100.0\,M_\odot$. The studies by Kroupa, Tout & Gilmore (1993) and Zoccali et al. (2000) support this IMF.

(3) We take a constant mass-ratio distribution in the current study,

$$n(1/q) = 1, \qquad 0 \le 1/q \le 1, \tag{2}$$

where $q = M_1/M_2$.

(4) We assume that all stars are members of binary systems and that the distribution of separations is constant in $\log a$ (a is the separation) for wide binaries and falls off smoothly at close separations:

$$an(a) = \begin{cases} \alpha_{\rm sep}(\frac{a}{a_0})^m, & a \le a_0; \\ \alpha_{\rm sep}, & a_0 < a < a_1, \end{cases} \tag{3}$$

where $\alpha_{\rm sep} \approx 0.070$, $a_0 = 10\,R_\odot$, $a_1 = 5.75 \times 10^6\,R_\odot = 0.13\,\mathrm{pc}$ and $m \approx 1.2$. This distribution implies that there is an equal number of wide binary systems per logarithmic interval and that approximately 50 per cent of stellar systems are binary systems with orbital periods less than 100 yr.

In order to convolve the simulation result into colors or spectral energy distribution (SED), we adopt the latest version of BaSeL library (see Lejeune et al 1997, 1998 for a description), which gives the colors and SEDs of stars with a wide range of metallicity Z, surface gravity $\log g$ and effective temperature $T_{\rm eff}$. The library does not cover the surface gravity range for hot subdwarfs, and we therefore calculated emergent fluxes for solar metallicity hot subdwarfs using plane-parallel static model stellar atmospheres computed with ATLAS9 (Kurucz 1992) and adopting the assumption of local thermodynamic equilibrium, and the range for $\log g$ is 5.0 to 7.0 with a spacing of $\Delta \log g = 0.2$, the range for $T_{\rm eff}$ is 10 000 K to 40 000 K with $\Delta T = 1000$ K.

3. RESULTS AND DISCUSSION

In our investigation, we evolve a simple stellar population (SSP), in which all the stars have the same metallicity and the same age, or a mixed stellar population (MSP) which consists of two SSPs, a major one and a minor one. The major population has solar metallicity and an age of 10 Gyr, while the minor one has a solar metallicity and an age t. The minor population fraction f is the ratio of minor population mass to the total mass of the MSP, and $f = 100\,\%$ means the MSP is actually a SSP with an age t.

Figure 1 is a comparison between the UV spectrum from our model and that of M 49 from the Hopkins Ultraviolet Telescope (HUT) (from Brown et al. 1997). The model is a solar metallicity MSP with a total stellar mass of $4.7 \times 10^{10} M_\odot$ and a major population age of 10 Gyr. The minor population fraction is $f = 0.28\,\%$, and the minor population has an age of 0.5 Gyr. Actually we fixed the age of the major population according to local galaxy ages derived by Terlevich & Forbes (2002) and the minor population fraction, and obtained the best fit when the minor population age is 0.5 Gyr (the details of the fitting process will be described in another publication). The fraction of $f = 0.28\,\%$ is below the detecting limit for recent star formation. We see that the fit is satisfactory.

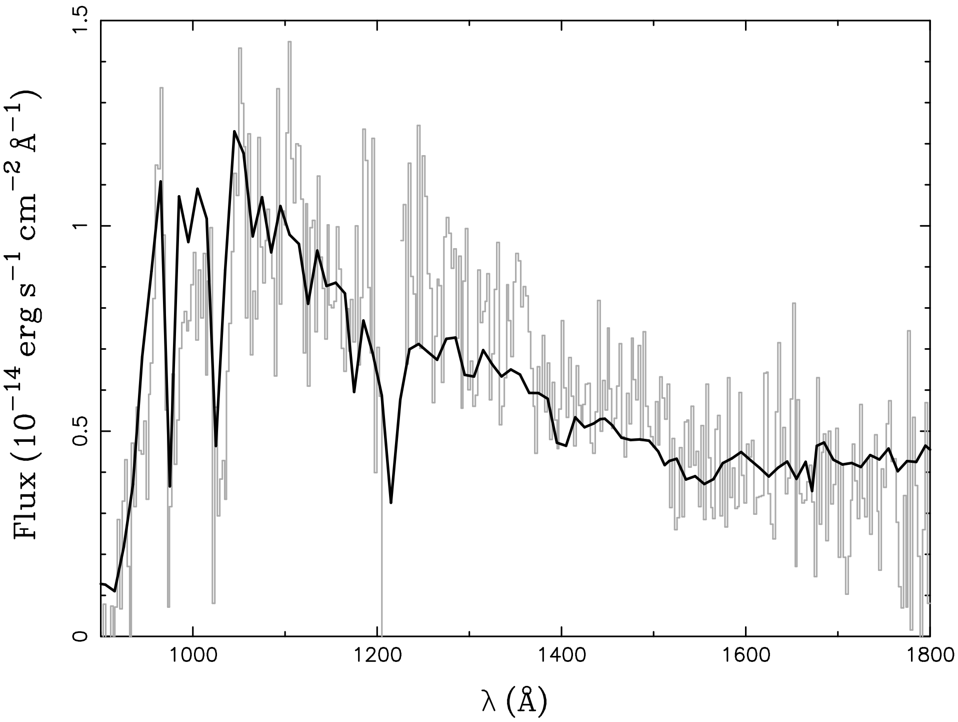

Fig. 1. A fit to the UV spectrum of elliptical galaxy M 49 obtained using the Hopkins Ultraviolet Telescope (HUT) (taken from Brown et al. 1997). The HUT data are shown by the grey histogram, while the thick solid line is from our model.

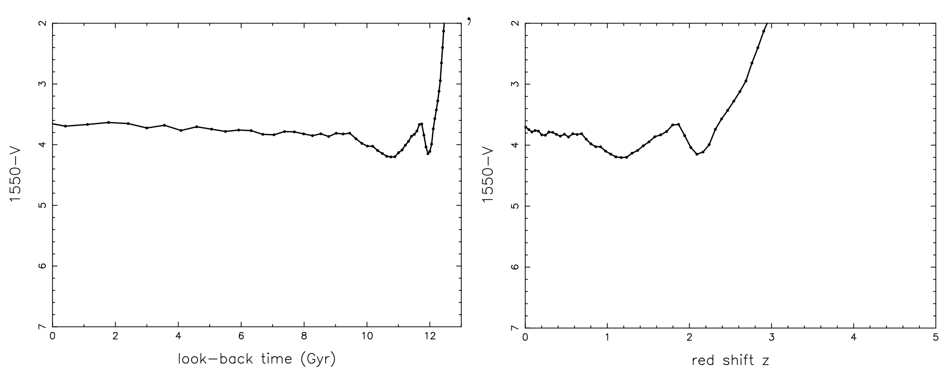

Fig. 2. The UV-upturn vs. look-back time (the left panel) and the UV-upturn vs. redshift (the right panel) from our model.

The magnitude of UV-upturn is defined by Burstein et al. (1988) as *1550–V* = –2.5 $\log(f_{1550}/f_V)$, where f_{1550} is the energy flux at 1550 Å and f_V – the flux in the V passband. Figure 2 is the UV-upturn versus the look-back time or the redshift for a SSP. The look-back time is defined as $t_\mathrm{L} = 13\,\mathrm{Gyr} - t_\mathrm{SSP}$, where t_SSP

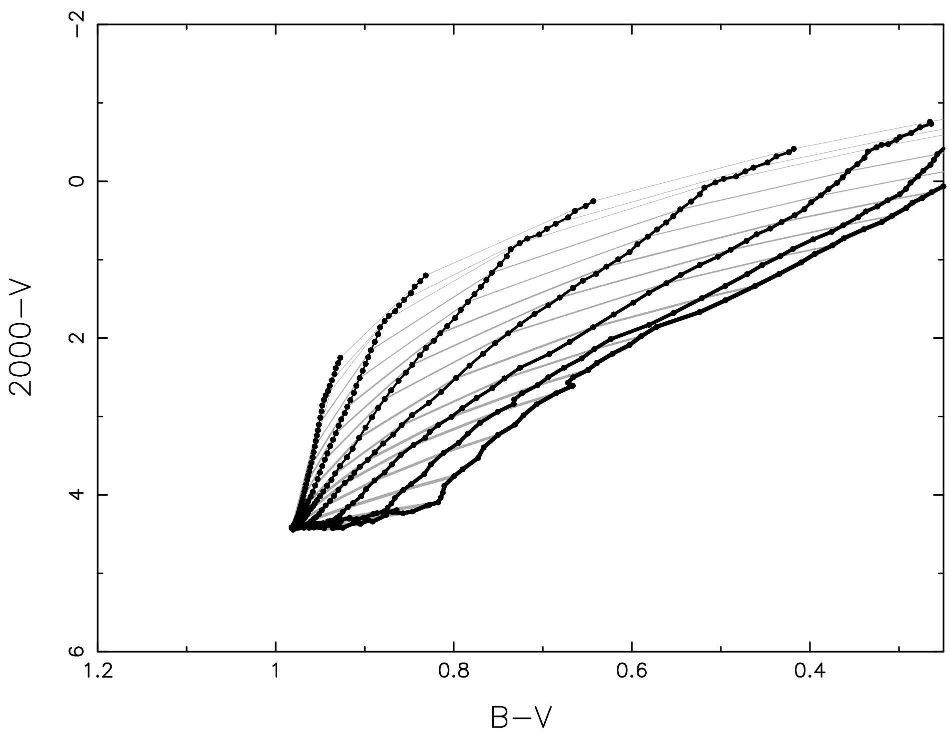

Fig. 3. *2000–V* vs. *B–V* for a mixed stellar population composed of a major and a minor population. The major population is with solar metallicity and with an age of 10 Gyr. The grey lines from top to bottom are for minor population age of $\log(t/\mathrm{Gyr}) = -1.0, -0.9, -0.8, -0.7 \ldots$, the dark solid lines from left to right are for minor population fractions of 0.1 %, 0.32 %, 1 %, 3.2 %, 10 %, 32 % and 100 %, while 100 % means that the mixed population is actually a single population (i.e., minor population only).

is the age of the SSP. We also convert the look-back time to redshift by adopting a flat universe and a Hubble time of 13.7 Gyr. As we see from Brown et al. (2003), UV-upturn does not depend much on redshift, and Figure 2 is consistent with the observations. Lee et al. (2005) tried to explain UV upturn-redshift relation by assuming that the post AGB (PAGB) mass decreases with redshift. However, the mass should increase with redshift from standard stellar evolution theory.

Figure 3 is the diagram of $\mathit{2000} - V$ vs. $B - V$ for a solar metallicity MSP with a major population of 10 Gyr and a minor population of varying age and fraction. The figure can be used to explain the observation of far-ultraviolet emission of early-type galaxies (see Fig. 2 of Deharveng et al. 2002).

Figure 4 is the diagram of $FUV - NUV$ vs. $FUV - r$, where FUV and NUV are magnitudes in the FUV and NUV passbands of the *Galaxy Evolution Explorer* (GALEX) and r is the magnitude in the r passband of the Sloan Digital Sky Survey (SDSS). If we compare our result to the systematics of the UV-upturn in a GALEX/SDSS sample of early-type galaxies (Fig. 3 of Rich et al. 2005), we find that the red-quiescent early-type galaxies in their sample have low level recent star formation.

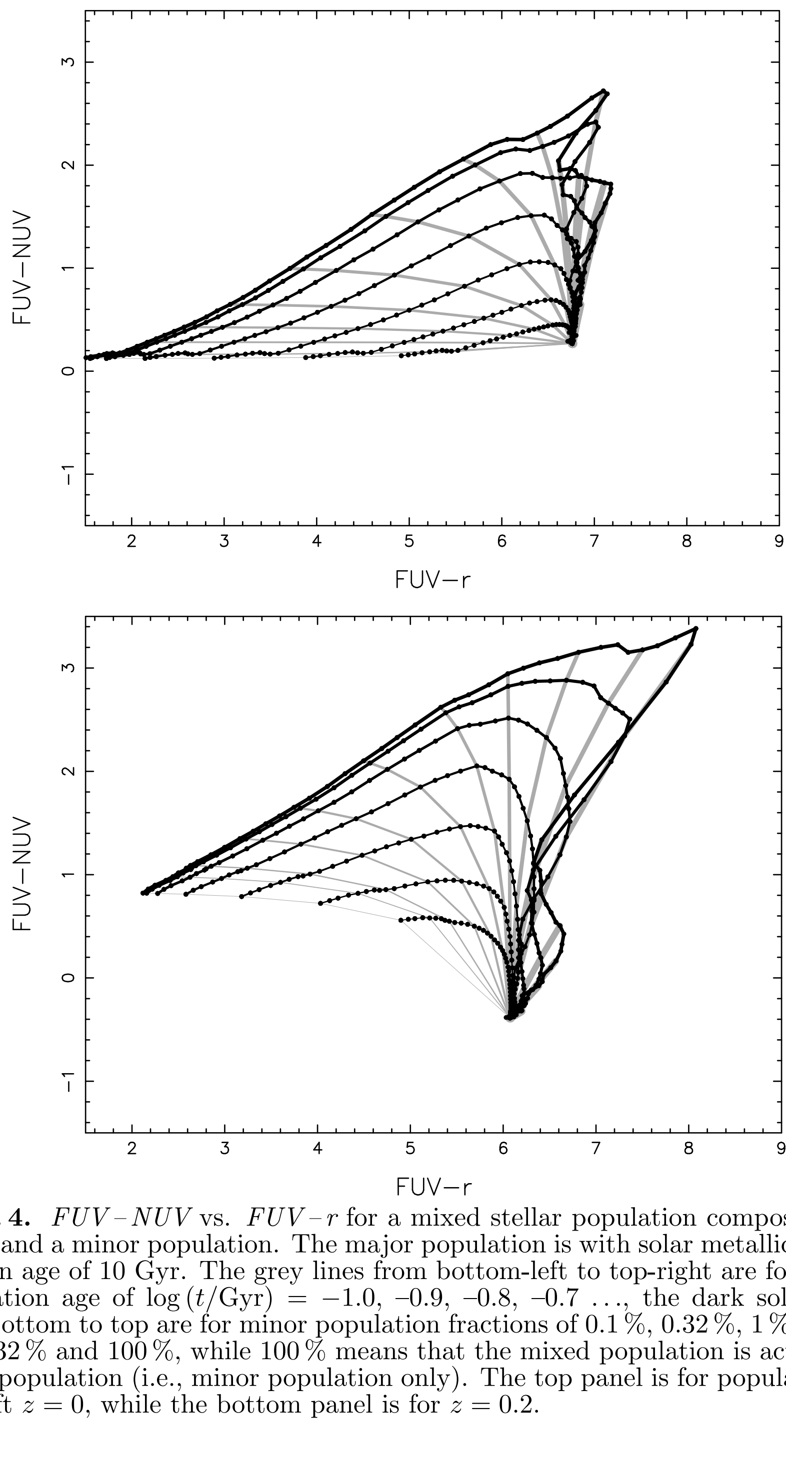

Fig. 4. $FUV-NUV$ vs. $FUV-r$ for a mixed stellar population composed of a major and a minor population. The major population is with solar metallicity and with an age of 10 Gyr. The grey lines from bottom-left to top-right are for minor population age of $\log(t/\mathrm{Gyr}) = -1.0, -0.9, -0.8, -0.7 \ldots$, the dark solid lines from bottom to top are for minor population fractions of 0.1 %, 0.32 %, 1 %, 3.2 %, 10 %, 32 % and 100 %, while 100 % means that the mixed population is actually a single population (i.e., minor population only). The top panel is for population at redshift $z = 0$, while the bottom panel is for $z = 0.2$.

4. CONCLUSIONS

We conclude that the binary model of hot subdwarfs of Han et al. (2002, 2003) is needed to understand the UV-upturn phenomenon of elliptical galaxies. Our model could be a useful tool in finding low level recent star formation.

REFERENCES

Bressan A., Chiosi C., Fagotto F. 1994, ApJS, 94, 63

Brown T. M., Bowers C. W., Kimble R. A., Ferguson H. C. 2000, ApJ, 529, L89

Brown T. M., Bowers C. W., Kimble R. A., Sweigart A. V. 2000, ApJ, 532, 308

Brown T. M., Ferguson H. C., Davidsen A. F. 1995, ApJ, 454, L15

Brown T. M., Ferguson H. C., Davidsen A. F., Dorman B. 1997, ApJ, 482, 685

Brown T. M., Ferguson H. C., Deharveng J. M., Jedrzejewski R. I. 1998, ApJ, 508, L139

Brown T. M. et al. 2003, ApJ, 584, L69

Burstein D., Bertola F., Buson L. M., Faber S. M., Lauer T. R. 1988, ApJ, 328, 440

D'Cruz N. L., Dorman B., Rood R. T., O'Connell R. W. 1996, ApJ, 466, 359

Deharveng J.-M., Boselli A., Donas J. 2002, A&A, 393, 843

Dorman B., O'Connell R. W., Rood R. T. 1995, ApJ, 442, 105

Eggleton P. P., Tout C. A., 1989, in *Algols*, ed. A. H. Batten, Kluwer Academic Publishers, Dordrecht, p. 164

Ferguson H. C. et al. 1991, ApJ, 382, L69

Han Z. 1998, MNRAS, 296, 1019

Han Z., Podsiadlowski Ph., Eggleton P. P. 1994, MNRAS, 270, 121

Han Z., Podsiadlowski Ph., Eggleton P. P. 1995a, MNRAS, 272, 800

Han Z., Eggleton P. P., Podsiadlowski Ph., Tout C. A. 1995b, MNRAS, 277, 1443

Han Z., Podsiadlowski Ph., Maxted P. F. L., Marsh T. R., Ivanova N. 2002, MNRAS, 336, 449

Han Z., Podsiadlowski Ph., Maxted P. F. L., Marsh T. R. 2003, MNRAS, 341, 669

Kjærgaard P. 1987, A&A, 176, 210

Kurucz R. L. 1992, in *The Stellar Populations in Galaxies*, IAU Symp. 149, eds. B. Barbuy & A. Renzini, Kluwer Academic Publishers, Dordrecht, p. 225

Lee Y. W. 1994, ApJ, 430, L113

Lee Y. W. et al. 2005, ApJ, 619, L103

Lejune T., Cuisinier F., Buser R. 1997, A&AS, 125, 229

Lejune T., Cuisinier F., Buser R. 1998, A&AS, 130, 65

Maxted P. F. L., Heber U., Marsh T. R., North R. C. 2001, MNRAS, 326, 1391

Miller G. E., Scalo J. M. 1979, ApJS, 41, 513

O'Connell R. W. 1999, ARA&A, 37, 603
Park J. H., Lee, Y. W. 1997, ApJ, 476, 28
Rich R. M. et al. 2005, ApJ, 619, L107
Tantalo R., Chiosi C., Bressan A., Fagotto F. 1996, A&A, 311, 361
Terlevich A. I., Forbes D. A. 2002, MNRAS, 330, 547
Yi S. K., Demarque P., Kim Y. C. 1997a, ApJ, 482, 677
Yi S. K., Afshari E., Demarque P., Oemler Jr. A. 1995, ApJ, 453, L69
Yi S. K., Demarque P., Oemler Jr. A. 1997b, ApJ, 486, 201
Yi S. K., Demarque P., Oemler Jr. A. 1998, ApJ, 492, 480

Baltic Astronomy, vol. 15, 25–31, 2006.

HOT SUBDWARFS IN THE GALACTIC BULGE

G. Busso[1], S. Moehler[1], M. Zoccali[2], U. Heber[3] and S. K. Yi[4]

[1] *Institut für Theoretische Physik und Astrophysik der Universität Kiel, Leibnizstrasse 12, D-24098 Kiel, Germany*

[2] *Departamento de Astronomia y Astrofisica, Pontificia Universidad Catolica de Chile, Avenida Vucuna Mackenna 4860, 782-0436 Macul, Santiago, Chile*

[3] *Remeis-Sternwarte, Astronommisches Institut der Universität Erlangen-Nürnberg, Sternwartstrasse 7, 96049 Bamberg, Germany*

[4] *Department of Physics, University of Oxford, Keble Road, Oxford OX1 3RH, U.K.*

Received 2005 August 1

Abstract. Recent observations and theories suggest that extreme horizontal branch (EHB) stars and their progeny should be the cause of the UV excess that many elliptical galaxies show in their spectra. Since the Galactic bulge is the closest representation of an old, metal-rich spheroid in which we are able to study the EHB scenario in detail, we obtained spectra of bulge EHB star candidates and we confirm their status as hot evolved stars. It is the first time that such stars are unambiguously observed in the Galactic bulge.

Key words: galaxies: elliptical – Galaxy: bulge – stars: hot subdwarfs

1. INTRODUCTION

The spectra of elliptical galaxies and bulge regions of spiral galaxies in many cases show a strong and unexpected increase in flux at wavelength shorter than 2500 Å. This feature, called "UV excess", was one of the most important discoveries of satellite-based UV astronomy (Code & Welch 1969) but also a puzzle, since it required the existence of hot stars in these old metal-rich systems (see Burstein et al. 1988 and references therein). After a long debate, most people agree that the observed UV radiation is mainly produced by very hot extreme horizontal branch stars (burning helium in their core) and their progeny, as Post-EarlyAGB and AGB-manqué stars (O'Connell 1999; Greggio & Renzini 1990, 1999; Dorman et al. 1995; Yi et al. 1998). This view is supported by spectroscopic (Ferguson et al. 1991; Brown et al. 1997, 2002) and photometric (Brown et al. 2002) UV observations of extragalactic systems. Near-UV HST observations of Brown et al. (2000) in M 32 detected for the first time individual EHB star candidates in an elliptical galaxy. The best fit to the observations is achieved with evolutionary tracks for helium- and metal-rich populations, since in this case EHB stars have the longest lifetimes in the temperature range required to reproduce the UV excess (cf. Bressan et al. 1994).

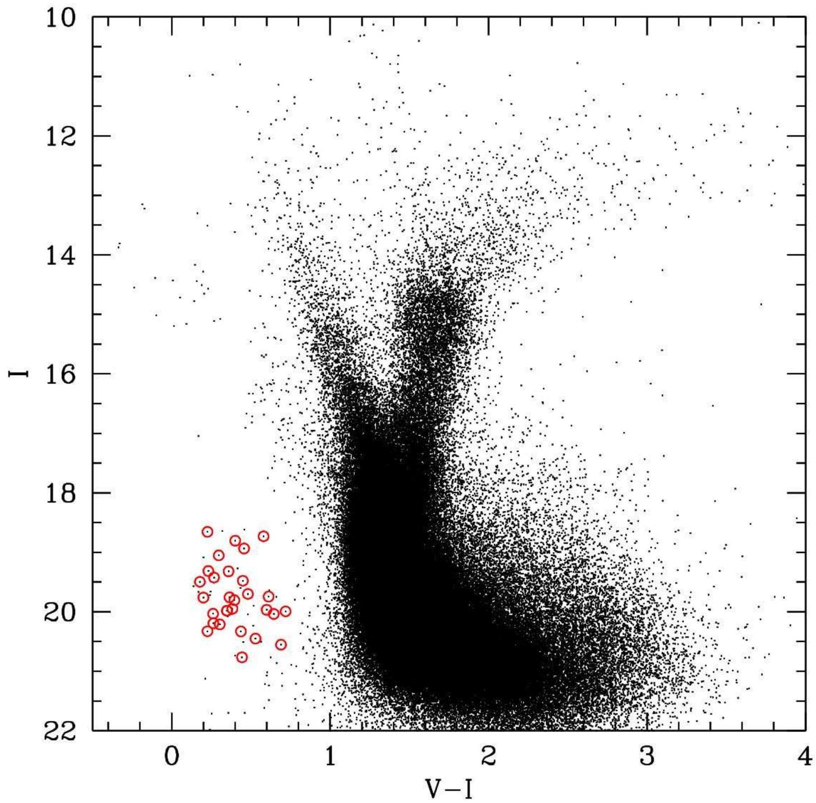

Fig. 1. Color-magnitude diagram of the Galactic bulge. Our targets are marked by circles.

The closest system similar to an elliptical galaxy with respect to age and metallicity for which it is possible to resolve stars is the Galactic bulge. The vast majority of EHB stars known in the Milky Way belongs however, to the metal-poor spheroid or to the disk population (where they show up as so-called subdwarf B (sdB) stars).

The only sdB candidates known in the bulge were found in the two massive globular cluster NGC 6388 and NGC 6441 (Rich et al. 1997; Busso et al. 2004), which are anyway not typical for the bulge population. The situation changed recently: Terndrup et al. (2004) found candidates in their survey for EHB stars in the Galactic bulge, and Wide Field Imager observations of a field toward the Galactic bulge (Zoccali et al. 2003) show a sequence of hot stars that are good candidates for EHB stars (see Figure 1). Using the values of Villeneuve et al. (1995) for scale height and space density of local field sdB stars, along a distance of 4.5 to 11 kpc within the field of view of WFI only less than 10 sdB stars are expected, while in our case about 140 candidates are found. Since they could be cool foreground stars (instead of reddened hot stars), we obtained spectroscopy of 29 candidates in order to derive effective temperatures and surface gravities and then, by means of comparison with HB models, to check their evolutionary status.

2. OBSERVATIONS

2.1. Target selection

Our spectroscopic targets were selected from the photometric catalogue of bulge stars obtained from Zoccali et al. 2003 (see Figure 1). We have chosen the stars with magnitude $18 < I < 21$ and color $0 < V - I < 0.8$ and among them we selected the most isolated ones.

2.2. VLT observations

We obtained medium-resolution spectra ($R \sim 1200$) of 29 candidates EHB stars at the VLT-UT1 (Antu) with FORS2. We used the multi-object spectroscopy (MXU) mode of FORS2 with the standard collimator, a slit width of $0.7''$ and grism B600, which allows to obtain spectra in the range between 3650 and 5200 Å(not all candidates though have spectra so extended because of the different positions on the CCD).

2.3. Data reduction

The data reduction was performed as described in Moehler et al. (2004) except for the following points. Due to the long exposure times (from 2700 s to 5400 s) the scientific observations contained a large number of cosmic rays and were therefore corrected with the algorithm described in Pych (2004). Regarding the subtraction of the sky background, we used two different methods depending on whether the target star in the slitlet was isolated or not. If the star was isolated, meaning any other stars in the slitlets were well enough separated from our target to identify regions uncontaminated by any stellar source, we approximated the spatial distribution of the sky background by a constant. If the slitlet showed severe crowding, meaning that the spectra of different stars were overlapping, we fitted each stellar profile with a Lorentzian function so that the whole spatial profile was reproduced by the sum of all the profiles; all the profiles but that one of the target were then subtracted (for details see Moehler & Sweigart 2006). With the extraction of the spectra, we saw that some (5 of 29) of our targets were actually cool stars. Therefore we did not proceed further with the reduction for these stars. The spectra were flux calibrated using standard stars spectra and corrected for any Doppler shifts determined from Balmer lines, as in Moehler et al. (2004).

3. ANALYSIS

Some examples of the spectra are shown in Figure 2. To fit the spectra (except for one He-rich one) we used ATLAS9 model atmospheres for solar metallicity (Kurucz 1993) to account for effects of radiative levitation (see Moehler et al. 2000 for details), from which we calculated spectra with Lemke's version of the LINFOR program (developed originally by Holweger, Steffen and Steenbock at Kiel University). The use of NLTE models or of LTE models with higher metallicity does not significantly change the results.

To establish the best fit, we used the routines developed by Bergeron et al. (1992) and Saffer et al. (1994), as modified by Napiwotzki et al. (1999), which employ a χ^2 test. The 1σ error necessary for the calculation of χ^2 is estimated from the noise in the continuum regions of the spectra. The fit program normalizes model spectra and observed spectra using the same points for the continuum definition.

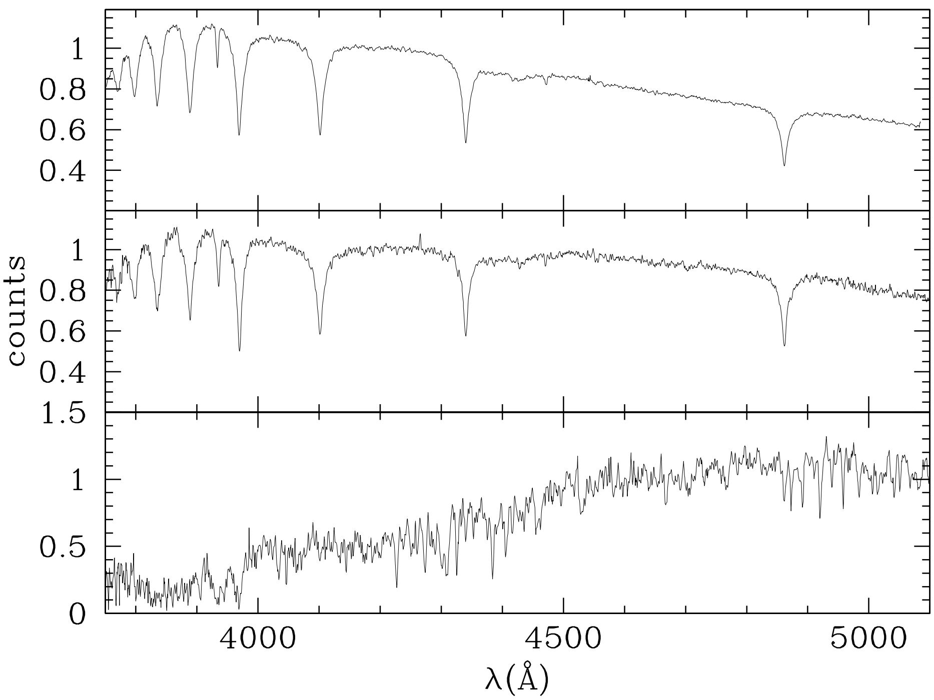

Fig. 2. Spectra of a few sdB star candidates. Top and central panel: typical spectra of newly detected hot stars with strong Balmer lines. Bottom panel: for comparison the totally different spectrum of a cool star.

We used the Balmer lines Hβ to H10 (excluding Hϵ to avoid the Ca II H line), the He I lines at 4026, 4388, 4471, 4921 Åand the He II lines at 4542 and 4686 Å.

We obtained the atmospheric parameters $T_{\rm eff}$, $\log g$ and helium abundances, and we calculated the absolute V and I magnitudes expected for these values, assuming $M_\star = 0.5\,M_\odot$. We left out one star because the fit was really bad. Considering a distance from the Galactic center of $\sim$ 8.5 kpc and a bulge radius of $\sim$1.5 kpc, we found that most of these objects are indeed bulge stars: of 23 hot stars, 13 stars are in the bulge within 1σ and 3 are in the bulge within 3σ.

This is also confirmed by the radial velocities found from the Doppler shift. The field we explored is centered at Galactic coordinates $\ell = 0°$, $b = -6°$, toward the Galactic center, so that the expected radial velocities for disk stars are around 0 km s^{-1}. Our velocities are distributed in a range between -200 and $+300$ km s^{-1}, in agreement with Terndrup et al. (1995).

Finally we compared our results with horizontal branch theoretical tracks: in Figure 3 we plotted in the $T_{\rm eff}$ vs. $\log g$ diagram the values found for those stars which belong to the bulge. The error bars are the formal errors from the fit procedure, but we are aware that the formal errors are underestimates (Napiwotzki, priv. comm.). The evolutionary tracks are from Yi et al. (1997) with metallicity $Z = 0.004$ and helium abundance $Y = 0.2416$. The Zero Age Horizontal Branch

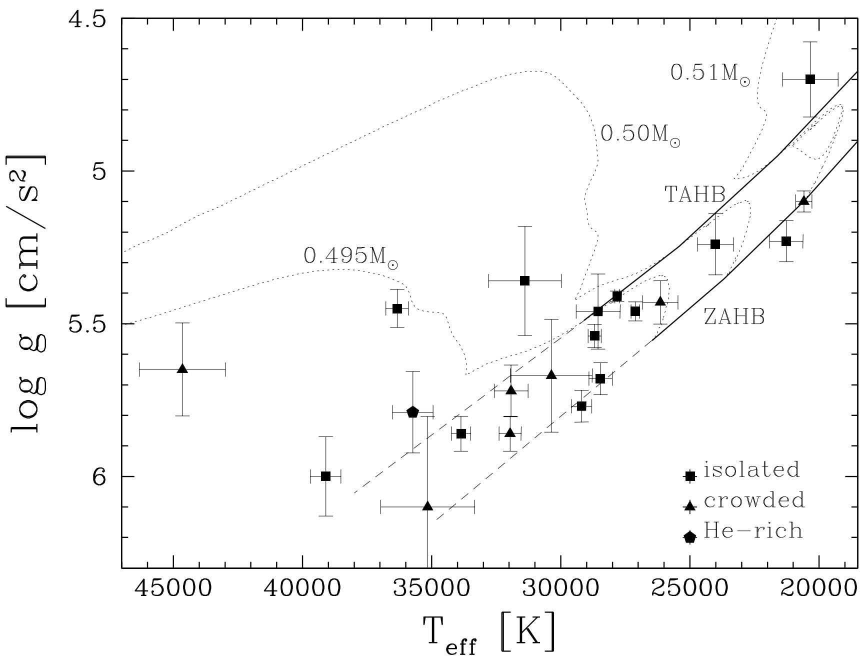

Fig. 3. T_{eff} vs. $\log g$) diagram. The squared symbols indicate the isolated stars; the triangles indicate the crowded stars and the pentagon is the He-rich star. The ZAHB and TAHB (Yi et al. 1997) and evolutionary tracks with metallicity $Z = 0.004$ and helium abundance $Y = 0.2416$ for 0.495, 0.50 and 0.51 $M_{\odot}$ are plotted. The dashed lines are extrapolated from the ZAHB and TAHB tracks.

(ZAHB), where the star starts to burn helium in its core quietly, and the Terminal Age Horizontal Branch, where the star burned the 99 % of the helium, are shown together with evolutionary tracks for stars with total masses of 0.495, 0.50 and 0.51 $M_{\odot}$. Since the theoretical lower limit for the mass of an EHB star is the core mass of the progenitor on the red giant branch ($\sim 0.45\,M_{\odot}$) while our tracks end at 0.495 $M_{\odot}$, we extrapolated the ZAHB and TAHB to lower masses (dashed curves in Figure 3). Proper models for lower masses will be calculated and used in a later paper. The observed points agree quite well with the theoretical tracks, therefore these objects are indeed EHB stars; some objects are above the TAHB meaning that they are in the post-HB phase and then evolving as AGB-manqué stars.

Finally we want to mention that all stars except one (which is helium-rich) are helium deficient as expected from diffusion.

5. CONCLUSIONS

We observed spectra of EHB star candidates in the Galactic bulge, from which we estimated the atmospherical parameters T_{eff} and $\log g$, confirming their evolutionary status. From the calculated radial velocities and distances we verified their membership to the bulge. This is the first time that such kind of stars are observed in the bulge, and with their spectra we are going to construct the integrated spectrum of the Galactic bulge from the UV to the optical, following the method described in Santos et al. (1995). The method consists in the construction of the integrated spectrum using a spectral library (in our case it will have to be a library extended to the UV) and the information contained in the spectroscopic and photometric observations. Regarding the spectral library, we will group the similar spectra, obtaining various groups of different spectral type, luminosity class and metallicity. For each group the average spectrum will be calculated, in order to obtain a better S/N. We will divide the color-magnitude diagram of the bulge in boxes, and each box will be associated to one of the library average spectra by means of the color index. The integrated spectrum will be the sum of the average spectra, scaling the contribute of each component keeping in account how many stars there are in each box.

This study will verify the role, so far only predicted, of EHB stars regarding the UV excess in elliptical galaxies.

ACKNOWLEDGMENTS. We are grateful to the ESO staff, especially those at the Paranal Observatory, for all their help during the observations. G.B. acknowledges support from the Deutsche Forschungsgemeinschaft via grant Mo 602/8.

REFERENCES

Bergeron P., Saffer R. A., Liebert J. 1992, ApJ, 394, 228

Bressan A., Chiosi C., Fagotto F. 1994, ApJS, 94, 63

Brown T. M., Ferguson H. C., Davidsen A. F., Dorman B. 1997, ApJ, 482, 685

Brown T. M., Bowers C. W., Kimble R. A., Sweigart A. V., Ferguson H. C. 2000, ApJ, 532, 308

Brown T. M., Ferguson H. C., O'Connell R. W., Ohl R. G. 2002, ApJ, 568, 19

Burstein D., Bertola F., Buson L. M., Faber S. M., Lauer T. R. 1988, ApJ, 328, 440

Busso G., Piotto G., Cassisi S. 2004, in *Stars in Galaxies*, eds. M Bellazzini, A. Buzzoni & S. Cassisi, Mem. Soc. Astron. Italiana, 75, 46

Code A. D., Welch G. A. 1969, ApJ, 228, 95

Dorman B., O'Connell R. W., Rood R. T. 1995, ApJ, 442, 105

Ferguson H. C., Davidsen A. F., Kriss G. A. et al. 1991, ApJ, 382, L69

Greggio L., Renzini A. 1990, ApJ, 364, 35

Greggio L., Renzini A. 1999, in *UV Astronomy in Italy*, eds. L. M. Buson & D. de Martino, Mem. Soc. Astron. Italiana, 70, 691

Kurucz R. L. 1993 in *ATLAS9 Stellar Atmospheric Program*, http://kurucz.harvard.edu

Moehler S., Sweigart A. V., Landsman W. B., Heber U. 2000, A&A, 360, 120

Moehler S., Sweigart A. V., Landsman W. B., Hammer N. J., Dreizler S. 2004, A&A, 415, 313

Moehler S., Sweigart A. V. 2006, Baltic Astronomy, 15, 41 (these proceedings)

Napiwotzki R., Green P. J., Saffer R. A. 1999, ApJ, 517, 399

O'Connell R. W. 1999, ARA&A, 37, 603

Pych W. 2004, PASP, 116, 148

Rich R. M., Sosin C., Djorgovski S. G. et al. 1997, ApJ, 484, L25

Saffer R. A., Bergeron P., Koester D., Liebert J. 1994, ApJ, 432, 351

Santos J. F. C., Bica E., Dottori H., Ortolani S., Barbuy B. 1995, A&A, 303, 753

Terndrup D. M., Sadler E. M., Rich R. M. 1995, ApJ, 110, 1774

Terndrup D. M., An D., Hansen A. et al. 2004, Ap&SS, 291, 247

Villeneuve B., Wesemael F., Fontaine G., Carignan C., Green R. F. 1995, ApJ, 446, 646

Yi S. K., Demarque P., Oemler A. J. 1997, ApJ, 486, 201

Yi S. K., Demarque P., Oemler A. J. 1998, ApJ, 492, 480

Zoccali M., Renzini A., Ortolani S. et al. 2003, A&A, 399, 931

Baltic Astronomy, vol. 15, 33–39, 2006.

SUPER-HELIUM-RICH STARS IN GLOBULAR CLUSTERS: THE ORIGIN OF EXTREME HORIZONTAL-BRANCH

S.-J. Joo[1], Y.-W. Lee[1], S.-J. Yoon[1,2], S.-I. Han[1], C. Chung[1], C. H. Ree[1], Y.-C. Kim[1], Y.-J. Sohn[1] and S. K. Yi[1,2]

[1] *Center for Space Astrophysics and Department of Astronomy, Yonsei University, Seoul 120-749, Korea*

[2] *Department of Physics, University of Oxford, Keble Road, Oxford OX1 3RH, U.K.*

Received 2005 August 1

Abstract. Recent observations of the globular cluster ω Centauri have shown that it has a double main sequence (MS), with a minority population of bluer and fainter MS well separated from a majority population of MS stars. Here we confirm that this special feature can only be reproduced by assuming a large range of helium abundance among several distinct populations in this cluster. We further show that the same helium enhancement required to reproduce this special feature on the MS can by itself reproduce the extreme horizontal-branch (EHB) stars observed in ω Cen, which are hotter than and separated from the majority population of normal HB stars. We also discuss the possibility that similar phenomena observed in the HB of other globular clusters are also due to the helium enhancement. If confirmed by further observations, this would establish that the third parameter that influences globular cluster color-magnitude diagram (CMD) morphology, in addition to metallicity and age, is indeed helium abundance.

Key words: globular clusters: individual (ω Centauri) – stars: abundances – stars: evolution – stars: horizontal-branch

1. INTRODUCTION

The Hubble Space Telescope snapshot survey of Galactic globular clusters has shown that the presence of extreme horizontal-branch (EHB) stars is not an unusual phenomenon among relatively massive globular clusters, which suggests that a third parameter, in addition to metallicity and age, is needed in order to explain the peculiar features observed on the HBs of these clusters (Piotto et al. 2002). It has been suggested for some time that more than one epoch of star formation and the accompanying helium and other elements enhancements in some globular clusters might be responsible for the presence of bimodal HBs and the EHB stars (D'Antona et al. 2002; D'Antona & Caloi 2004). While it has already been known that the HB morphology is very sensitive to helium abundance (see, e.g., Lee et

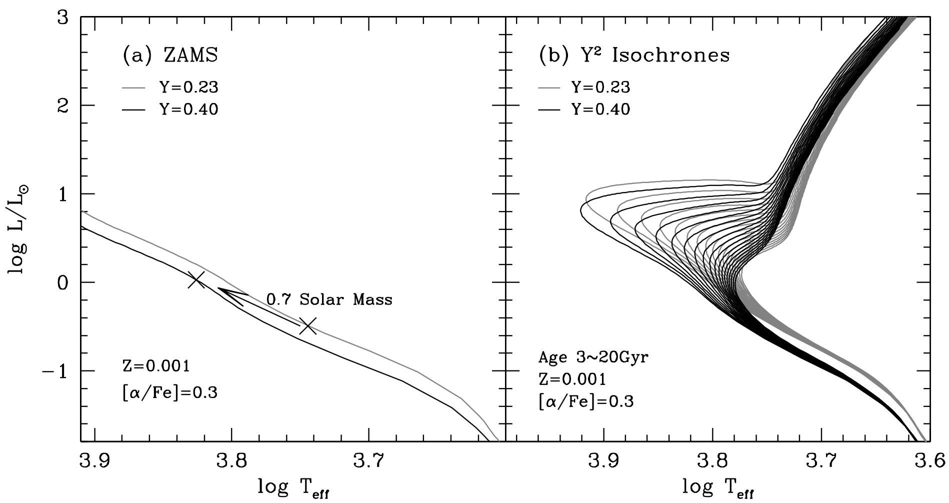

Fig. 1. New sets of Y^2 isochrones with helium enhancement. Panel (a) demonstrates the effect of helium enhancement on the zero-age main sequence for a given mass, while panel (b) illustrates the effect on the isochrones.

al. 1994), what is needed is a firm evidence that such a special helium enrichment indeed occurs in some globular clusters. This is because a star cluster is widely believed to be a coeval and chemically homogeneous system, and also the required helium enrichment is far more than that expected from standard chemical evolution models in galactic scales (i.e., $\Delta Y/\Delta Z = 1\sim 2$).

The first good evidence that some stars in a globular cluster are actually enhanced in helium came from the recent observations of ω Cen. In particular, recent analyses with isochrones (Norris 2004) and spectroscopy (Piotto et al. 2005) of the MS stars in ω Cen have shown that a large helium abundance variation is needed to reproduce the double MS (Bedin et al. 2004) observed in this cluster. Although more work is needed for a specific chemical evolution model devoted for ω Cen to understand the origin of this unusually strong helium enrichment, these observations and analyses have nevertheless provided a compelling evidence that a minority population of stars at least in one globular cluster are indeed enhanced in helium. In this paper, we report our progress in constructing population models with the super-helium-rich scenario.

2. EFFECT OF HELIUM ENHANCEMENT

In order to investigate the effect of helium abundance on the observed features in the CMD, we have first calculated new sets of Yonsei-Yale (Y^2) stellar evolutionary tracks and isochrones with helium enhancements (Kim et al. 2002; Kim et al. 2005). These tracks adopted most up-to-date input physics including a new equation of state for the low mass stars. Figure 1 demonstrates the effect of helium enrichment on the HR diagram. Helium-rich stars, in general, are brighter and bluer for a given mass because of their higher core temperature (Fig. 1a), however, since they evolve faster than helium-poor stars, they would have smaller masses for a given age, and therefore the helium-rich MS appears both bluer and

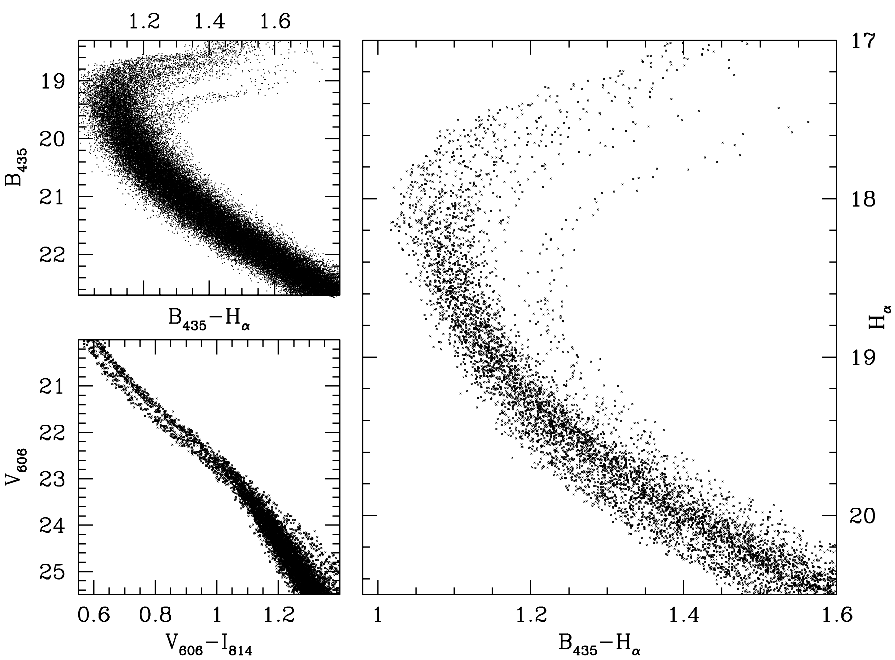

Fig. 2. Model CMDs for the main-sequence and subgiant-branch parts of ω Cen. These figures are to be directly compared with the observations by Bedin et al. (2004; see their Fig. 1).

fainter than the helium-poor MS on the isochrone (Fig. 1b). For the same reason, the mass at the tip of the red-giant-branch (RGB) of a helium-rich population is smaller than that of a helium-poor one, so that helium-rich HB stars have smaller total masses than helium-poor stars, which shifts their positions to the blue in the CMD (Lee et al. 1994).

3. POPULATION MODELS

Based on our new isochrones and the HB evolutionary tracks of Sweigart (1987) extrapolated to $Y \sim 0.4$,[1] population synthesis models are constructed following the techniques developed by Lee et al. (1990) and Park & Lee (1997). In Figure 2 we present the model CMDs for the MS and subgiant-branch (SGB) parts, based on the assumption that the helium abundances for the three most metal-rich populations are significantly enhanced among five populations with different metallicities in ω Cen (Sollima et al. 2005). These CMDs were specifically constructed with the passbands, photometric errors and total numbers of stars comparable to the observed ones of Bedin et al. (2004; see their Fig. 1), so that they can be directly compared with each other. The values of helium abundance and age are

[1] We are now in the process of constructing new sets of helium enhanced HB tracks fully consistent with our isochrones. Based on our preliminary models for ZAHB, we have confirmed that there is no serious systematic difference between our HB models and those of Sweigart (1987). We also verified that the extrapolation in Y does not produce a critical problem, by using the Sweigart & Gross (1976) HB tracks where the helium abundance is extended to $Y = 0.4$.

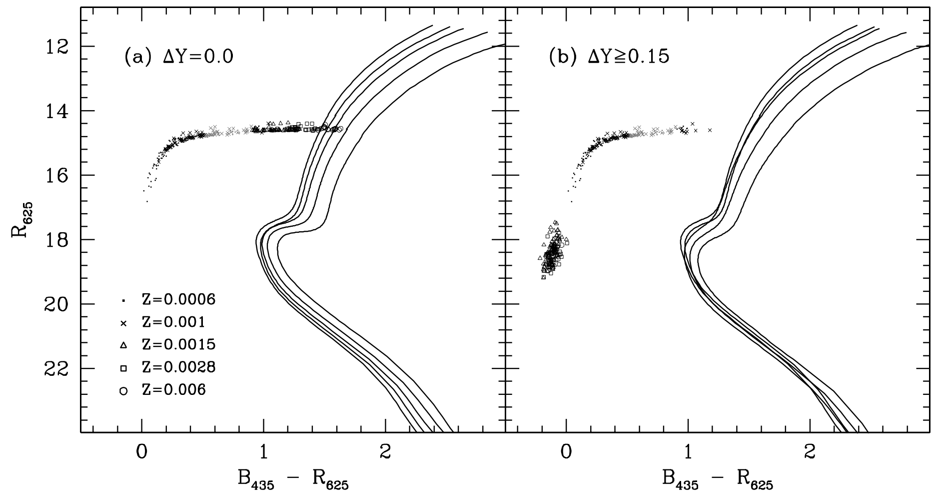

Fig. 3. Model CMDs for ω Cen. Panel (a) is for the case in which all five populations in ω Cen have the same helium abundance, while panel (b) is for the case in which the helium abundances for the metal-rich populations are significantly enhanced as in Table 1. Only the case of $\Delta Y \geq 0.15$ can reproduce the observed features on the MS and HB simultaneously. We adopted $(m-M)_R = 14.3$ and $E_{B-R} = 0.19$ in our models.

adjusted until the best matches between the models and the observed CMDs are obtained, while those for the metallicity are mostly fixed by the RGBs. Table 1 lists the input parameters used in our best model simulations. Similarly, in Figure 3, we compare two models constructed under different assumptions regarding the helium enhancement. As is clear from Figures 2 and 3, we confirm the conclusion from previous works that a large variation in helium abundance is indeed needed to reproduce the observed features on the MS to RGB, including the double MS, where the minority population of the bluer and fainter MS is both more metal-rich and super-helium-rich ($\Delta Y = 0.15$) compared to the majority population of the metal poor redder one.

In Figure 3 we have also presented corresponding synthetic HB models, which should be compared with the observed CMD by Ferraro et al. (2004; see their

Table 1. Input parameters in our best simulation of ω Cen. We adopted [α/Fe]=0.3 and η=0.46 for the mean mass-loss on the RGB. Population ratios were from Sollima et al. (2005).

Population	Z	Y	Age (Gyr)	Mass Loss ($M_\odot$)	Fraction
1	0.0006	0.231	13	0.168	0.42
2	0.001	0.232	13	0.178	0.27
3	0.0015	0.38	12	0.172	0.17
4	0.0028	0.40	11.5	0.177	0.08
5	0.006	0.42	11.5	0.201	0.05

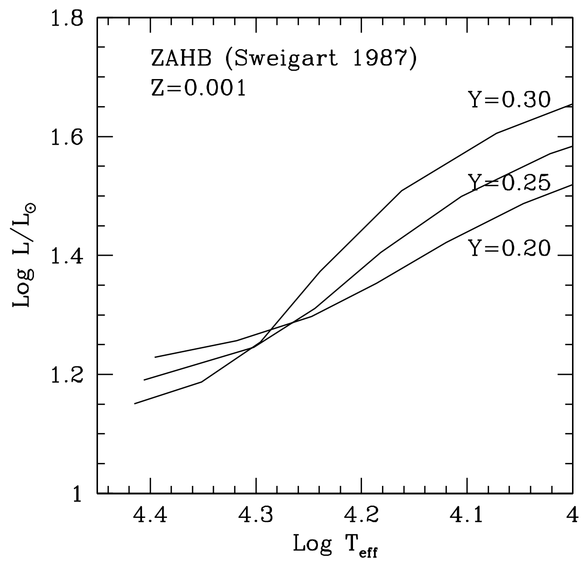

Fig. 4. The zero-age HB sequences with different helium abundances (Sweigart 1987).

Fig. 2, also see Fig. 1 of Lee et al. 2005). From models in Fig. 3a, we can see that the HB morphology generally gets redder with increasing metallicity, and the models fail to reproduce the EHB population. However, the models in Fig. 3b naturally reproduce the EHB stars observed in ω Cen with the same helium enhancements needed to reproduce the unique features on the MS. The fact that the three most metal-rich populations, including progeny of the bluer and fainter MS, all piled up on the extremely blue HB in Fig. 3b is a consequence of the large difference in helium abundance that easily overcomes the metallicity effect. In our model calculations, nothing other than the standard Reimers (1977) empirical relation was employed to estimate the amount of mass-loss on the RGB as a function of the input parameters adopted, and therefore the presence of extreme HB stars is solely the effect of helium enhancement. Under the same scenario, the complex features on the HBs of other globular clusters, such as NGC 2808, can be also explained by large internal variations of helium abundance (Lee et al. 2005; see also D'Antona et al. 2005).

An independent test for the helium-rich scenario might be provided from the FUV photometry of extreme HB stars, because the zero-age HB (ZAHB) locus is very sensitive to helium abundance. As Figure 4 illustrates, in general, helium-rich HB stars are brighter than helium-poor ones, but this trend is reversed when the effective temperature reaches ~19 000 K. This is because extremely hot HB stars have very thin envelopes, with an almost negligible energy output from the hydrogen-burning shell. The total energy output is then mostly sustained by the helium-burning core, and since helium rich stars have a smaller core mass, they have a lower surface luminosity (Sweigart 1987). According to Sweigart (1987), EHB stars, therefore, would be fainter than HB stars as a result of the helium enhancement. The observed trends in UV CMD of EHB and blue HB stars in NGC 2808 (Brown et al. 2001) and ω Cen (Whitney et al. 1994) support our prediction (see Fig. 4 of Lee et al. 2005). It is important to note that spectroscopic analyses of the EHB stars in ω Cen and NGC 2808 (Moehler et al. 2002; Moehler et al. 2004) have shown anomalously high helium abundances up to about 0.3–1.0. While Moehler et al. interpreted this with the late hot flasher scenario (Brown et al. 2001), we believe that at least some of this helium enrichment might be also understood from our scenario.

4. DISCUSSION

The good agreements between the models and the observations for the appearance and population ratio of EHB stars in ω Cen suggest that the third parameter that controls HB morphology, in addition to metallicity and age, might be helium abundance. This in turn suggests that whenever the relative age is estimated from the HB morphology (Lee et al. 1994; Rey et al. 2001), a better result would be obtained by ignoring extreme HB stars or similar peculiar features on the HB. Fortunately, the effect of helium abundance on the MS and RGB is relatively small, and in most globular clusters with EHB stars, the expected helium-rich populations are a minority in terms of the population ratio. Therefore, the age dating from MS and RGB is likely to be less affected by the minority populations of helium-rich stars in these clusters. However, when one infers the relative age or other physical parameters from the integrated-light colors and spectra of globular clusters and early-type galaxies, the possible contamination from helium-rich populations should still be carefully considered, as they would make the observed colors bluer, especially in the UV. Further observations and modeling of globular clusters with peculiar features on their HBs will undoubtedly help us to establish the super-helium-rich scenario as the origin of EHB stars found in globular clusters.

ACKNOWLEDGMENTS. Support for this work was provided by the creative research initiative program of the Korean ministry of science and technology, for which we are grateful.

REFERENCES

Bedin L. R., Piotto G., Anderson J., Cassisi S. et al. 2004, ApJ, 605, L125

Brown T. M., Sweigart A. V., Lanz T., Landsman W. B., Hubeny I. 2001, ApJ, 562, 368

D'Antona F., Bellazzini M., Caloi V., Fusi Fecci F., Galleti S., Rood R. T. 2005, ApJ, in press

D'Antona F., Caloi V. 2004, ApJ, 611, 871

D'Antona F., Caloi V., Montalban J., Ventura P., Gratton R. 2002, A&A, 395, 69

Ferraro F. R., Sollima A., Pancino E., Bellazzini M. et al. 2004, ApJ, 603, L81

Kim Y.-C., Demarque P., Yi S. K., Alexander D. R. 2002, ApJS, 143, 499

Kim Y.-C. et al. 2005, in preperation

Lee Y.-W., Demarque P., Zinn R. 1990, ApJ, 350, 155

Lee Y.-W., Demarque P., Zinn R. 1994, ApJ, 423, 248

Lee Y.-W., Joo S.-J., Han S.-I., Chung C. et al. 2005, ApJ, 621, L57

Moehler S., Sweigart A. V., Landsman W. B., Dreizler S. 2002, A&A, 395, 37
Moehler S., Sweigart A. V., Landsman W. B., Hammer N. J., Dreizler S. 2004, A&A, 415, 313
Norris J. E. 2004, ApJ, 612, L25
Park J.-H., Lee Y.-W. 1997, ApJ, 476, 28
Piotto G., King I. R. Djorgovski S. G., Sosin C. et al. 2002, A&A, 391, 945
Piotto G., Villanova S., Bedin L. R., Momany Y. et al. 2005, ApJ, 621, 777
Reimers D. 1977, A&A, 57, 395
Rey S.-C., Yoon S.-J., Lee Y.-W., Chaboyer B., Sarajedini A. 2001, AJ, 122, 3219
Sollima A., Ferraro F. R., Pancino E., Bellazzini M. 2005, MNRAS, 357, 265
Sweigart A. V. 1987, ApJS, 65, 95
Sweigart A. V., Gross P. G. 1976, ApJS, 32, 367
Whitney J. H., O'Connell R. W., Rood R. T. et al. 1994, AJ, 108, 1350

Baltic Astronomy, vol. 15, 41–48, 2006.

THE NATURE OF THE HOT STARS IN THE BULGE OF GLOBULAR CLUSTER NGC 6388 †

S. Moehler[1] and A. V. Sweigart[2]

[1] *Institut für Theoretische Physik und Astrophysik, Christian-Albrechts-Universität zu Kiel, D-24098 Kiel, Germany*

[2] *NASA Goddard Space Flight Center, Code 681, Greenbelt, MD 20771, U.S.A.*

Received 2005 August 1

Abstract. The metal-rich bulge globular clusters NGC 6388 and NGC 6441 show distinct blue horizontal-branch tails in their color-magnitude diagrams. They are thus strong cases of the well known *Second Parameter Problem.* In addition, the horizontal branches in these globular clusters show an upward tilt toward bluer colors, which cannot be explained by canonical evolutionary models. We will discuss several scenarios which have been proposed to explain these two features and present observations obtained to test these scenarios.

Key words: stars: horizontal branch, stars: evolution, globular clusters: individual: NGC 6388

1. INTRODUCTION

Ever since its discovery over 30 years ago (Sandage & Wildey 1967; van den Bergh 1967), the 2nd parameter effect has stood as one of the major unsolved challenges in the study of the Galactic globular clusters. While it was recognized quite early that the horizontal branch (HB) becomes redder on average with increasing metallicity, many pairs of globular clusters are known with identical metallicities but markedly different HB morphologies, e.g., M 3 versus M 13. Thus some parameter(s) besides metallicity (the 1st parameter) must affect the evolution of the HB stars in these globular clusters. Possible 2nd parameter candidates include the globular cluster age, mass-loss along the red giant branch (RGB), helium abundance Y, α-element abundance, cluster dynamics, stellar rotation, deep mixing, etc.

HST observations by Rich et al. (1997) have found that the metal-rich globular clusters NGC 6388 and NGC 6441 ([Fe/H] ≈ -0.5) contain an unexpected population of hot HB stars and therefore show a prominent 2nd parameter effect. Ordinarily metal-rich globular clusters have only a red HB clump. However, NGC 6388 and NGC 6441 possess extended blue HB tails containing $\sim 15\,\%$ of the total HB population. Quite remarkably, the HBs in both clusters slope upward with decreasing B–V with the stars at the top of the blue tail being nearly 0.5 mag brighter in V than the well-populated red HB clump. Moreover, the RR Lyrae variables in these clusters have unusually long periods for the cluster metallicity,

† Based on observations from the European Southern Observatory, Chile (prop. 69.D-0231)

leading Pritzl et al. (2000) to suggest that NGC 6388 and NGC 6441 may represent a new Oosterhoff group. For all of these reasons the HBs of NGC 6388 and NGC 6441 are truly exceptional.

In the next section we will discuss the implications of NGC 6388 and NGC 6441 for the 2nd parameter effect and will review a number of scenarios for explaining the HB morphology of these clusters. The following sections will then describe the high and medium resolution spectra that we have obtained to test these scenarios.

2. HB MORPHOLOGY: PROBLEMS AND SCENARIOS

The presence of hot HB stars in globular clusters as metal-rich as NGC 6388 and NGC 6441 may provide an important diagnostic for understanding the 2nd parameter effect for the following reason. In intermediate-metallicity globular clusters such as M 3 the HB spans a wide range in color that extends both blueward and redward of the instability strip. The location of a star along the HB is then quite sensitive to changes in the stellar parameters. In fact, this is why the HB is "horizontal". In metal-rich globular clusters, however, the situation is quite different. Due to their high envelope opacity, metal-rich HB stars are normally confined to a red clump. To move such stars blueward requires a larger change in the stellar structure. Thus any 2nd parameter candidate capable of producing hot HB stars in a metal-rich globular cluster might also have other observational consequences. Indeed, the upward sloping HBs in NGC 6388 and NGC 6441 suggest that the 2nd parameter in these globular clusters is affecting both the temperature and luminosity of the HB stars.

Can canonical models explain the upward sloping HBs in NGC 6388 and NGC 6441? In principle, one could produce hot HB stars in these globular clusters by increasing the cluster age or by enhancing the amount of mass-loss along the RGB. Rich et al. (1997) considered both of these possibilities but found neither of them to be satisfactory because the required increase in the cluster age is quite large and because the frequency of stellar interactions within the cores of these clusters seems too low to produce the additional RGB mass-loss. This conclusion was further supported by the theoretical HB simulations of Sweigart & Catelan (1998, hereafter SC98). They found that the HB morphology predicted by canonical HB models is flat in the (M_V vs. B–V) plane. Increasing the cluster age or the RGB mass-loss simply moves the models blueward in B–V without increasing their luminosity. Thus canonical HB models cannot account for the HB morphology of NGC 6388 and NGC 6441. In particular, two of the most prominent 2nd parameter candidates – age and RGB mass-loss – do not work.

This failure of canonical HB models to produce upward sloping HBs has prompted the study of other noncanonical solutions. Theoretical models show that the HB luminosity at a fixed metallicity depends on two parameters: the helium abundance Y and the core mass M_c. This fact led SC98 to suggest three noncanonical scenarios involving increases in either Y or M_c which might potentially produce upward sloping HBs.

The first ("high-Y") scenario assumes that the stars in NGC 6388 and NGC 6441 formed with a high primordial helium abundance due to a peculiar chemical enrichment history in these clusters. From theoretical models we know that HB tracks at high helium abundances have very long blue loops which deviate considerably from the zero-age HB (ZAHB). The HB simulations of SC98 show that such high-Y tracks can indeed produce upward sloping HBs as seen in NGC 6388 and NGC 6441 provided Y is very large ($\gtrsim 0.4$). However, this scenario can be ruled out because it predicts too large a value for the number ratio R of HB stars to RGB stars brighter than the HB (Layden et al. 1999) as well as too bright a luminosity for the RGB bump (Raimondo et al. 2002).

The second ("rotation") scenario is based on the fact that internal rotation within an RGB star can delay the helium flash, thereby leading to a larger core mass and to greater mass-loss near the tip of the RGB. This increase in M_c together with the corresponding decrease in M will shift a star's HB location towards higher effective temperatures and luminosities. HB simulations show that this scenario can also produce upward sloping HBs similar to those observed in NGC 6388 and NGC 6441. The problem, however, is to understand how the blue HB stars could have the high rotation rates required by this scenario.

The third ("helium-mixing") scenario is motivated by the large star-to-star abundance variations which are found among the red-giant stars within individual globular clusters and which are sometimes attributed to the mixing of nuclearly processed material from the vicinity of the hydrogen shell out to the stellar surface (Kraft 1994). The observed enhancements in Al are particularly important because they indicate that the mixing is able to penetrate deeply into the hydrogen shell (Cavallo et al. 1998). Such mixing would dredge up fresh helium together with Al, thereby enhancing the envelope helium abundance and leading to a brighter RGB tip luminosity and hence greater mass-loss. Thus a helium-mixed star would arrive on the HB with both a higher envelope helium abundance and a lower mass and would therefore be both bluer and brighter than its canonical counterpart - just what is needed to produce an upward sloping HB. Indeed, the HB simulations of SC98 confirm that helium mixing can produce HB morphologies similar to those in NGC 6388 and NGC 6441. However, the existence of helium mixing can be questioned on several grounds. The O-Na and Mg-Al anticorrelations observed in turnoff stars of NGC 6752 by Gratton et al. (2001) indicate that the Al enhancements are more likely due to primordial pollution from an earlier generation of asymptotic-giant-branch (AGB) stars than to deep mixing on the RGB. It is also questionable whether the mixing currents could overcome the large gradient in the mean molecular weight within the hydrogen shell of a RGB star. Thus helium mixing seems unlikely.

A number of additional solutions have been offered to explain the HB morphologies of NGC 6388 and NGC 6441. One of the earliest solutions, suggested by Piotto et al. (1997), was a spread in metallicity. In this case the blue HB stars would be metal-poor compared to the stars in the red HB clump. Because the HB becomes brighter in V with decreasing metallicity, the blue HB stars would also be brighter. Thus a metallicity spread might also produce an upward sloping HB. This possibility was studied by Sweigart (2002), who showed that upward sloping HBs similar to those in NGC 6388 and NGC 6441 would require the stars at the top of the blue HB tail to be approximately 2 dex more metal-poor than the stars in the red HB clump. However, Raimondo et al. (2002) have noted that the progenitors of the blue HB stars should appear as a population of metal-poor giants lying well to the blue of the metal-rich RGB. Since such metal-poor giants are not seen in the color-magnitude diagrams of NGC 6388 and NGC 6441, Raimondo et al. (2002) conclude that any metallicity spread must be small.

Piotto et al. (1997) also suggested that NGC 6388 and NGC 6441 might contain two stellar populations with different ages. This possibility has been further explored by Ree et al. (2002). Their population models for NGC 6388 and NGC 6441 are able to produce blue HB stars provided these stars are older by 1.2 Gyr and metal-poor by 0.15 dex compared to the stars in the red HB clump. Such a small difference in metallicity between the blue and red HB stars avoids the problem with the missing metal-poor giants discussed above. However, while such models might produce bimodal HBs, they do not produce an upward sloping HB. As shown by SC98, differences in age merely move an HB star horizontally along the HB, and, as shown by Sweigart (2002), a metallicity difference of 0.15 dex is too small to produce a significant HB slope. Thus the Ree et al. (2002) models do not account for a key property of the HBs in NGC 6388 and NGC 6441. Ree et al. (2002) also suggest that the long RR Lyrae periods might be explained if these stars are highly evolved from the blue HB. While such stars would have long periods, they would also evolve rapidly across the instability strip on their way to the AGB. Explaining the observed number of RR Lyrae stars under such a scenario would therefore be very difficult (Pritzl et al. 2002).

A more promising possibility is based on the suggestion by D'Antona & Caloi (2004) that the stars in globular clusters with blue HB tails are born in two events: a first generation of helium-normal stars and a second generation of helium-rich stars which subsequently form from the ejecta of the intermediate-mass AGB stars of the first generation. Since a helium-rich star has a lower turnoff mass at a given age, it will be bluer on the HB than a helium-normal star. It will also be brighter due to the increased energy output of the hydrogen-burning shell. Thus the spread in the internal helium abundance predicted by this scenario will lead to a spread in color along the HB, with the red clump stars corresponding to the helium-normal, first generation stars and the blue tail stars being progressively more helium-rich as the effective temperature increases. An upward sloping HB is a natural consequence of this spread in helium. The fact that the HB slope is more prominent in NGC 6388 and NGC 6441 than in other blue tail globular clusters may be simply due to their higher metallicity which requires a larger increase in helium in order to force a star blueward of the red clump. We emphasize that this scenario differs from the high-Y scenario, mentioned above, in which all of the stars are helium-rich and the helium-mixing scenario in which the spread in helium arises from deep mixing on the RGB.

All of the above scenarios which can produce an upward sloping HB predict that the gravities of the blue HB stars should be lower than the gravities of canonical blue HB stars. In 1998 we observed some of the brighter objects in both clusters ($B < 18$; four stars in NGC 6388, three in NGC 6441) to test this prediction. Unfortunately the results only added to the confusion as most of the stars had *higher gravities* than predicted by canonical evolution (Moehler et al. 1999). It took us four years and three rejected proposals to convince the ESO TAC to give us observing time for another test of the above described scenarios: With proposal 69.D-0231 we obtained high resolution spectra of four cool blue HB stars in NGC 6388 to determine their metallicities and rotation velocities. In addition, we observed medium resolution spectra of about a dozen blue HB stars along the blue tail to determine their effective temperatures and surface gravities. By comparing the observed values to those predicted by the various scenarios, we hope to distinguish among the scenarios.

3. HIGH RESOLUTION SPECTROSCOPY

The high resolution spectra were obtained with the UVES spectrograph at the ESO VLT with the standard setting DIC1 (390+564) and a slit width of 1″. This setting covers the wavelength ranges 3720–4520 Å in the blue arm and 4605–5585 Å and 5674–6610 Å in the red arm (2 CCDs) at a resolution of 45 000 (blue) and 37 000 (red). This is the same setting as used by the SPY project (Karl et al., these proceedings). We therefore reduced the data with the UVES context within MIDAS, with the additional correction by a flat field shifted in wavelength direction as done by the SPY consortium to avoid ripples in the resulting one-dimensional spectrum. The details will be described in a forthcoming paper.

3.1. Analysis and results

To analyze the high resolution spectra, we first estimated effective temperatures from B–V colors corrected for a reddening of 0.37 mag. Keeping these temperatures fixed, we estimated the surface gravities by fitting the Balmer line profiles as described in Moehler et al. (2004). Using these values we did a first abundance determination by spectrum synthesis, using the LINFOR program*. Then we changed the effective temperature until the abundances from Fe I and Fe II agreed to within 0.15 dex. The surface gravity was again determined by fitting the Balmer line profiles. Figure 1 shows a section of the spectra of three HB stars together with the synthesized spectrum (the fourth star is the coolest one and therefore most difficult to analyze due to severe line blending). We find no significant deviations from the overall metallicity of NGC 6388 in these spectra and therefore no supporting evidence for a possible metal deficiency in these blue HB stars. We also do not find rotation velocities in excess of 10 km s^{-1}, which is in good agreement with the values found for blue HB stars in other globular clusters. We do find a *very tentative* evidence for a possible helium enrichment. In this temperature range, however, the helium lines are very weak and extremely sensitive to temperature variations, so that we so not want to place much emphasis on this *possible* result.

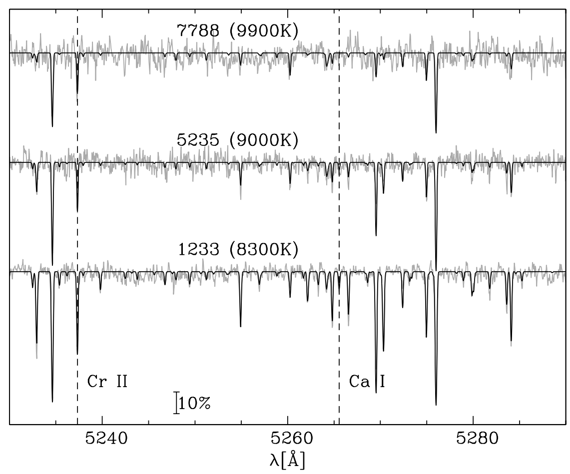

Fig. 1. Small section of the UVES spectra for the three hotter stars. The black line is the synthetic spectrum for each star and the unmarked lines are all iron lines.

4. MEDIUM RESOLUTION SPECTROSCOPY

The medium resolution spectra of stars along the blue tail were obtained with the multi-object spectroscopy mode MOS of FORS2, again at the ESO VLT.

* For a description see http://a400.sternwarte.uni-erlangen.de/∼ai26/linfit/linfor.html

We used the grism 600B with a slit width of 0.6″, corresponding to a resolution of 1200 and a wavelength range of 3700 Å to 5200 Å for all spectra. The wavelength range extended to blue or redder regions depending on the position of the slitlet on the CCD. The data were reduced as described in Moehler et al. (2004), except for the sky subtraction.

The MOS observations were obtained in very crowded fields, and due to the fact that several stars were observed simultaneously, we could not orient the individual slitlets in a way to avoid nearby stars. Therefore most slitlets contain spectra of several stars, in many cases overlapping so strongly that it is impossible to directly extract the spectrum of our intended target (see Figure 2). In order to account for this overlap we proceeded as follows.

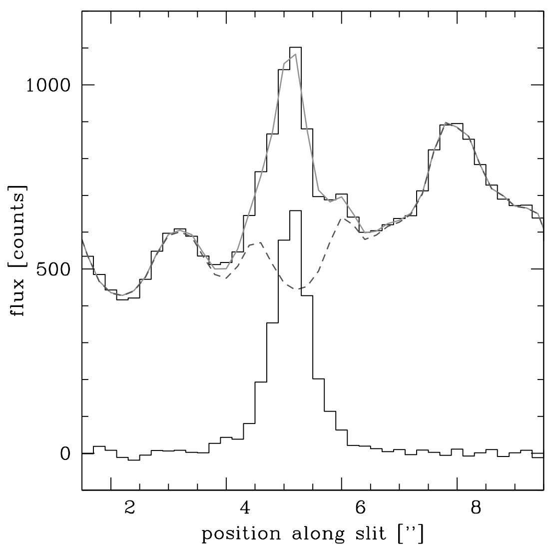

Fig. 2. The spatial light distribution along one slitlet. The upper histogram is the observed light distribution, the light continuous line gives the fit of all sources, the light dashed line marks the subtracted sky background. The lower histogram is the spatial profile of the sky subtracted image.

- We corrected the curvature of the FORS2 spectra.
- We averaged the wavelength-calibrated two-dimensional spectra along their dispersion axis between 3500 and 5200 Å (roughly the range which is later used for fitting the line profiles), thereby producing a one-dimensional spatial profile along the slitlet (cf. Figure 2, upper histogram).
- The one-dimensional spatial distribution of light was fitted with a combination of Moffat functions, i.e.,

$$I_{(x)} = bck + \sum_{j=1}^{n} I_{j(x)}$$

$$\text{with} \qquad I_{j(x)} = a_j \left(1 + \frac{4(x-b_j)^2}{c^2}\right)^{-d}.$$

For each profile the parameters a_j (amplitude) and b_j (position) were fitted individually, whereas the parameters c and d, which determine the profile width and shape (and should depend only on the seeing and instrumental broadening), had to be the same for all objects within one slitlet. We used up to 13 individual profiles to fit the full spatial light distribution along one slitlet (see Figure 2, light solid line).

- After achieving a good fit to the observed spatial profiles we kept the parameters b_j, c and d fixed and used these profiles to fit the spatial profile now at

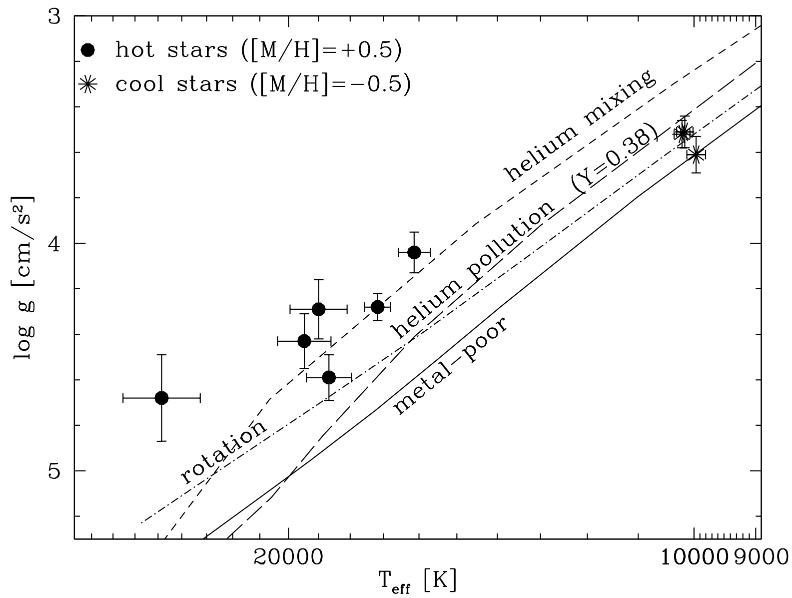

Fig. 3. Effective temperatures and surface gravities for our target stars as derived from line profile fits. Three stars have temperatures below 8000 K, where we do not trust the fit procedure, and one star showed a prominent G-band in its spectrum after the sky subtraction and was therefore not analyzed. For comparison we show the tracks discussed in Section 2.

every wavelength step. The amplitudes a_j and the spatial constant *bck* (for the true sky background) were allowed to vary with wavelength, in order to describe the various spectra.

- The sum of all profiles *minus the target profile* were then used as sky background (cf. Figure 2, dashed line) and subtracted from the wavelength calibrated two-dimensional image. The resulting image – containing only the target spectrum – was again averaged over the same wavelength range as above to verify the quality of the sky correction (see Figure 2, lower histogram).

4.1. Analysis and results

We then fitted the Balmer and helium line profiles to determine effective temperatures, surface gravities and helium abundances as described in Moehler et al. (2004), using a solar metallicity model grid to account for the effects of radiative levitation. The resulting values of $T_{\rm eff}$ and log g are shown in Figure 3, together with tracks describing the scenarios mentioned in Section 2. Obviously the hot stars show significantly lower gravities than expected. To verify if this is a luminosity effect or rather a reduction and/or analysis artifact, we used these values to estimate masses for the stars. While the three stars around 10 000 K show an average mass of 0.52 $M_\odot$, the hot stars have an average mass of 0.28 $M_\odot$, which is too low by almost a factor of 2. We therefore suspect that the sky subtraction did not work sufficiently well to really isolate the light from the hot stars. Tests with the spectra indicate that sky subtraction problems may also be the cause for the unexpectedly high gravities found previously by Moehler et al. (1999).

5. CONCLUSIONS

From our high resolution data (which include two of the three stars at 10 000 K in Figure 3) we find no supporting evidence for the low metallicity scenario. The atmospheric parameters of the stars at about 10 000 K also do not support the helium mixing scenario. The medium resolution data of the hotter and visually fainter stars unfortunately yield results that are apparently affected by systematic errors. As the hotter stars are fainter by at least 1.2 mag in B compared to the stars at about 10 000 K, the systematic problems are most probably due to crowding problems, which are more severe for fainter stars. Despite our best efforts, which yielded spectra without obvious evidence for contamination in all but one case, we apparently did not succeed in extracting from the observed data the information related *only* to the intended target. This should serve as a warning that observations in crowded regions are difficult, especially, if the targets are selected from HST observations (as was the case here).

ACKNOWLEDGMENTS. We want to thank the staff at the Paranal Observatory for obtaining the observations for us.

REFERENCES

Cavallo R. M., Sweigart A. V., Bell R. A. 1998, ApJ, 492, 575

D'Antona F., Caloi V. 2004, ApJ, 611, 871

Gratton R. G., Bonifacio P., Bragaglia A. et al. 2001, A&A, 369, 87

Kraft R. P. 1994, PASP, 106, 553

Layden A. C., Ritter L. A., Welch D. L., Webb T. M. A. 1999, AJ, 117, 1313

Moehler S., Sweigart A. V., Catelan M. 1999, A&A, 351, 519

Moehler S., Sweigart A. V., Landsman W. B., Hammer N. J., Dreizler S. 2004, A&A, 415, 313

Piotto G., Sosin C., King I. R. et al. 1997, in *Advances in Stellar Evolution*, eds. R. T. Rood & A. Renzini, Cambridge University Press, Cambridge, p. 84

Pritzl B. J., Smith H. A., Catelan M., Sweigart A. V. 2000, ApJ, 530, L41

Pritzl B. J., Smith H. A., Catelan M., Sweigart A. V. 2002, AJ, 124, 949

Raimondo G., Castellani V., Cassisi S., Brocato E., Piotto G. 2002, ApJ, 569, 975

Ree C. H., Yoon S.-J., Rey S.-C., Lee Y.-W. 2002, in *Omega Centauri, a Unique Window into Astrophysics*, eds. F. van Leeuwen, J. D. Hughes & G. Piotto, ASP Conf. Ser., 265, 101

Rich R. M., Sosin C., Djorgovski S. G. et al. 1997, ApJ, 484, L25

Sandage A., Wildey R. 1967, ApJ, 150, 469

Sweigart A. V. 2002, in *Highlights of Astronomy*, ed. H. Rickman, ASP, San Francisco, p. 292

Sweigart A. V., Catelan M. 1998, ApJ, 501, L63 (SC98)

van den Bergh S. 1967, AJ, 72, 70

Baltic Astronomy, vol. 15, 049–052, 2006.

NEW CANDIDATE EHB STARS IN THE OPEN CLUSTER NGC 6791: LOOKING LOCALLY INTO THE UV-UPTURN PHENOMENON

L.M. Buson[1], E. Bertone[2], A. Buzzoni[3] and G. Carraro[4,5,6]

[1] *INAF - Osservatorio di Padova, Italy*
[2] *INAOE, Puebla, Mexico*
[3] *INAF - Osservatorio di Bologna, Italy*
[4] *Dept. de Astron. Univ. de Chile, Santiago. Chile*
[5] *Astronomy Dept., Yale Univ., USA*
[6] *Dip. di Astronomia, Univ. di Padova, Italy*

Received 2005 August 1

Abstract. Relying on U and B imagery at the Italian Telescopio Nazionale Galileo (TNG), we report here the discovery of a sample of 13 new UV-bright post-HB candidate stars in the field of the Galactic open cluster NGC 6791. Owing to its super-solar metal content ([Fe/H] $\gtrsim$ 0.2 dex) and estimated age ($t \gtrsim$ 8 Gyr), this cluster represents the nearest and ideal stellar aggregate to match the distinctive properties of the evolved stellar populations possibly ruling the UV-upturn phenomenon in elliptical galaxies and bulges of spirals. Our ongoing spectroscopic follow-up of this unique UV-bright sample will allow us to assess – once cluster membership of the candidates is properly checked – the real nature (e.g., sdB, sdO, AGB-manqué or EHB stars) of these hot sources and their link with the ultraviolet excess emerging from low-mass, metal-rich evolutionary environments of external galaxies.

Key words: stars: sudwarfs – stars: horizontal-branch – ultraviolet: stars

1. INTRODUCTION

Since its early discovery (Code 1969), the so-called UV-upturn phenomenon in old stellar populations of ellipticals and spiral bulges (namely the abrupt rise in the UV continuum emission shortward of $\lambda \sim 2000$ Å) has been the subject of growing theoretical analyses intended to establish its origin and evolution (see, e.g., Greggio & Renzini 1990 and O'Connell 1999, for reviews).

Both theory and observations currently seem to converge towards the "Extreme Horizontal Branch" (EHB) scenario as the main factor responsible for the phenomenon (Dorman et al. 1995; Brown 2004). If this is the case, models show that hot HB stars with helium core mass $M_{\rm core} \lesssim 0.52\ M_\odot$ can escape the standard post-HB evolution (that would culminate with the planetary-nebula event at the end of the asymptotic giant branch evolution), and directly reach the high-temperature region of the HR diagram ($T_{\rm eff} \gtrsim 30\,000$ K) to fade then along the white-dwarf cooling sequence (Dorman et al. 1993).

In this framework, the role of metallicity cannot yet be confidently assessed, however, as we face two conflicting scenarios relying either on a metal-poor evolution (naturally giving rise to a blue HB morphology, see Park & Lee 1997) or a metal-rich case, where the onset of UV emission needs at least a fraction of stars to exceed some critical threshold in [Fe/H] (Greggio & Renzini 1990; Bressan et al. 1994; Buzzoni 1995; Dorman et al. 1995). In this regard, one should be aware that even the high-resolution UV spectroscopy provided by FUSE for the UV-brightest elliptical NGC 1399 turned out to be inadequate to solve the problem, as it mainly probes the photospheric abundance of hot stars, likely perturbed by diffusion effects and therefore not fully indicative of the true metallicity of the whole galaxy stellar population (Brown et al. 2002).

2. NGC 6791: THE UNEXPECTED SHORTCUT

Photometric observations of evolved UV-bright stars in external galaxies are still confined to the relevant case of M 31 and its satellite system (e.g., Bertola et al. 1995; Brown et al. 1998, 2000), and no suitable spectroscopy for single stars is available to date.

Surprisingly enough, the close Galactic open cluster NGC 6791, less than 5 kpc away (Friel 1995; Carraro et al. 1999), turned out to be a highly valuable candidate to address the issue of the EHB UV-bright stars, standing out as a sort of backyard "Rosetta Stone" to assess the UV emission of spheroids much farther away. This cluster is actually one of the brightest ($L_V \sim 6.3\,10^3\ L_\odot$), oldest ($t \gtrsim 8$ Gyr) and metal-rich ([Fe/H]$\gtrsim +0.2$) ones (King et al. 2005; Stetson et al. 2003; Carraro et al. 1999), and hosts a significant fraction of sdB/O stars (Kaluzny & Rucinski 1995; Kaluzny & Udalski 1992, see Fig. 1) interpreted by Yong et al. (2000) as EHB stars with $T_{\rm eff}$ in the range 24–32 000 K, as confirmed by ground and space-borne (UIT and HST) observations (Liebert et al. 1994; Landsman et al. 1998).

3. OBSERVATIONS AND REDUCTIONS

In 2003 we started a specific observing program aiming at imaging a large field of NGC 6791 in the Johnson U and B passbands with the LRS FOSC camera at the 3.5 m Italian Telescopio Nazionale Galileo (TNG) at La Palma. Taking advantage of its 0.275 arcsec/px scale and its wide (9.4×9.4 arcmin) field of view, this imager allowed us to carry out a suitable (16×16 arcmin) and accurate (± 0.01 mag) survey of the cluster region. Resulting CMDs, based on 330 s B and 1200 s U exposures, are shown in Fig. 2. Data have been reduced with IRAF packages CCDRED, DAOPHOT, ALLSTAR and PHOTCAL, making use of the point spread function method (Stetson 1987).

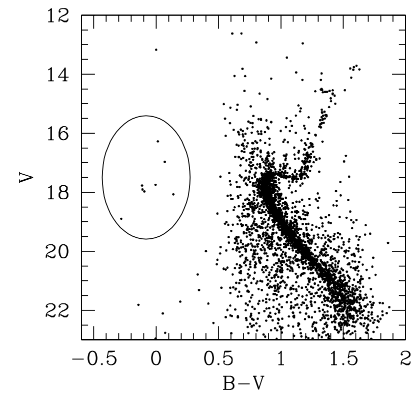

Fig. 1. The Kaluzny & Rucinski (1995) C-M diagram of NGC 6791, based on CCD photometry at the ESO 2.1 m telescope (only best photometric sample plotted here). Yong et al. (2000) provided a good fit to these data with a ([Fe/H], t) = (0.33 dex, 8 Gyr) model, predicting however a red HB morphology clumped about $(B-V) \simeq 1.3$, and clearly missing the eight hot (supposedly EHB) stars singled out in the plot.

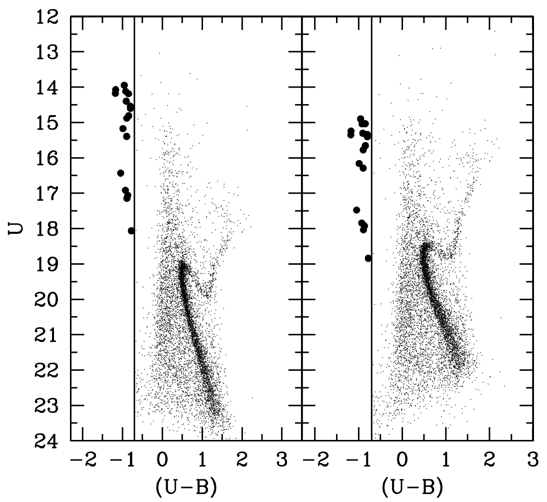

Fig. 2. Combined U vs. U–B and B vs. U–B diagrams of the field of NGC 6791 explored with TNG LRS. Big solid dots mark our 13 newly discovered UV-bright sources with U–$B < -0.7$ (vertical line) together with four objects (the clump about $U \sim 17$) including three member sdB and one sdO from the sample of faint blue stars by Kaluzny & Udalski (1992).

4. TOWARDS THE FUTURE

The analysis of Fig. 2 shows a cleanly detected sample of 13 new UV-bright objects, bluer than U–$B < -0.7$, and consistent with sdB/O stars, that sums up to the four EHB candidates (the clump of stars around $U \sim 17$) previously found in this color range by Kaluzny & Udalski (1992).*

Our current observational campaign, making use of several spectroscopic facilities at TNG and other telescopes, will provide us with both low- (~ 10 Å FWHM) and mid- (~ 6 Å) resolution spectra along the full optical range (3500–8000 Å) for these newly identified targets, assessing their cluster membership and, for those positive cases, allowing us to settle the effective temperature and surface gravity of each star by fitting the observed spectral energy distribution with the new

* Although about 2 mag brighter than the Kaluzny & Udalski (1992) candidates, our targets might still be consistent with an sdB/O classification, recalling the large spread in the bolometric correction to U and B magnitudes and the allowed temperature range compatible with the observed scatter in the U–B color (see Johnson 1966).

UVBLUE and BLUERED synthetic spectral libraries (Rodriguez-Merino et al. 2005; Bertone et al. 2003) of appropriate metallicity. Among others, such a complete sample of *bona fide* EHB stars will also provide a first reliable estimate of the lifetime and global UV energetic budget associated to the EHB evolution relying on the so-called "Fuel Consumption Theorem" of Renzini & Buzzoni (1986).

REFERENCES

Bertola F., Bressan A., Burstein D., Buson L. M., Chiosi C., di Serego Alighieri S. 1995, ApJ, 438, 680

Bertone E., Buzzoni A., Rodriguez-Merino L. H., Chavez M. 2003, in *Modelling of Stellar Atmospheres*, IAU Symp. 210, eds. N. E. Piskunov, W. W. Weiss & D. F. Gray, ASP, San Francisco

Bressan A., Chiosi C., Fagotto F. 1994, ApJS, 94, 63

Brown T. M. 2004, Ap&SS, 291, 215

Brown T. M., Ferguson H. C., Deharveng J.-M., Jedrzejewski R. I. 1998, ApJ, 508, L139

Brown T. M., Bowers C. W., Kimble R. A., Sweigart A. V., Ferguson H. C. 2000, ApJ, 532, 308

Brown T. M., Ferguson H. C., O'Connell R. W., Ohl R. G. 2002, ApJ, 568, L19

Buzzoni A. 1995, ApJS, 98, 69

Carraro G., Girardi L., Chiosi C. 1999, MNRAS, 309, 430

Code A. D. 1969, PASP, 81, 475

Dorman B., Rood R. T., O'Connell R. W. 1993, ApJ, 419, 596

Dorman B., O'Connell R. W., Rood R. T. 1995, ApJ, 442, 105

Friel E. D. 1995, ARA&A, 33, 381

Greggio L., Renzini A. 1990, ApJ, 364, 35

Johnson H. L. 1966, ARA&A, 4, 193

Kaluzny J., Rucinski S. M. 1995, A&AS, 114, 1

Kaluzny J., Udalski A. 1992, Acta Astron., 42, 29

King I. R., Bedin L. R., Piotto G., Cassisi S., Anderson J. 2005, AJ, 130, 626

Landsman W. Bohlin R. C., Neff S. G., O'Connell R. W., Roberts M. S., Smith A. M., Stecher T. P. 1998, AJ, 116, 789

Liebert J., Saffer R. A., Green E. M. 1994, ApJ, 107, 1408

O'Connell R. W. 1999, ARA&A, 37, 603

Park J.-H., Lee Y.-W. 1997, ApJ, 476, 28

Renzini A., Buzzoni A. 1986 in *Spectral Evolution of Galaxies*, eds. C. Chiosi & A. Renzini, Reidel, Dordrecht, p. 195

Rodriguez-Merino L. H., Chavez M., Bertone E., Buzzoni A. 2005, ApJ, 626, 411

Stetson P. B. 1987, PASP, 99, 191

Stetson P. B., Bruntt H., Grundahl F. 2003, PASP, 115, 413

Yong H., Demarque P., Yi S. 2000, ApJ, 539, 928

Baltic Astronomy, vol. 15, 53–60, 2006.

SPECTROSCOPIC SEARCH FOR BINARIES AMONG EHB STARS IN GLOBULAR CLUSTERS *

C. Moni Bidin[1,2], R.A. Mendez[2], S. Moehler[3], G. Piotto[1], A. Recio-Blanco[1,4] and Y. Momany[1]

[1] *Dipartimento di Astronomia, Universtitá di Padova, Vicolo dell'Osservatorio 2, 35122 Padova, Italy*

[2] *Departamento de Astronomía, Universidad de Chile, Casilla 36-D, Santiago, Chile*

[3] *Institut für Theoretische Physik und Astrophysik, Christan-Albrechts-Universität zu Kiel, D-24098 Kiel, Germany*

[4] *Observatoire de la Côte d'Azur, Dpt. Cassiopée, CNRS UMR 6202, B.P. 4229, F-06304 Nice, Cedex 04, France*

Received 2005 August 1

Abstract. We performed a spectroscopic search for binaries among hot horizontal branch stars in globular clusters. We present final results for a sample of 51 stars in NGC 6752 and preliminary results for the first 15 stars analyzed in M 80. The observed stars are distributed along all the HBs in the range $8000 \leq T_{\rm eff} \leq 32\,000$ K, and have been observed during four nights. Radial velocity variations were measured with the cross-correlation technique. We analyzed the statistical and systematic errors associated with the measurements in order to evaluate the statistical significance of the observed variations. No close binary system has been detected, neither among cooler stars nor among the sample of hot EHB stars (18 stars with $T_{\rm eff} \geq 22\,000$ K in NGC 6752). The data corrected for instrumental effects indicate that the radial velocity variations are always below the 3σ level of ~ 15 km s^{-1}. These results are in sharp contrast with those found for field hot subdwarfs, and open new questions about the formation of EHB stars in globular clusters and possibly of the field subdwarfs.

Key words: stars: horizontal branch – hot subdwarfs – binaries: spectroscopic – globular clusters: individual (NGC 6752, M 80)

1. INTRODUCTION

Although stellar evolution theory has successfully identified horizontal branch (HB) stars as post-core helium flash stars of low initial mass (Hoyle & Schwarzschild 1955; Faulkner 1966), we still lack a comprehensive understanding of their nature. There is a general agreement that the hottest HB stars (EHB) must have suffered a heavy mass-loss during their evolution, keeping only a thin envelope ($\sim 0.02\ M_\odot$), but their specific formation mechanism remains unclear. The bi-

---

* Based on observations with the ESO Very Large Telescope at Paranal Observatory, Chile (proposal ID 69.D-0682).

narity of EHB stars, as proposed by many authors (Mengel et al. 1976; Heber et al. 2002) can provide an explanation, since in a close binary system the mass-loss can be enhanced through a number of different binary evolution channels (Han et al. 2002). Binaries have been found to be very common among field subdwarf B-type stars (sdBs), considered to be the counterparts of the cluster EHB stars. Maxted et al. (2001) estimated that 69±9 % of sdB stars are close binaries with periods $P \leq 10$ days, and Han et al. (2003) by binary population synthesis techniques predicted a 76–89 % binary fraction. From the recent investigation of Morales-Rueda et al. (2003) it appears clear that close binaries with periods $P \leq 5$ days and semiamplitudes of the radial velocity variation $K \geq 50$ km s^{-1} are very common among sdBs. Nevertheless the binary scenarios, extensively investigated by Han et al. (2002), are not free from problems as shown by Lisker et al. (2005). Moreover a more recent survey of Napiwotzki et al. (2004) found a significantly lower binary fraction among the sdB sample (42 %), showing that we are still far from a full understanding of this kind of stars. With this contribution we investigate a sample of EHB stars in globular clusters, searching for evidence of the presence of close binaries among them.

2. OBSERVATIONS AND DATA REDUCTION

In the globular cluster NGC 6752 we selected 51 target stars from the photometric data of Momany et al. (2002). We chose to perform a more complete investigation distributing the sample along the entire HB, from cooler stars ($T_{\rm eff} \approx 8000$ K) to hot EHB stars ($T_{\rm eff} \geq 20\,000$ K), although our attention was focused toward the EHB sample among which we expected to find a high fraction of close binary systems. The targets were divided into three stellar fields for multiobject spectroscopy. The positions of the targets in the color-magnitude diagram of the cluster are shown in Figure 1. In Figure 2 we indicate their radial distribution with respect to the cluster center. The spectra were collected during four nights of observation (2002 June 12–15) at the VLT-UT4 telescope with the FORS2 spectrograph in MXU mode. During each night, up to two pairs of 1800 s exposures were obtained in each field with a grism 1400V+18 (0.5″ wide slits, 1.2 Å resolution), except in the third night in field A, where only one single exposure was acquired, and the first night in field C, where no observations were performed. In Table 1, the UT of the start of the pair of 1800 s exposures is shown.

Table 1. UT of the start of the exposures (hours and minutes).

Field	Night			
	12	13	14	15
A	8:43	2:44 3:56	9:34	7:47
B	5:55 6:59	5:08	8:33	8:58
C	–	8:04	6:39 7:33	6:36

Due to different positions of the slits on the mask, the spectra covered slightly different spectral ranges, but in each spectrum the Hβ line was always present, except for star 14 in field C, that has been excluded from our analysis.

The data reduction has been performed with standard MIDAS procedures, as described in detail in Moehler et al. (2004) and Moni Bidin et al. (2005). During the same observing run similar data were acquired also for 32 HB stars in M 80.

3. MEASUREMENTS

Radial velocity (RV) variations have been measured with the cross-correlation (CC) technique (Tonry & Davis 1979) with the *fxcor* IRAF task. Before coadding the single 1800 s exposures in pairs we performed a CC between them in order to verify that no significant RV variation had occurred. For every star each spectrum has been cross-correlated with all the others, performing 10 CCs for each star in fields A and B, and 6 in field C, covering different temporal intervals from one hour to 3.1 days.

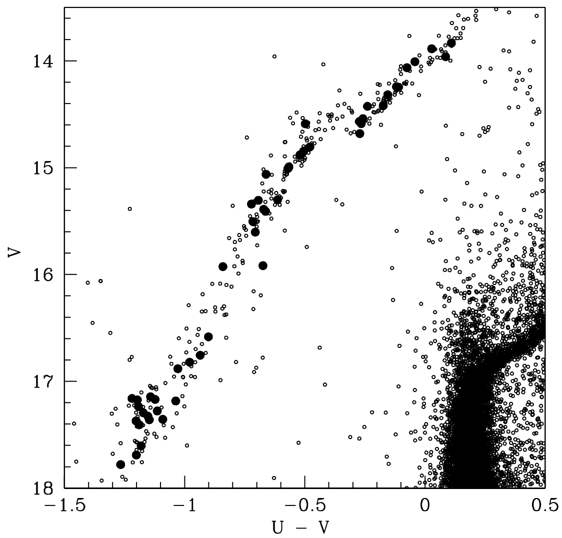

Fig. 1. Positions of the observed stars in the color-magnitude diagram of NGC 6752. Data from Momany et al. (2002).

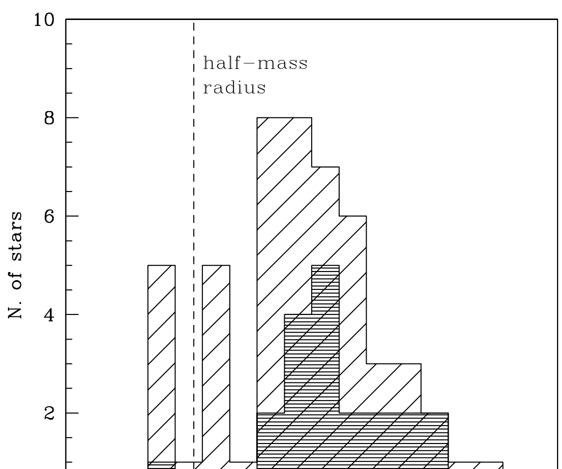

Fig. 2. Radial distribution of the observed stars. The dark shaded area indicates hot stars ($T_{\rm eff} \geq 20\,000$ K). The half-mass radius from Harris (1996) is also indicated.

Our analysis was focused on the Hβ line, cross-correlating the 4830–4890 Å spectral range. Nevertheless, all the measurements have been repeated also at other wavelengths, cross-correlating the entire spectra, with and without Hβ and Hγ when present in the spectral range. In each CC the position of the center of the cross-correlation function (CCF) has been determined with a Gaussian fit (for example, see Recio-Blanco et al. 2004 for a description of the procedure). In the measurements of hot stars it has been often impossible to cross-correlate the entire spectra without the Hβ line, and we selected spectral intervals with the strongest He lines instead, in order to minimize the noise included in the CC procedure and obtain a CCF with a clear peak. We also applied a Fourier filter of various shapes (Brault & White 1971) to the noisy spectra, obtaining always better CCFs but substantially unchanged results.

The [OI] 5577 Å sky line has been used as zero-point in order to correct the spectral shifts due to differences between lamp and star spectra.

We have been forced to correct the data for a systematic effect due to different positions of stars inside the slits in different nights. The effect was up to 10–12 $\mathrm{km\,s^{-1}}$. On the slit images (without grism), acquired just before each pair of exposures, we measured the position of the stars with respect to the center of the slit with a Gaussian fit of the stellar profile parallel to the dispersion direction. Then we translated the displacements between the frames to $\mathrm{km\,s^{-1}}$ with the instrumental relation 1 pixel = 38.2 $\mathrm{km\,s^{-1}}$ and applied them as corrections to the RV variations. A trend with Y position was evident, but with a certain scatter due to random errors, and we opted to derive the final corrections from the values obtained from the least-square solution of this relation, in order to avoid to introduce additional noise to the results.

This procedure gave corrections very similar to the RV variations measured, indicating both that the removal of the systematic effect had been successful and that the RV variations observed were due only to it.

We measured absolute RVs in order to check the cluster membership of our targets, by means of CCs with the template star HD 188112, a binary sdB star with known ephemeris (Heber et al. 2003). These RVs have undergone similar correction procedures as described before. The errors (1σ) of these measures are 6–10 $\mathrm{km\,s^{-1}}$. All the stars show an absolute RV in agreement with that of the cluster (–27.9 $\mathrm{km\,s^{-1}}$, Harris 1996) within 2σ and can be considered RV cluster members.

4. ERROR ANALYSIS

The detection of binary systems in our survey is strongly dependent on a proper estimate of the error budget. We performed an accurate analysis of all the sources of errors and estimated their values (σ). Finally, all the error sources have been combined in quadrature. The resulting errors are about 3–5 km $\mathrm{s^{-1}}$, with the exception of some measurements for hotter stars, where the low S/N sometimes increased the total error up to 7.5 km $\mathrm{s^{-1}}$. In Table 2 we summarize the contribution of each error source and the corresponding ranges (1σ). The CC error is evaluated directly from the CC theory (Tonry & Davis 1979).

Table 2. Estimates of errors.

Error	Range of values (km $\mathrm{s^{-1}}$)
σ_{CC}	0.5-2 (Hβ) 1-5 (weak lines)
σ_{wlc}	1.4-1.6
σ_{sky}	1.5
σ_{disp}	0.7-1.4
$\sigma_{\mathrm{fit+ext}}$	0.7-1.5 (cooler stars) 2.1-3.5 (hotter stars)

The wavelength calibration (wlc) error has been measured on the lamp images calibrated with the coefficients obtained in the wlc procedure, analyzing the position of nine bright lamp lines.

The errors introduced by the corrections for the sky line position, σ_{sky}, and for the displacement of the star inside the slits, σ_{disp}, have been estimated from the dispersion of the corrections around the least-square solution when plotted against the Y positions.

We identified two additional sources of errors: the choice of the "best fit" of CCF peak and the extraction of the spectra. In fact a different extraction can

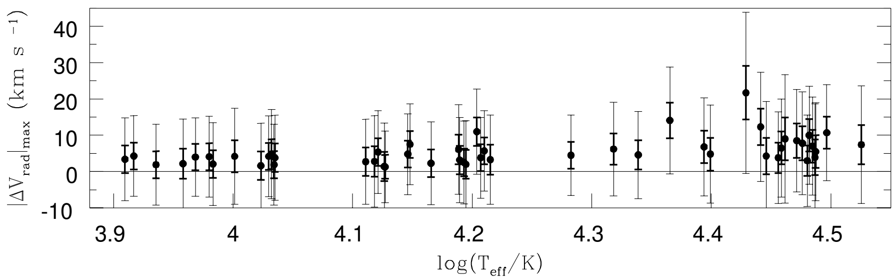

Fig. 3. Maxima of RV variations (in absolute value) measured in Hβ as a function of the temperature of the stars. The thick error bar indicates the 1σ interval, the thin one – 3σ.

cause a slightly different line profile; the CC procedure is sensitive enough to reveal it. In measurements on hot stars these have been identified as the main source of error. We evaluated them together extracting all the spectra a second time in a different manner and performing new measures in Hβ with different fits and, finally, measuring the dispersion $\sigma_{\rm fit+ext}$ of the differences between these new data and the previous ones. This error was strongly dependent on the S/N of the spectra. Then we divided the targets into two groups (stars cooler and hotter than $\sim$20 000 K).

5. RESULTS

5.1. Results from Hβ

In Figure 3 we summarize the results obtained from measurements in the Hβ wavelength range, where we obtained the most reliable data. All the RV variations are small, lower than 15 km s^{-1}, except for one star, and are never greater than the estimated 3σ interval. They are only slightly higher for hotter stars, but with larger errors due to decreasing S/N in the spectra. We therefore conclude that *none of the observed RV variations can be considered statistically significant.*

Star 15 in field A exhibited higher RV variations in the third night, and the higher datum plotted in the figure (21.7 km s^{-1}) refers to these measurements. We consider this result interesting but particularly dubious, because it was obtained in the only not-summed spectrum (a single 1800 s exposure, as mentioned before), where all the stars tended to show higher RV variations due to the increased noise, and a comparable variation is never seen in any of the other observing nights.

5.2. Results from other lines

The results from CCs involving the entire spectral range did not provide additional information, because they always repeated the results already obtained with Hβ. This is due to the sensitivity of CC technique to the stronger line, and the extreme difference in strength between Balmer and others lines in our spectra.

The results obtained with Hγ, when present in the spectra, always confirm the ones obtained in Hβ wavelength range. The differences are always lower than 10 km s^{-1}, with just a handful of exceptions in agreement with a Gaussian distribution given the evaluated σ value.

None of the variations measured with weak lines ever exceeds the evaluated

3σ value, confirming the previous conclusions. The measurements with weak metallic lines have given very good results for cooler stars, mainly in the range $11\,500 \leq T_{\rm eff} \leq 18\,000$ K due to the presence of many lines induced by radiative levitation of heavy elements (Glaspey et al. 1989; Behr 2003). In these cases the differences between the measured variations and the ones in Hβ are really small, always below 4 km s^{-1}. For hotter stars the low S/N and the lack of lines complicated the measurements, and the results are less reliable. Occasionally the difference reaches 30 km s^{-1}, but always in the sense of limiting the highest RV variations measured in Hβ and never emphasizing them. In fact, the stars, that show the highest variations in Figure 3, do not show great variation in these measurements.

5.3. Detection probability

In order to better understand our results, we calculated the probability of detecting a binary in our observations as a function of the period P. We assumed circular orbits and a mass of 0.5 $M_\odot$ for each component, in order to relate the semiamplitude of the RV variation to the period. These assumptions are representative of typical binary systems observed among field sdBs. We repeated the calculations assuming a companion of 0.1 $M_\odot$. Systems with a low-mass companion are a minority among field sdBs, but their presence is well established. Our survey is not sensitive enough for this kind of systems, except for the shortest periods, and from our results we cannot draw interesting conclusions about them. The probabilities are shown in Figure 4 (the solid line for a 0.5 $M_\odot$ companion and the dotted line – for 0.1 $M_\odot$).

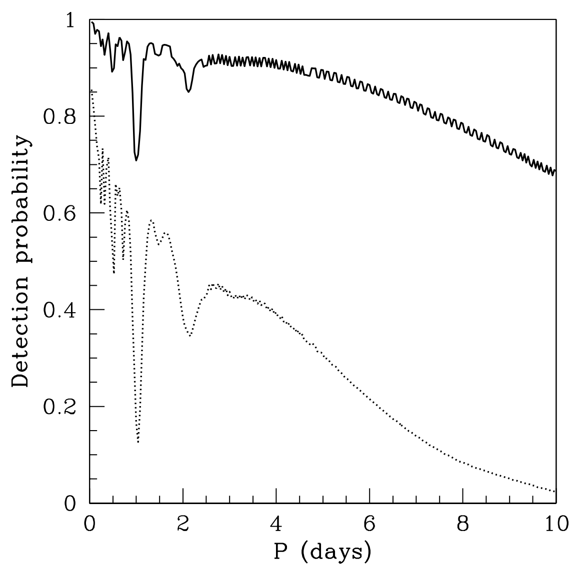

Fig. 4. Probability of detecting a binary in our observations.

5.4. Results for M 80

Since this is a work in progress we are still unable to show a plot similar to Figure 3 for the stars observed in M 80. Nevertheless we can point out that the preliminary analysis of the first 15 stars in this cluster gives the results similar to what obtained in NGC 6752. The variations are small, the highest values being around 20 km s^{-1}. Only two RV variations exceed 15 km s^{-1}, similarly to what was observed in NGC 6752. It must be emphasized that the results on M 80 are going to be less significant than in the case of NGC 6752 both because the stars are much fainter and the errors are larger, and because strong wind from north during the observing run prevented us from observing this cluster in the first two nights, so that the detection probability is reduced. We evaluated a loss of sensitivity of about 20–25 % for periods up to 5 days (compared to that in NGC 6752), which, for longer periods, drops rapidly to very low values.

6. CONCLUSIONS

The results shown in Figure 3 indicate that there is no close binary system in our sample, neither among cooler stars, nor among EHB targets. All the RV variations are within the estimated errors and are significantly lower than what expected. In the compilation of Morales-Rueda et al. (2003) for all field binary sdB stars with known periods, the RV semi-amplitudes are always greater than 30 km s^{-1}. These binary systems would be easily detectable in our survey. If the binary fraction of EHB stars in NGC 6752 were 69 %, as found by Maxted et al. (2001) in the field, we would expect that 13±2 of our 18 stars with $T_{\rm eff} \geq 22\,000$ K should be binaries. According to the period distribution found by Morales-Rueda et al. (2003) 80 % of them should have $P \leq 5$ days, and thus 9±2 binary systems should have been detected in our sample. The absence of evidence of their presence is in sharp contrast with these previous results, and can indicate a significant difference between sdB stars in and outside globular clusters.

In conclusion, most of the EHB stars in NGC 6752, and possibly in M 80, are not close binaries. These results pose a number of problems. First of all, we are forced to conclude that the dominant mechanism for the formation of these stars in globular clusters does not involve the interactions within a close binary system. Although the high close binary fraction among field sdBs indicates that binary interactions can play an important role, our results on the EHB stars in NGC 6752 indicate that there must be other mechanisms at work.

It is possible that in GCs there are different formation channels of EHB stars with respect to the main ones in the field. For example, dynamical evolution of GCs could remove the primordial binaries able to produce sdB stars, at least in the inner part of the cluster. This is an interesting possibility, which has already been proposed also to explain why the frequency of blue stragglers (BSs) in GCs is significantly smaller than the frequency of field BSs (Piotto et al. 2004), and the anticorrelation between the frequency of BSs in GC cores and the GC total mass (Davies et al. 2004). At the same time, the GC environment can favor different formation mechanisms for the EHB stars, like close encounters and collisions among stars (at least in the cluster cores), or even more complex scenarios like the ones proposed to explain the anomalous double main sequence population in Omega Centauri (Bedin et al. 2004 and Piotto et al. 2005) and in NGC 2808 (D'Antona et al. 2005). Apparently, in these two clusters, a second generation of stars could have formed from material polluted by SNe and/or intermediate mass AGB star ejecta. These stars have an enhanced He content and could explain the presence of the EHB in both clusters.

An extended survey of the presence of close binaries among cluster EHB stars, from the inner core to the outskirts of NGC 6752, and of the presence of binaries with low companions or with longer (100 days or so) periods in NGC 6752 and other clusters with EHBs, is absolutely needed in order to test the hypothesis of the environment effects on the main production channels of these stars.

We note also that Peterson et al. (2002) reported a high fraction of binaries among the same type of stars in the same cluster, but Peterson (priv. comm.) also pointed out that their sample is mainly located in the outer regions of the cluster.

In concluding this brief discussion, we note that Napiwotzki et al. (2004) suggested that the low binary fraction among field sdBs found in their survey could be due to contamination of the sample by halo and thick disk stars, absent in Maxted et al. (2001) sample since it included only bright (thin disk) stars. On average, our cluster EHB stars are expected to be older and possibly more metal-poor than the Napiwotzki et al. sample, and apparently, the fraction of binaries among them is even smaller than among thick disk-halo sdBs, suggesting a possible dependence on ages or metallicities or on a combination of these parameters.

ACKNOWLEDGMENTS. C.M.B. and R.A.M. acknowledge support by the Chilean Centro de Astrofísica FONDAP (No. 15010003). G.P. acknowledges support by MIUR, under the program PRIN03.

REFERENCES

Bedin L. R., Piotto G., Anderson J. et al. 2004, ApJ, 605, L125

Behr B. B. 2003, ApJS, 149, 67

Brault J. W., White O. R. 1971, A&A, 13, 169

D'Antona F., Bellazzini M., Caloi V. et al. 2005, ApJ, 631, 868

Davies M. B., Piotto G., De Angeli F. 2004, MNRAS, 349, 129

Faulkner J. 1966, ApJ, 144, 978

Glaspey J. W., Michaud G., Moffat A. F. J., Demers S. 1989, ApJ, 339, 926

Han Z., Podsiadlowski P., Maxted P. F. L., Marsh T. R., Ivanova N. 2002, MNRAS, 336, 449

Han Z., Podsiadlowski P., Maxted P. F. L., Marsh T. R. 2003, MNRAS, 341, 669

Harris W. E. 1996, AJ, 112, 1487

Heber U., Edelmann H., Lisker T., Napiwotzki R. 2003, A&A, 411, L477

Heber U., Moehler S., Napiwotzki R., Thejll P., Green E. M. 2002, A&A, 383, 938

Hoyle F., Schwarzschild M. 1955, ApJS, 2, 1

Lisker T., Heber U., Napiwotzki R. et al. 2005, A&A, 430, 223

Maxted P. F. L., Heber U., Marsh T. R., North R. C. 2001, MNRAS, 326, 1391

Mengel J. G., Norris J., Gross P. G. 1976, ApJ, 204, 488

Moehler S., Sweigart A. V., Landsman W. B., Hammer N. J., Dreizler S. 2004, A&A, 415, 313

Momany Y., Piotto G., Recio-Blanco A. et al. 2002, ApJ, 576, L65

Moni Bidin C., Moehler S., Piotto G. et al. 2005, A&A, submitted

Morales-Rueda L., Maxted P. F. L., Marsh T. R., North R. C., Heber U. 2003, MNRAS, 338, 752

Napiwotzki R., Karl C. A., Lisker T. et al. 2004, Ap&SS, 291, 321

Peterson R. C., Green E. M., Rood R. T., Crocker D. A., Kraft R. P. 2002, in *Omega Centauri, a Unique Window into Astrophysics*, ASP Conf. Ser., 265, 255

Piotto G., De Angeli F., King I. R. et al. 2004, ApJ, 604, L109

Piotto G., Villanova S., Bedin L. R. et al. 2005, ApJ, 621, 777

Recio-Blanco A., Piotto G., Aparicio A., Renzini A. 2004, A&A, 417, 597

Tonry J., Davis M. 1979, AJ, 84, 1511

Baltic Astronomy, vol. 15, 61–64, 2006.

NGC 6121-V46: A LOW-MASS DOUBLE DEGENERATE ELLIPSOIDAL VARIABLE IN A GLOBULAR CLUSTER

S. J. O'Toole[1], R. Napiwotzki[2], U. Heber[1], H. Drechsel[1], S. Frandsen[3], F. Grundahl[3] and H. Bruntt[4]

[1] *Remeis-Sternwarte Bamberg, Astronomisches Institut der Universität Erlangen-Nürnberg, Sternwartstrasse 7, D-96049 Bamberg, Germany*

[2] *Centre for Astrophysics Research, University of Hertfordshire, Hatfield AL10 9AB, U.K.*

[3] *Department of Physics and Astronomy, University of Aarhus, Ny Munkegade, DK-8000 Aarhus C, Denmark*

[4] *Niels Bohr Institute, Juliane Maries Vej 30, DK-2100 Copenhagen Ø, Denmark*

Received 2005 August 1

Abstract. The variable sdB known as V46 in the globular cluster M 4 has remained enigmatic since its discovery almost 10 years ago. We present here radial velocity measurements obtained from medium-resolution VLT/FORS2 spectra that show variations at twice the period of the luminosity changes. This implies that the system is an ellipsoidal variable. Unlike the other sdB binaries of this nature, the fundamental parameters of this star we derive suggest that it lies below the Zero Age Extreme Horizontal Branch. From the cluster distance and the gravity we determine the mass of V46 to be $\sim$0.19 $M_\odot$. This is too low to sustain core helium burning. From the mass function we derive a lower limit for the companion of only 0.26 $M_\odot$. We discuss the star's origin in the context of close binary evolution in the field and globular clusters.

Key words: stars: variable: general – stars: individual (NGC 6121-V46)

1. HISTORY AND MOTIVATION

It is now known that while the mass distribution of DA white dwarfs peaks at $\sim$0.6 $M_\odot$, there is also a subset of objects with masses $\leq$0.46 $M_\odot$ (Bergeron et al. 1992). Their low mass implies that they cannot ignite helium in their cores, and must have lost most of their envelope mass before reaching the tip of the red giant branch. The implication of this is that the stars must be in close binary systems, although recent results suggest that fewer than 50 % show radial velocity variations (Napiwotzki et al. 2005).

There are two kinds of known binaries containing helium-core white dwarfs (HeWDs): double degenerate systems, typically containing two low-mass white dwarfs (e.g., Nelemans & Tout 2005) and millisecond pulsar (MSP) systems. In the former case the lowest mass HeWD companion known has 0.31 $M_\odot$ (Marsh et al. 1995), while in the latter the masses are $\leq$0.2 $M_\odot$ (e.g., Callanan et al. 1998).

Recent discoveries suggest a link between HeWDs and a small subset of sdB stars. As part of a program to measure radial velocities of sdBs, Heber et al. (2003)

discovered that the apparently normal sdB HD 188112 lies below the Zero-Age Extreme Horizontal Branch (ZAEHB). The star's mass, determined from its trigonometric parallax, $T_{\rm eff}$ and $\log g$, to be only 0.24 $M_\odot$, is inconsistent with the lowest mass for the common envelope ejection model of Han et al. (2003). HD 188112 is a radial velocity variable with a minimum companion mass of 0.73 $M_\odot$, suggesting the primary is the progenitor of a helium core white dwarf, while the unseen companion is most likely a C/O white dwarf. Comparison with the evolutionary tracks of Driebe et al. (1998) supports this conclusion.

Since then, Liebert et al. (2004) have discovered another object lying below the ZAEHB. Comparison of the parameters of SDSS J123410.37-022802.9 (hereafter SDSS J1234) with the evolution tracks of Althaus et al. (2001) shows that this star has a mass in the range 0.18–0.19 $M_\odot$. Note that the mass is dependent on the evolution models adopted. A higher mass is found ($\sim$0.23 $M_\odot$) for SDSS J1234 when it is compared to the Driebe et al. tracks.

Kaluzny et al. (1997) discovered intensity variations with amplitude $\sim$1.9 % and period 1.045 h in the star now known as V46 in NGC 6121 (= M 4). The system was a puzzle from the beginning, with colors consistent with those of a cataclysmic variable, but no emission lines present in its spectrum. Mochejska et al. (2002) found that the spectrum is consistent with an sdB star. With the discovery of pulsations in sdB stars with periods of 0.75–2 hours (Green et al. 2003), it seemed possible that V46 was a member of this class. We therefore set out to clarify the object's nature.

2. IS IT AN EHB STAR?

A low resolution spectrum of V46 taken with the MMT was kindly provided by Janus Kaluzny. By means of Balmer line profile fitting we find $T_{\rm eff} = 16197 \pm 546$ K and $\log g = 5.75 \pm 0.108$; the star shows no helium lines. We used Detlev Koester's DA white dwarf grid (Finley et al. 1997) to derive these parameters. When we examine the position of V46 in the $T_{\rm eff}$ vs. $\log g$ plane (Figure 1), we find that it, like HD 188112 and SDSS J1234, lies below the ZAEHB. This means the star has not evolved via the EHB and strongly suggests that it too is the progenitor of a HeWD (similar to HD 188112).

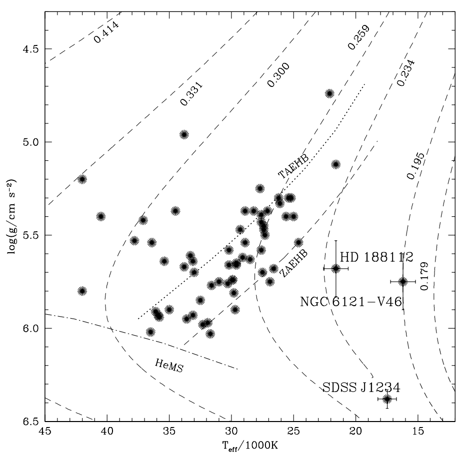

Fig. 1. Position of V46 in the $T_{\rm eff}$ vs. $\log g$ diagram.

If we consider the distance to the cluster M 4 (2.2 kpc, Rosenberg et al. 2000) and the surface gravity of V46, we find that it should have a mass of $\sim$0.19 $M_\odot$. In Figure 1 we show the post-RGB evolutionary tracks of Driebe et al. (1998) which suggest that V46 should have a mass of $\sim$0.195 $M_\odot$. This is very good agreement considering the uncertainties of the model physics, and is strong evidence that the star is a member of the cluster and not a foreground object. Using the VLT we have determined the nature of this system by measuring the radial velocity of V46.

3. THE NATURE OF NGC 6121-V46

We obtained 81 spectra with resolution ∼2100 using VLT/FORS2 with the 1400V grating in service mode. The only line visible in the spectra is Hβ, and the resulting S/N per 4 min exposure was 10–15. We measured the radial velocity of Hβ by cross correlation with a model spectrum at the temperature and gravity derived above. The velocity curve is shown at the top of Figure 2, while the power spectrum is shown at the bottom. It was calculated by fitting the curve with a range of periods using χ^2 minimization. Based on this method, we measure the period and ephemeris to be $\mathrm{HJD}(T_0) = 2453134.496797{+}0.087159{\times}E$, while the system velocity and semi-amplitude of the system are $\gamma = 31.3 \pm 1.6$ km/s and $K = 211.6 \pm 2.3$ km/s, respectively. Using this period and semi-amplitude we derive the mass function of the system to be $f(m) = 0.0855{\pm}\,0.0028\ M_\odot$. Taking the mass of the sdB to be 0.195 $M_\odot$, the minimum mass of the secondary is 0.26 $M_\odot$. We note that the period of the radial velocity variation is exactly twice that of the intensity variation, indicating that V46 is an ellipsoidal variable, similar to the previously known systems KPD 0422+5421 (Koen et al. 1998) and KPD 1930+2752 (Billéres et al. 2000; Maxted et al. 2000).

4. LIGHT CURVES

As well as a velocity curve, we have also obtained BVR light curves. These observations were made over April–June of 2001 to search for oscillations in red giants in M 4 (Bruntt 2003). They were obtained at the Danish 1.54 m at La Silla, Chile with DFOSC. We have attempted to determine the inclination angle of the system using a light curve analysis similar to that used for the sdB HS 2333+3927 (Heber et al. 2004). No eclipses have been detected. Due to the low amplitude of the ellipsoidal variations, the analysis is difficult. We kept the T_{eff} and mass of the sdB fixed at 16 200 K and 0.2 $M_\odot$, respectively, during the analysis, but could not find a unique solution. Even fixing the mass ratio arbitrarily at, e.g. $q = 3.0$, does not help. The fits from all solutions appear identical and have very similar χ^2 values. There must be a lower limit for the inclination since at some angle the deformation of the sdB will no longer be visible. To find this limit, we first set $q = 6.0$ and then decreased it in steps of 1.0. Again no unique solution could be found, meaning that unfortunately the light curves cannot place any constraints on the system. Nevertheless we can conclude that the companion must be a white dwarf, because the variations are ellipsoidal in nature and there is no sign of a reflection effect. The latter would be expected if it were a low-mass main-sequence star.

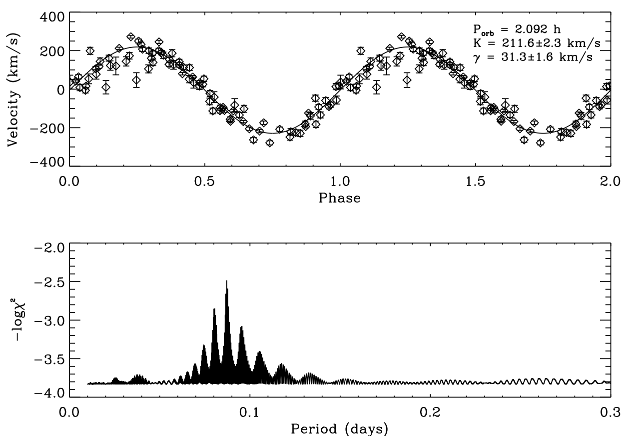

Fig. 2. Radial velocity curve and corresponding power spectrum of V46.

5. IMPLICATIONS

Despite not being able to constrain the inclination of the V46 system, we can still discuss the implications of its existence for close binary formation in globular clusters. Hansen et al. (2003) discussed low-mass HeWDs in globular clusters from a theoretical standpoint, and found that for the population of these stars in the core of NGC 6397 the companions are most likely C/O white dwarfs and not neutron stars. The likelihood of the companion of V46 being a neutron star is not high, since the inclination angle of the system would have to be $\leq 26°$, and there has been no detection at radio wavelengths of any neutron star in M 4 other than PSR B1620-26 (Lyne et al. 1988). We suggest therefore that V46's companion is either a C/O or HeWD. At the most probable inclination of 52° the mass of the companion is $\sim$0.40 $M_{\odot}$, making it an object with a helium core. We also point out that V46 lies outside the central part of M 4; more massive objects are expected to settle towards the core of a globular cluster.

REFERENCES

Althaus L. G., Serenelli A. M., Benvenuto O. G. 2001, MNRAS, 323, 471

Bergeron P., Saffer R. A., Liebert J. 1992, ApJ, 394, 228

Billéres M., Fontaine G., Brassard P. et al. 2000, ApJ, 530, 441

Bruntt H. 2003, PhD dissertation, University of Aarhus

Callanan P. J., Garnavich P. M., Koester D. 1998, MNRAS, 298, 207

Driebe T., Schönberner D., Blöcker T., Herwig F. 1998, A&A, 339, 123

Finley D. S., Koester D., Basri G. 1997, ApJ, 488, 375

Green E. M., Fontaine G., Reed M. D. et al. 2003, ApJ, 583, L31

Han Z., Podsiadlowski P., Maxted P. F. L., Marsh T. R. 2003, MNRAS, 341, 669

Hansen B. M. S., Kalogera V., Rasio F. A. 2003, ApJ, 586, 1364

Heber U., Drechsel H., Østensen R. et al. 2004, A&A, 420, 251

Heber U., Edelmann H., Lisker T., Napiwotzki R. 2003, A&A, 411, L477

Kaluzny J., Thompson I. B., Krzeminski W. 1997, AJ, 113, 2219

Koen C., Orosz J. A., Wade R. A. 1998, MNRAS, 300, 695

Liebert J., Bergeron P., Eisenstein D. et al. 2004, ApJ, 606, L147

Lyne A. G., Biggs J. D., Brinklow A., McKenna J., Ashworth M. 1988, Nature, 332, 45

Marsh T. R., Dhillon V. S., Duck S. R. 1995, MNRAS, 275, 828

Maxted P. F. L., Marsh T. R., North R. C. 2000, MNRAS, 317, L41

Mochejska B. J., Kaluzny J., Thompson I., Pych W. 2002, AJ, 124, 1486

Nelemans G., Tout C. A. 2005, MNRAS, 356, 753

Rosenberg A., Piotto G., Saviane I., Aparicio A. 2000, A&AS, 144, 5

Baltic Astronomy, vol. 15, 65–68, 2006.

DO EC 14026 STARS EXIST IN CLUSTERS?

M. D. Reed[1], D. Kilkenny[2] and D. M. Terndrup[3]

[1] *Missouri State University, Springfield, MO 65804, U.S.A.*

[2] *South African Astronomical Observatory, Cape Town, South Africa*

[3] *The Ohio State University, 140 W. 18th Avenue, Columbus, OH 43210, U.S.A.*

Received 2005 August 1

Abstract. We have began a program to search for pulsating sdB stars in open and globular clusters. Detection of pulsators in clusters would aid the understanding of their evolution, since the masses and metal content of the main-sequence progenitors would be known. Here we describe the beginning of our search during which we plan to observe about 100 sdB stars. A failure to detect any pulsators would suggest differences between sdB stars in clusters and in the field of the Milky Way (e.g., metallicity, binarity) which would need to be taken into account by any pulsation/evolution scenario.

Key words: stars: AGB and post-AGB, variable: general – clusters: individual (NGC 6791, NGC 188, NGC 6571, M 13, M 15, NGC 2808)

1. OBSERVATIONS AND ANALYSIS

To date we have observed more than 50 stars during 54 short data runs. Data were obtained for the open clusters using McDonald Observatory's 2.1 m telescope and for the globular clusters using the MDM Observatory's 2.4 m and the SAAO 1.9 m telescopes. All data were obtained using high-speed CCDs and processing was done using standard IRAF routines.

Differential light curves were produced using MOMF (Kjeldsen & Frandsen 1992). The accuracy of the photometry depended on several factors including the signal-to-noise (brightness) of the target and comparison stars, the number of available comparison stars, and of utmost importance for globular cluster fields, the seeing and how crowded the fields are compared to the resolution. A selection of some of the light curves and temporal spectra for sdB stars in NGC 6752 are provided in Figures 1 and 2. The dotted lines in Fig. 2 is the detection threshold discussed below.

Limits on time-series photometry can be a bit tricky as even noisy data can result in relatively flat temporal spectra (Howell 1992; Breger et al. 1994). To quantify the detection limits of our data, we used the 4σ approach of Breger et al. (1994). However, it is actually easier to detect pulsations than it might seem as during short data runs, the power can combine into unresolved peaks. (Likewise, unresolved pulsations can also cancel each other during a "beat.") For example, the highest amplitude mode of the known pulsator Feige 48 is about 5 mma when

Table 1. Detection limits for the target stars. Column 1 gives the star designation, column 2 the 4σ limit and column 3 indicates the percentage of (24) known pulsators that would be detectable at our threshold limit.

Target	Limit (mma)	%	Target	Limit (mma)	%	Target	Limit (mma)	%
				NGC 6791				
B3	3.9	92	B5	5.8	75	B9	4.6	92
B4	4.8	92	B6	3.0	92	B10	3.2	92
				NGC 188				
II-91	3.1	92	D702	1.9	96			
				NGC 1904				
Hill11	3.1	92	Hill34	3.1	92	Hill70	1.9	96
				NGC 2808				
6022	3.1	92	6816	1.9	96	6849	2	20
8750	3.1	92	9301	1.9	96	9863	2	20
14040	3.1	92	18899	1.9	96			
				ω Cen				
10123	3.1	92	C521	1.9	96	BC77702	4	20
D16003	3.1	92						
				NGC 6752				
S3616	3.0	92	S23768	2.2	92	S3936	2.0	96
S3422	2.5	92	S23665	2.0	96	S24268	2.0	96
S31695	3.0	92	S23407	5.0	75	S5610	4.5	92
S30963	3.2	92	S12087	7.0	58	S23975	25	8
S3008	2.8	92	S11517	3.9	92	S5719	14	25
S29988	3.0	92	S9135	3.0	92	S27622	3.8	92
S29704	2.2	92	S7935	3.0	92	S6224	3.3	92
S28234	3.5	92	S7860	4.3	92	S28073	2.0	92

resolved, but typically appears close to 8 mma in nightly runs that do not resolve the pulsations. Therefore, we examined our own observations of known sdBV stars, as well as those of the literature to estimate pulsation amplitudes of known sdBV stars from 2 hour data runs. This provides two detection limits:

(1) the 4σ limit, and

(2) a "likelihood" that we would detect pulsations. The percentage of known pulsators that would be detected at our 4σ limit from a 2 hour data run (of 24 known sdBV stars). These values are given in Table 1 and show that we are far more likely to have detected pulsations, were they occurring, than to have missed them for the majority of our targets.

2. RESULTS

Though this is a work-in-progress, we have already made significant progress and achieved some success. We have observed more than half of our goal of 100 stars, but have yet to ensure that all targets have appropriate temperatures and gravities for EC 14026-type pulsators. We have also not completed our photometry and analysis, yet are already aware that some stars will not have useful detection limits. During the 2004 January SAAO observing run, we became aware that

NGC 2808 was too faint for the seeing conditions and scampered for back-up targets. These stars were chosen on the basis of color, so should be EHB stars, but may not be sdB stars. In contrast, during our 2004 July SAAO observing run, the seeing was excellent and we obtained useful limits for nearly every target star on our list.

At this point in our analysis, we have not detected any pulsating stars, but it is too early to determine how significant our non-detection is. Yet we can state with some certainty that previously suspected open cluster pulsators B5 and D702 (Yong et al. 1998; Bailyn 1998) do not pulsate. We also examined our data for PG 1716-type pulsations. However, our observing runs were typically too short to discern, with any accuracy, whether or not such variations exist. In no case did we detect long period variations, even though the star B4 is known to vary with a period near 19 hours; far too long for us to detect. (However, for contrast we refer readers to the paper by Kilkenny et al. (2006) where a PG 1716-type pulsator *was* detected with just 2 hours of data!)

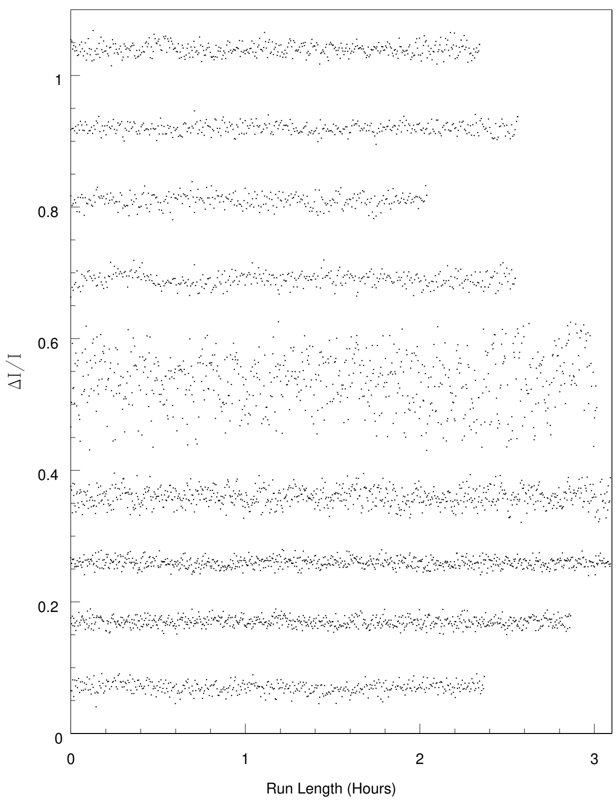

Fig. 1. Sample light curves for nine stars in NGC 6752 observed from SAAO.

Our efforts have been somewhat hampered by the fact that most of our targets are in the Southern Hemisphere, yet telescope time is very difficult to obtain there. The SAAO 1.9 m, though readily available and an excellent telescope, is a bit too small for most clusters while 4 m telescopes either lack appropriate instrumentation (CTIO) or are heavily constrained by queue schedules and allocation procedures (ESO).

ACKNOWLEDGMENTS. The Authors gratefully acknowledge Dr. Sabine Moehler for her finding charts for nearly all of our targets. This material is based upon work supported by the National Science Foundation under Grant No. 0307480. Any opinions, findings, and conclusions or recommendations expressed in this material are those of the author(s) and do not necessarily reflect the views of the National Science Foundation.

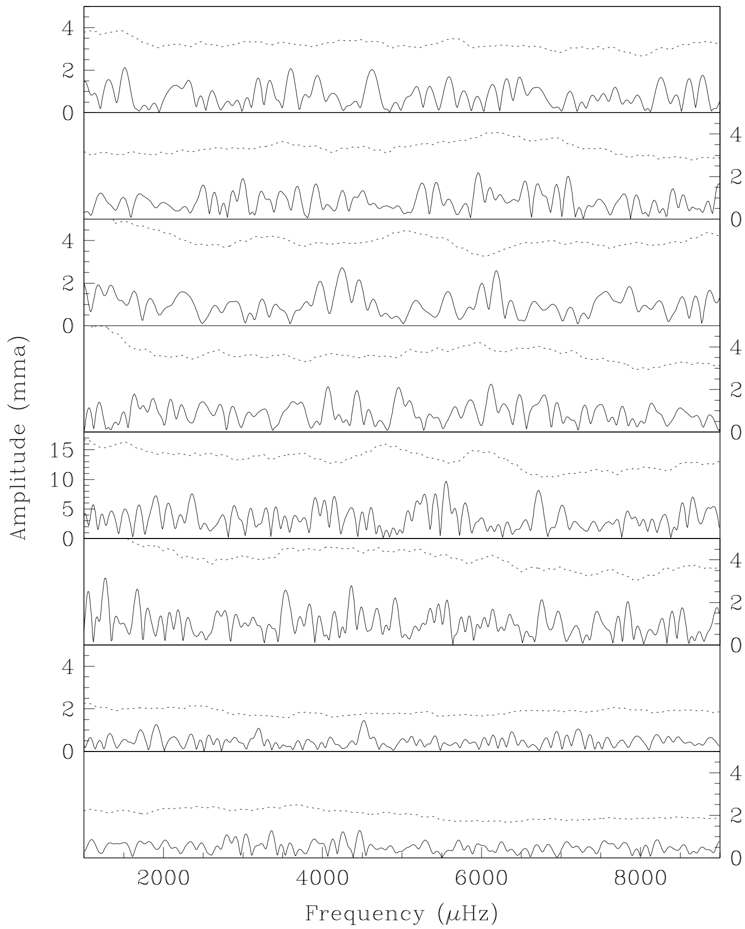

Fig. 2. Fourier transforms of the light curves in Fig. 1. Dashed lines are the 4σ detection limit.

REFERENCES

Bailyn C. D. 1998, private communication

Breger M., Ostermann W. M., Shi-Yang J. 1994, A&A, 289, 162

Howell S. B. 1992, in *Astronomical CCD Observing and Reduction Techniques*, ed. S. B. Howell, ASP Conf. Ser., 23, 105

Kilkenny D., O'Donoghue D., Reed M. D. et al. 2006, Baltic Astronomy, 15, 317 (these proceedings)

Kjeldsen H., Frandsen S. 1992, PASP, 104, 413

Yong H., Bailyn C. D., Demarque P. 1998, BAAS, 193.6403

Baltic Astronomy, vol. 15, 69–76, 2006.

HOT SUBDWARFS FROM LOW-DISPERSION SURVEYS – METHODS OF EXTRACTION AND AUTOMATIC ANALYSIS

C. Winter C. S. Jeffery A. Ahmad and D. R. Morgan
Armagh Observatory, College Hill, Armagh BT61 9DG, Northern Ireland

Received 2005 August 1

Abstract. We present our first attempts to construct an automatic system for extracting and analysing hot subdwarf spectra from a large set of unknown, low-resolution spectra. The first element in this system is a filtering technique, based on Principal Components Analysis (PCA), which is used to extract hot subdwarf candidates from the unknown data. We field-test the PCA filter on a test data set obtained from the SDSS, and initial results are illuminating. The second element in the system is an automatic pipeline for providing spectral classification and parameterisation of hot subdwarf candidates. Classification is carried out by an artificial neural network, and parameterisation by a χ^2 minimiser over a set of LTE model atmospheres. We combine both elements to extract and analyse a set of 282 hot subdwarf candidates obtained from the SDSS. As such, this work is the first step toward constructing a fully automated tool for analysing large data sets.

Key words: methods: data analysis – methods: numerical – stars: fundamental parameters – stars: subdwarfs – stars: Hertzsprung-Russell (HR) and C-M diagrams

1. INTRODUCTION

Modern digital sky surveys, such as the Sloan Digital Sky Survey (SDSS), are able to produce extremely large data sets which contain observations of millions of objects. To extract and process data of relevance to a particular line of research in a time-efficient manner requires the astronomer to employ automated methods to help sift through the soup of objects not necessarily of interest and then analyse any resulting candidate objects.

As such, we are attempting to construct an automated filtering tool to assist in locating hot subdwarf candidates from any set of low-dispersion spectra. These will then be submitted to an automated analysis pipeline from which classifications and physical parameterisations are derived.

The filtering tool is based around the multivariate statistical technique called Principal Components Analysis (PCA) which can be used to identify patterns in an N-dimensional data set. Our intention is to employ PCA as a coarse spectral classifier to distinguish between hot subdwarf-like objects, and objects/data of little interest, e.g., white dwarfs, QSOs, incomplete or low SNR exemplars. As a test, we apply the tool to a sample of spectra obtained from the SDSS.

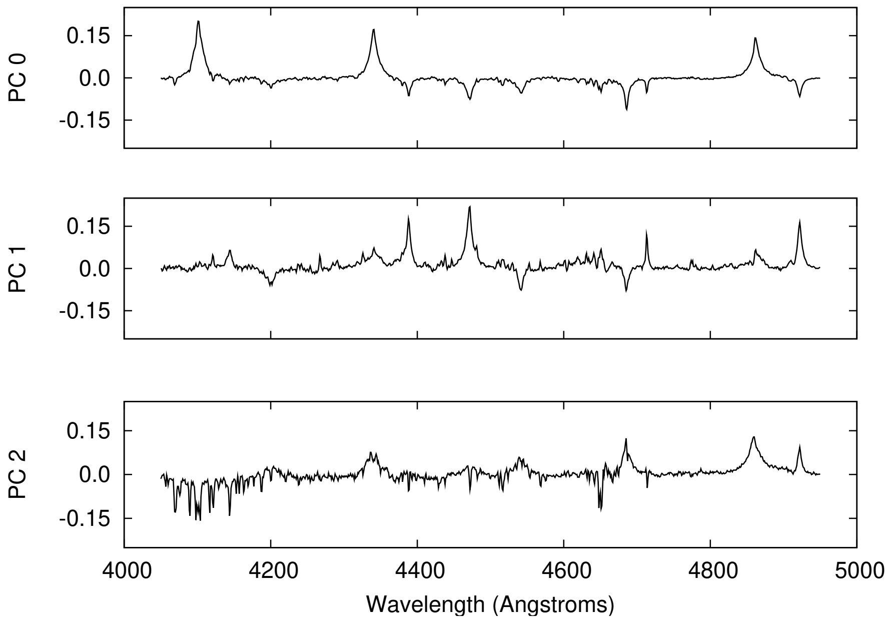

Fig. 2. First three principal components. Eigenfluxes are plotted against wavelength.

The automated analysis pipeline will allow us to gain insight into large volumes of spectra in a short amount of time. At present, the pipeline accepts a quantity of spectra, prepares them for analysis, and simultaneously feeds them to an artificial neural network (ANN), which has been trained to perform classifications using the Drilling et al. (2005) system, and a spectral optimisation toolkit which determines physical parameters by fitting each spectrum to a grid of LTE model atmospheres. Herein, we present the first application of the automated pipeline to a collection of 282 hot subdwarf candidates extracted from the SDSS with the aid of the PCA filter.

2. PRINCIPAL COMPONENTS ANALYSIS FILTER

2.1. Background

The basic idea behind PCA is to describe the variation of an N-dimensional data set in terms of a set of uncorrelated variables, each of which is a mutually-orthogonal linear combination of the original variables. Geometrically speaking, PCA is a rotation and scaling of a data set onto a new set of orthonormal vectors. The vectors (principal components) represent the directions of greatest variance in the data, and are a natural means for classifying the data set. If the first few vectors account for most of the variance in the original data, then they can be used to summarise the data with little loss of information – thus a reduction in dimensionality is achieved.

Technically, the principal components (PCs) are found by calculating the eigenvectors of the covariance matrix of an N-dimensional data set. A complete derivation of the technique can be found in, e.g., Murtagh & Heck (1987).

PCA has been applied on several occasions to the classification of astronomical spectra. Deeming (1964) applied the technique to stellar spectral classification, Connolly et al. (1995) used it to classify galaxy spectra, and Francis et al. (1992) applied it to the classification of quasar spectra. The dimensionality reduction capabilities of PCA have been used in conjunction with artificial neural networks, for example, Storrie-Lombardi et al. (1994).

2.2. Filter construction

We construct our PCA-based filter from the set of hot standards used in the classification system of Drilling et al. (2005). The spectra, which are at a resolution of 2.5 Å, were velocity corrected and resampled onto a uniform wavelength grid of 4050–4950 Å at a dispersion of 1 Å per pixel before performing the PCA. The first three of the derived PCs are shown in Figure 1. One can immediately notice that the first PC (PC 0) distinguishes between H and He lines. The second PC (PC 1) differentiates between He I and He II. This reification makes sense as it is the hydrogen and helium lines which vary most across all of the Drilling et al. (2005) spectra. Weaker lines, and uncorrelated features, such as noise, are distributed across the remaining less significant PCs. The first three derived PCs account for 69% of the variance present in the set of hot standards, and we use them to summarise the data set and to construct our filter.

If we consider the $(3 \times n)$ matrix, $\mathbf{E}$, of these eigenvectors, we can find the 3-dimensional projection vector, $\mathbf{p}$, of a spectrum projected onto the PCs by,

$$\mathbf{p} = \mathbf{x} \cdot \mathbf{E}, \tag{1}$$

where $\mathbf{x}$ is a vector of fluxes of dimension n.

Using the projection vector, we can then derive a reconstructed version of the original spectrum, $\mathbf{x_{rec}}$ by,

$$\mathbf{x_{rec}} = \sum_{k=1}^{k=3} p_k \mathbf{e}_k, \tag{2}$$

where p_k is the k^{th} element of the projection vector, $\mathbf{p}$, and $\mathbf{e}_k$ is the k^{th} eigenvector stored in matrix $\mathbf{E}$. The RMS error between $\mathbf{x}$ and $\mathbf{x_{rec}}$ can be used to differentiate between unknown stars which are most like the Drilling et al. (2005) hot standards, and those objects which we wish to discard.

2.3. Test application

We have applied the PCA filter to a test sample of ∼4600 spectra from the SDSS Data Release 3 database. Our selection criteria naively rely upon the classifications assigned automatically by the SDSS reduction pipeline. The SQL query used is as follows:

```
SELECT s.plate, s.mjd,s.fiberid
FROM BESTDR3..SpecPhotoAll as s
WHERE s.specClass = dbo.fSpecClass('STAR')
AND (s.primTarget & (dbo.fPrimTarget('TARGET_STAR_BHB')
     + dbo.fPrimTarget('TARGET_STAR_SUB_DWARF')) > 0)
AND (s.objType = 2)
```

Each spectrum was velocity corrected using the redshift as derived by the SDSS spectroscopic processing pipeline and stored in the FITS file header, and subsequently resampled onto the same wavelength grid as the Drilling et al. (2005) hot standards before being reconstructed by the PCA filter.

At present, the reconstruction filter is successful in filtering out objects with spectroscopic features that differ significantly from those of the hot subdwarfs, e.g., the white dwarfs in our test sample, or incomplete spectra.

The filter also allows a SNR threshold to be determined beyond which all samples can be discarded on the principle that they are too noisy for further analysis. Unfortunately, the filter does not readily allow the extraction of objects that are spectroscopically similar to subdwarfs but which contain small, yet important, differences that set them apart somehow. For instance, the test data sample, because it was selected based on the automatic classifications given by the SDSS (which are not very precise), contained many A- and F-type BHB stars which were clearly not subdwarfs because of very strong Balmer lines and the appearance of metal lines, and also other objects with weaker Balmer lines but containing the molecular G-band.

In calculating the reconstruction error of such spectra, the simple RMS error measure is not sensitive enough to allow small differences to influence the final error value in any meaningful way. The error calculation could be enhanced perhaps by introducing a weighting scheme, however, although these stars may have much in common with subdwarfs spectroscopically, they are very dissimilar photometrically and can be avoided easily by searching the SDSS by color.

3. AUTOMATED ANALYSIS PIPELINE

3.1. Outline

The input for our analysis pipeline comes from the PCA filter described in the previous section. The filter does still admit a number of false positives at this stage, so a manual inspection of the data is necessary.

Candidate spectra are subjected to a data preparation stage. The SDSS continuum fitting procedure does not do a great job in most cases, so we renormalise the calibrated spectra using a cubic spline fitting algorithm. The normalised spectra are then resampled onto a uniform wavelength grid of 4050–4950 Å, at a dispersion of 1 Å per pixel, ready for further analysis.

Classification is performed by an artificial neural network (ANN) which has been trained to classify onto the system defined by Drilling et al. (2005). This is an MK-like system which extends and refines the earlier work of Drilling (1996) and Jeffery et al. (1997) – it defines a spectral type (analogous to MK spectral classes), luminosity class and a helium class based on H, He I and He II line strengths. The ANN can classify onto this system with approximate errors (1σ) of ± 2 subtypes for spectral type, ± 1 subclass for luminosity class, and ± 4 subclasses for the helium class.

Physical parameters ($T_{\rm eff}$, $\log g$, $\log(n{\rm He}/n{\rm H})$) are derived from candidate spectra by χ^2 fitting to a grid of LTE model atmospheres. This is performed automatically by our spectrum optimisation toolkit, SFIT2 (Jeffery et al. 2001). To accommodate the physical diversity of the hot subdwarfs, our grid of model atmospheres coarsely covers the parameter space $T_{\rm eff}$: 15 000–50 000; $\log g$: 3–6; nHe:

0.001–0.999.

3.2. SDSS data samples

We selected two samples of spectra from the SDSS Data Release 3 database. The first sample consists of all the hot standard stars used for SDSS spectrophotometric calibrations.

Our second sample was selected based on photometric colors. Although the SDSS spectroscopic processing pipeline does make an attempt to classify stellar spectra, we learned in section 2.3 that it does not do so in any great detail, so we cannot rely upon the SDSS classifications to accurately extract a complete sample of subdwarf candidates from the database. Our selection criteria are summarised in the following SQL query:

```
SELECT s.fiberID,s.mjd,s.plate
FROM BESTDR3..SpecPhotoAll as s
WHERE s.psfMag_u < 21
AND (s.psfMag_u - s.psfMag_g) < 0.7
AND (s.psfMag_g - s.psfMag_r) < -0.1
AND s.specClass <> dbo.fSpecClass( QSO )
```

After passing all the retrieved spectra through our PCA filter, manually extracting any false positives and removing samples occurring in both data sets, we obtained a final sample of 282 hot subdwarf candidates. A summary of data set statistics is given in Table 1.

Table 1. With the combination of our PCA filter and visual selection, we were able to extract 282 unique subdwarf candidates from a total of 8171 spectra retrieved from the SDSS.

Data set	Spectra retrieved	Candidates extracted
Hot standards	1417	152
Color-color	6754	249
Total	8171	401 (282 Unqiue)

3.3. Results

Classification and parameterisation results for the 282 SDSS spectra are presented in Figure 2. The analogues between the classification parameters and physical parameters can be clearly seen by comparing the left-hand plots with the right-hand plots in Figure 2.

We note the patterns visible in the $\log g$ vs. $T_{\rm eff}$ plot: the gap at approximately $T_{\rm eff} \approx 20,000$K, $\log g \approx 4.5$; and the line extending leftwards at $\log g \approx 5.0$. We are unsure as to their nature, but the work of Green et al. (2006) discovered similar patterns from an analysis of an independent set of subdwarf stars.

An example of the model atmosphere fits and corresponding ANN classification of four stars from the sample are presented in Figure 3.

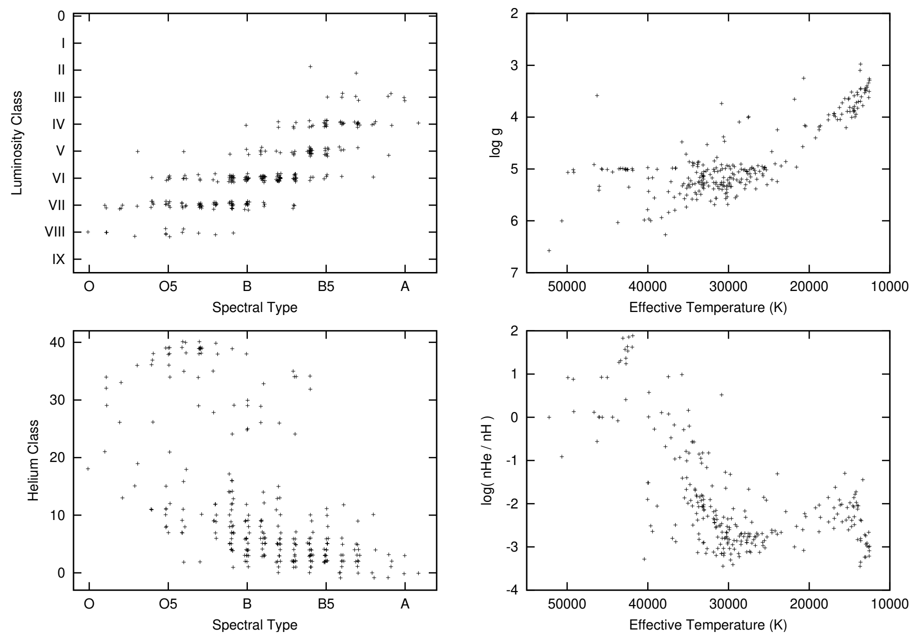

Fig. 2. Results of classifying and parameterising the 282 hot subdwarf candidates extracted from the SDSS. Classifications are presented in the two left-hand plots, with parameterisations presented in the two right-hand plots. The analogues between classification parameters and physical parameters is clearly evident.

4. FUTURE DIRECTIONS

The automatic filtering and analysis pipeline presented here is a part of what will be a more extensive system for automatic spectral analysis (see Jeffery 2003).

Given the nature of the hot subdwarfs, our use of LTE model atmospheres represents a problem for the analysis of very hot stars wherein NLTE effects become more apparent. However, our analysis pipeline can be easily extended to incorporate third-party model atmosphere codes that will allow us to address this issue in future work. We have used this study to help us refine our analysis pipeline and uncover the main hazards in dealing with large quantities of data. As we work to further improve the system, we must also tackle a number of issues, such as:

• **Data management.** Keeping track of different data sets, selection criteria, extracted candidates, their classifications and parameterisations, and maintaining general order when working with large quantities of spectra is an important task. Doing it manually is time-consuming, prone to user-forgetfulness, and can result in unfortunate industrial accidents (`rm -fr *`)[1].

• **Visualisation and interaction.** Analysing large data sets presents the problem of how to visualise thousands of spectra in a meaningful way. Also, when results have been obtained, the user must be able to produce plots and interact

[1] This is the Unix shell incantation which wipes clean the files in a user's current working directory and all its sub-directories.

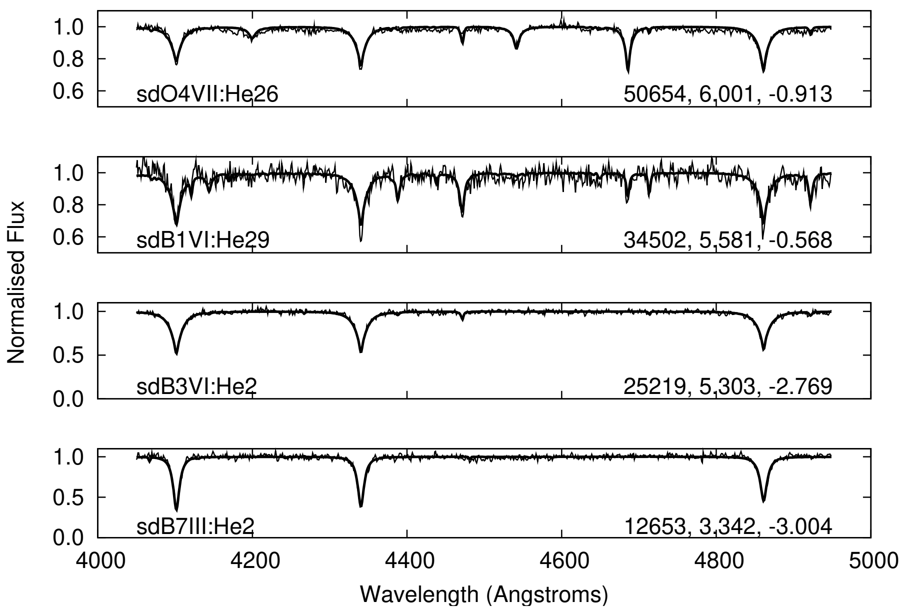

Fig. 3. A selection of stars from the set of 282 subdwarf candidates. The bottom-left of each plot details that star's spectral type as determined by the ANN, and the derived physical parameters are given at the bottom-right ($T_{\rm eff}$, $\log g$, $\log(n{\rm He}/n{\rm H})$). The thicker line in each plot is the best-fit model determined by SFIT2.

with them such that objects of interest can be displayed, allowing the data to be explored and connections to be made.

ACKNOWLEDGEMENTS. This work was carried out as part of the CosmoGrid project, funded under the Programme for Research in Third Level Institutions (PRTLI) administered by the Irish Higher Education Authority under the National Development Plan and with partial support from the European Regional Development Fund.

REFERENCES

Connolly A. J., Szalay A. S., Bershady M. A., Kinney A. L., Calzetti D. 1995, AJ, 110, 1071

Deeming T. J. 1964, MNRAS, 127, 493

Drilling J. S. 1996, in *Hydrogen Deficient Stars*, eds. C. S. Jeffery & U. Heber, ASP Conf. Ser., 96, 461

Drilling J. S., Jeffery C. S., Moehler S., Heber U., Napiwotzki R. 2005, in preparation

Francis P. J., Hewett P. C., Foltz C. B., Chaffee F. H. 1992, ApJ, 398, 476

Green E. M., Fontaine G., Hyde E. A., Charpinet S., Chayer P. 2006, Baltic

Astronomy, 15, 167

Jeffery C. S. 2003, in *Stellar Atmosphere Modeling*, eds. I. Hubeny, D. Mihalas & K. Werner, ASP Conf. Ser., 288, 137

Jeffery C. S., Drilling J. S., Harrison P. M., Heber U., Moehler S. 1997, A&AS, 125, 501

Jeffery C. S., Woolf V. M., Pollacco D. L. 2001, A&A, 376, 497

Murtagh F., Heck A., 1987, *Multivariate Data Analysis*, Reidel, Dordrecht

Storrie-Lombardi M. C., Irwin M. J., von Hippel T., Storrie-Lombardi L. J. 1994, Vistas in Astronomy, 38, 331

Baltic Astronomy, vol. 15, 77–80, 2006.

A SPECTROSCOPIC SEARCH FOR NEW SDB STARS FROM THE GALEX SURVEY

J. Rhee[1,2], M. Seibert[1], R. H. Østensen[3], S. K. Yi[4], S.-C. Rey[5], R. M. Rich[6], L. Bianchi[7] and Y.-W. Lee[2]

[1] *Space Astrophysics Laboratory, California Institute of Technology, MC 405-47, 1200 East California Boulevard, Pasadena, CA 91125, U.S.A.*

[2] *Center for Space Astrophysics, Yonsei University, Seoul 120-749, S. Korea*

[3] *Isaac Newton Group, E-37800 Santa Cruz de La Palma, Canary Islands, Spain*

[4] *Department of Physics, University of Oxford, Keble Road, Oxford OX1 3RH, U.K.*

[5] *Department of Astronomy and Space Sciences, Chungnam National University, Daejeon 305-764, S. Korea*

[6] *Department of Physics and Astronomy, University of California at Los Angeles, Los Angeles, CA 90095, U.S.A.*

[7] *Department of Physics and Astronomy, Johns Hopkins University, Baltimore, MD 21218, U.S.A.*

Received 2005 August 1

Abstract. We have recently initiated a systematic search for the UV-bright, subdwarf B (sdB) stars in the Milky Way. The sdB stars are core He-burning stars with very thin H envelopes and are known to be immediate progenitors of white dwarfs, but their formation mechanism is still enigmatic. For instance, it is not clear whether such objects are born as single stars or can form only in binary systems. The number ratio of sdB stars in each Galactic stellar population (i.e., thin disk, thick disk and halo) may give a clue to which of the suggested formation mechanisms dominates: the binary scenario or the RGB-peel-off scheme. This approach was hampered by the lack of identified sdB stars belonging to the thin disk and halo. Thus, it is of primary importance to find new sdB stars that are faint (halo) and lie at lower Galactic latitudes (thin disk). In this contribution, we will describe the motivation and plan for our spectroscopic survey and preliminary results based on pilot observations for 34 sdB star candidates from the GALEX All-sky Imaging Survey.

Key words: stars: early-type – stars: subdwarfs – surveys

1. INTRODUCTION

The UV bright, hot subdwarf B (sdB) stars are considered to be core He-burning stars of 0.5 $M_\odot$ with very thin H envelopes of $M_{\rm env} \leq 0.02 M_\odot$ (Heber 1986). In the Galactic field, they are characterized by H-dominated atmospheres with $T_{\rm eff} \approx 24\,000$–$30\,000$ K and $\log g > 5$. Their counterparts in globular clusters are generally recognized to be extended horizontal-branch (EHB) stars found as the faint and blue tail of the horizontal-branch (HB) in clusters such as NGC 6752 and M 13. These observations suggest that the UV-bright stars might be populous enough to account for much of the UV uptrun phenomenon observed in elliptical galaxies and spiral galaxy bulges (Greggio & Renzini 1990; O'Connell 1999; Yi et al. 1999). The sdB stars are known to be immediate progenitors of low mass white dwarfs (WDs), although they consist of only a small fraction of whole sample of WD progenitors (Saffer et al. 1994). In their past, sdB stars must have experienced a core He flash and substantial mass-loss during or after the red giant branch (RGB) phase. But, it is still a mystery how the mass-loss mechanism in the sdB star's progenitor manages to remove all but a tiny fraction of the H envelope exactly at the same time when the He core has attained the canonical sdB mass of 0.5 $M_\odot$ required for the He flash. This project aims to study the sdB population in the Galaxy, which may shed light on their still enigmatic formation process.

2. WHY LOOK FOR "NEW" SDB STARS?

Major formation channels of sdB stars can be divided into two scenarios: (1) single sdB stars are created from the enhancement of stellar wind near the RGB tip which strips off the H envelope (D'Cruz et al. 1996), and (2) sdB stars are formed from close binary evolution with strong mass transfer by a companion (Mengel et al. 1976). Previous observational results are not in contradiction with either scenario (Maxted et al. 2001; Altmann et al. 2004). The RGB-peel-off models predict a depletion of the HB stars in the middle temperature range (HBA stars) as metallicity increases, while stars at the hot and cold ends of HB (sdB and Red HB stars) should be abundant at all metallicities. Thus, as proposed by Altmann et al. (2004), the number ratio of sdB stars in each stellar population may provide a clue to answer which formation mechanism can be dominating. If the binary scenario is the most significant process, the number ratio of sdB stars in the thin disk, thick disk and halo would be similar to that of other evolved, low-mass stars. In the RGB-peel-off scheme, sdB stars would be more dominant over HBA stars in the thin disk. Unlike the known case of HBA stars (e.g., Altmann & de Boer 2000), this approach was hampered by the lack of identified sdB stars belonging to the thin disk and halo. Therefore, it is particularly important to increase the number of identified sdB stars with faint magnitudes (halo) and at lower Galactic latitudes (thin disk), and GALEX can provide useful targets for it.

It has lately been confirmed that large He abundance variations (ΔY) among stars can not only naturally reproduce the EHB stars in ω Cen, but can also explain the large spread of FUV magnitude for the EHB stars in NGC 2808 (Lee et al. 2005). They have suggested He abundance being a third parameter which influences HB morphology of such clusters, other than metallicity and age. Spectroscopic distances of these field sdB stars will be derived from stellar radii and angular diameters: the former is based on the surface gravity measured from the spectra and a canonical mass of 0.5 $M_\odot$, and the latter is obtained from comparing model atmosphere flux with dereddened NUV photometry. We then expect to be able to determine absolute $M_{\rm FUV}$ of sdB stars at an accuracy of 0.2 magnitude owing to the spectroscopic distances and GALEX FUV photometry, and thus reasonable ΔY among the sdB stars by the comparison of, if any, observed $M_{\rm FUV}$ spread and the predictions derived from isochrones. This would permit us to systematically obtain ΔY of sdB stars as a function of stellar population in order to study the global third parameter effect of the Galaxy.

It has been known that sdO stars have a larger scale height ($\geq$ 1.0 kpc, Thejll et al. 1994) than sdB stars ($\sim$ 0.5 kpc, Villeneuve et al. 1995), which is inconsistent

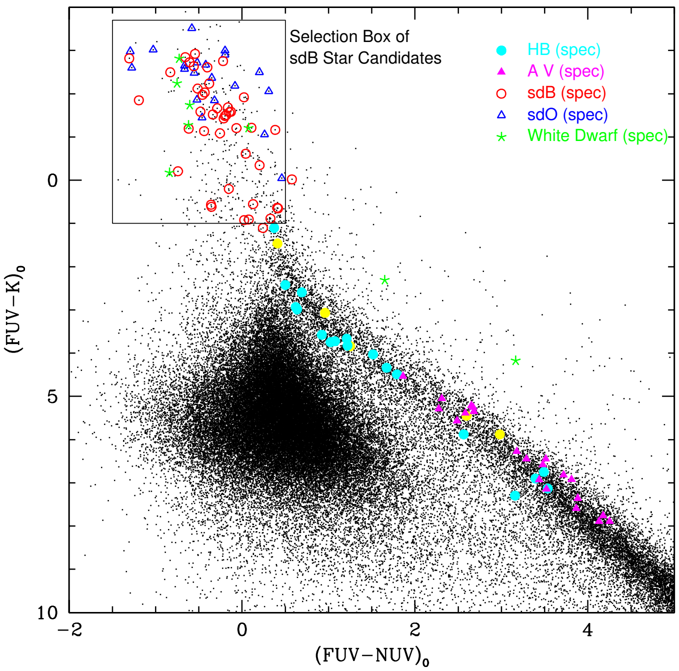

Fig. 1. GALEX AIS objects from about 1000 fields in GR1, also matched in 2MASS. Spectroscopically known sdB/O, WD, HB and A V stars are marked by different symbols. The sdB and sdO stars are clearly separated.

with an evolutionary connection between sdB and sdO stars. But, a larger scale height of 0.9 kpc has recently been obtained including "fainter" (but still $B \leq 16$) sdB stars (Altmann et al. 2004). This implies that a correct scale height can only be obtained with a sample without limiting magnitude bias.

3. CANDIDATE SELECTION

The public GALEX Release (GR1) of All-sky Imaging Survey (AIS) data was made in 2004 December. We performed cross-matching of the GALEX and 2MASS catalogs for some 3000 AIS fields (∼3500 deg^2). As seen in Figure 1, two-color diagram efficiently separates sdB/O stars because the FUV–NUV color provides relatively long temperature baseline (spectral type) for hot stars, while the FUV–K_S color is useful for classification between stellar and non-stellar objects. Our empirical comparison with spectroscopically known sdB/O stars agrees well with the above expectation. It should be pointed out that replacing 2MASS K_S with SDSS i or USNO-B I gives a similar result, so our sdB candidate stars should reach apparent magnitude NUV ≈ 20 ($B \approx 20$), four magnitudes fainter than for the Palomar Green survey (Green et al. 1986) which was one of the most extensive surveys for sdB star in the past. Using this method, we have selected a sample of some 1000 sdB star candidates over a range of depths and sky-coverages.

4. OBSERVATIONS, RESULTS AND PLANS

We have performed pilot spectroscopic observations for 34 sdB star candidates with the KPNO 2.1 m telescope and GoldCam, McDonald 2.7 m telescope and LCS and Lick 3.0 m telescope and KAST between 2004 June and 2005 May. Based on the visual inspection of spectra and measurements of $D_{0.2}$ (average width of Hγ and Hδ lines at 20% below continuum) and R_c (average depth of Hγ and Hδ lines) employed in Beers et al. (1992), the medium-resolution (1–3 Å) spectroscopy has revealed that the sample consists of 14 sdB, 5 narrow-lined B, 8 WD, 4 HBB with He lines and 3 normal B stars. Based on the preliminary detection rate of sdB stars (14/34) and the number of our sdB star candidates ($N \geq 1000$), we expect to "newly" confirm more than 400 *bona fide* sdB stars in the halo and thin disk as well as in the thick disk. In the future, more sophisticated methods will be employed to determine stellar parameters (log g, $T_{\rm eff}$, and He abundance) accurately. Using observing time awarded at the CTIO 4.0 m, KPNO 2.1 m and Lick 3.0 m telescopes, we plan to complete a spectroscopic survey of some 1000 sdB star candidates by early 2006. Radial velocities determined from our spectroscopy, combined with proper motions from astrometric surveys such as UCAC2 (Zacharias et al. 2004), USNO-B (Monet et al. 2003) and future space missions (Gaia and SIM), will provide us with full space motions and thus allow us to assign population membership for the sdB stars. Indeed, this huge data set of GALEX sdB stars, which reach the entire UV visible Milky Way, will eventually help us broaden our understanding about their formation/evolution mechanism and Galactic structure.

ACKNOWLEDGMENTS. We are grateful to the referee, Sabine Moehler, for her careful review of the paper and a number of thoughtful suggestions. We gratefully acknowledge support for this work from NASA grant GALEX GI 04-0000-0096. J. R. and Y.-W. L. appreciate partial support by the Korean Ministry of Science and Technology through the Creative Research Initiative Program.

REFERENCES

Altmann M., de Boer K. S. 2000, A&A, 353, 135
Altmann M., Edelmann H., de Boer K. S. 2004, A&A, 414, 181
Beers T. C., Doinidis S. P., Griffin K. E., Preston G. W., Shectman S. A. 1992, AJ, 103, 267
D'Cruz N. L., Dorman B., Rood R. T., O'Connell R. W. 1996, ApJ, 466, 359
Green R. F., Schmidt M., Liebert J. 1986, ApJS, 61, 305
Greggio L., Renzini A. 1990, ApJ, 364, 35
Heber U. 1986, A&A, 155, 33
Lee Y.-W., Joo S.-J, Han S.-I. et al. 2005, ApJ, 621, L57
Maxted P. F. L., Heber U., Marsh T. R., North R. C. 2001, MNRAS, 326, 1391
Mengel J. G., Norris J., Gross P. G. 1976, ApJ, 204, 488
Monet D. G., Levine S. E., Canzian B. et al. 2003, AJ, 125, 984
O'Connell R. W. 1999, ARA&A, 37, 603
Saffer R. A., Bergeron P., Koester D., Liebert J. 1994, ApJ, 432, 351
Thejll P., Bauer F., Saffer R. et al. 1994, ApJ, 433, 819
Villeneuve B., Wesemael F., Fontaine G., Carignan C., Green R. F. 1995, ApJ, 446, 646
Yi S., Lee Y.-W., Woo J.-H. et al. 1999, ApJ, 513, 128
Zacharias N., Urban S. E., Zacharias M. I. et al. 2004, AJ, 127, 3043

Baltic Astronomy, vol. 15, 81–84, 2006.

SEARCHING FOR THE "MISSING" PG HOT SUBDWARFS IN SDSS AND GALEX DATA

R. A. Wade[1] M. A. Stark[1] R. F. Green[2] and P. R. Durrell[3]

[1] *Department of Astronomy & Astrophysics, Pennsylvania State University, 525 Davey Lab., University Park, PA 16802, U.S.A.*

[2] *NOAO, P.O. Box 26732, Tucson, AZ 85726-6732, U.S.A.*

[3] *Department of Physics and Astronomy, Youngstown State University, Youngstown, OH 44555-2001, U.S.A.*

Received 2005 July 28

Abstract. Many EHB stars have been found in short-period binaries, where the companions in these post-common envelope systems are either white dwarfs or dM stars; these systems are catalogued as hot subdwarfs because the subdwarf is the more luminous component. Hypothesized Roche-lobe overflow systems (with more massive companions) may largely be uncatalogued, since the G band or Ca II K line from the companion may have caused them to be overlooked or discarded. In particular, many candidate objects were excluded from the PG catalog because of such spectroscopic indicators. Could these rejects include large numbers of "missing" hot subdwarfs? We have examined 2MASS, SDSS and GALEX archival data for large subsets of these rejected stars and conclude that only a handful (about 3%) show indications of binarity; most are consistent with (single) metal-poor F stars, as was originally supposed.

Key words: binaries: close – stars: horizontal-branch – ultraviolet: stars

1. HYPOTHETICAL "MISSING sdB" STARS

Binary population synthesis (BPS) models suggest that many core-helium burning, thin hydrogen envelope objects ("sdB stars") are not yet discovered, hidden in binary systems with luminous (non-degenerate) relatively cool companions. The existing catalogs of sdB stars would therefore be significantly biased, and a clear picture of the true situation regarding formation and current population of sdB stars is lacking. It is desirable to learn whether these proposed hidden populations of sdB stars actually exist.

It has been suggested (Han et al. 2002, 2003) that the stars that were rejected from the Palomar-Green (PG: Green, Schmidt & Liebert 1986, GSL86) survey for ultraviolet-excess (UVX) objects are a potential rich source for some types of these. During the PG survey, candidate UVX objects were those with (transformed) $U-B < -0.46$. Because of the large errors in $U-B$, $\sigma \approx 0.38$, the color selection was supplemented by classification spectroscopy, for more accurate temperature information. Many candidate UVX targets were indeed excluded from the final

PG catalog, because their spectra showed the Ca II K line (or the G band) in absorption. These rejected K-line stars were inferred to be metal-poor subdwarf F or G stars that crept into the candidate list owing to a combination of low metal-line blanketing and photometric errors.

In the alternative BPS view, these "PG-rejects" could be binaries containing sdB or sdO stars. The cool star would contribute a K line and make the blended U–B color marginal for the PG color criterion, giving a result similar to a metal-poor subdwarf. In this interpretation, therefore, the PG-rejects actually belong in the PG catalog, and moreover would constitute important evidence in favor of certain binary formation channels for sdBs.

2. THE SAMPLE OF REJECTED (K-LINE) STARS

Here we use broad-band photometry over extended wavelength ranges to assess two large subsamples from the list of PG rejects. This allows the spectral energy distribution of a composite hot+cool system to be distinguished from that of a single star. From the master catalog of 1125 PG-rejects (RW & RFG, in preparation), we found 291 stars that are present in both the Two-Micron All-Sky Survey (2MASS) Point Source Catalog and the Sloan Digital Sky Survey (SDSS) DR2 survey region, and we identified 103 stars that have GALEX observations accessible in the first Data Release. These samples are almost completely non-overlapping.

3. THE SDSS/2MASS DATASET: COLOR-COLOR DIAGRAMS

Of the 291 K-line stars that overlap 2MASS/SDSS, we consider here the 173 stars with Sloan r magnitudes in the range 14.00 to 16.00 (median $r = 14.86$) that have non-flagged (unsaturated) magnitudes in at least 4 of the 5 passbands of the SDSS (*ugriz*) photometric system (136 have all 5 optical magnitudes). All of these 173 stars have detections in the 2MASS J, H and K_s bands.

We plotted the 173 K-line stars in both g–r vs. u–g and r–K_s vs. g–r diagrams, along with 199 PG stars that have been classified as hot subdwarfs. We compared these with loci for the Population I main sequence, metal-poor main sequence and metal-poor giants (representing horizontal branch stars). We also considered three sequences of composite (binary) models. These combine the light from a hot subdwarf star ($T_{\rm eff} = 25\,000$ K, $30\,000$ K and $35\,000$ K; M_V derived from the zero-age EHB calculations of Caloi 1972) with the light from a cool main-sequence (MS) companion. These sequences emerge from the hot end of the stellar locus (faintest, coolest companions at this end), loop away from the single-star locus, and then loop back to meet the stellar locus at a (single-star) $T_{\rm eff} \approx 10\,000$ K. At this end, the 'cool' (A or F star) companion dominates.

In these diagrams, the recognized PG hot subdwarfs and the K-line PG-rejects are very different groups of stars. In this sense, the spectroscopy carried out by GSL86 succeeded in improving on the photographic U–B color selection. Some catalogued PG hot subdwarfs clearly are composite objects (Stark & Wade 2003; Reed & Stiening 2004). Most PG-reject stars, however, are consistent with being single stars, just as they were interpreted to be by GSL86. Except for a few outliers, they are not EHB+MS binary systems.

4. FITTING THE PG-REJECT STARS AS SINGLE STARS

We fitted the observed magnitudes for the 173 stars with model magnitudes, derived from the synthetic photometry done by the Padova group (Girardi et al. 2002, 2004). We considered all Padova models with $T_{\rm eff}$ in the range 4000–50 000 K, $4.0 < \log g < 5.0$ and metallicities between solar and [M/H] $= -2.5$.

For each of the 173 stars, we scaled each model in brightness to find the best fit. We chose as the best overall model, the one that gave the smallest reduced chi-square statistic, χ^2_ν. Seven outliers have either large χ^2_ν or unusual $T_{\rm eff}$ or $\log g$. All of the remaining 166 PG-rejects can be fitted as single stars with $T_{\rm eff}$ in the range 5000–7100 K. The χ^2_ν values for these 166 non-outliers are acceptably small, given our present understanding of the SDSS error estimates, our neglect of interstellar reddening, etc. Most of these stars (136 of 166) are preferably fitted with low-metallicity models, [M/H] $= -1.0$ or below, consistent with the GSL86 interpretation that these are metal-poor F and G subdwarfs.

Two of the outliers have SDSS spectra. They show Mg Ib, Na D and Ca II infrared triplet absorption, but the continua are blue. Both stars lie among the composite models in the color-color diagrams. A plausible model for the first is a 30 000–35 000 K hot subdwarf plus a $T_{\rm eff} \approx 6000$ K MS star. A plausible model for the second outlier is a $\sim 30\,000$ K hot subdwarf plus a $T_{\rm eff} \sim 7500$ K MS star. The other outliers lie either close to the hot single-star locus or the sequences of composite models; one may be a blue horizontal branch star.

5. THE GALEX DATASET

The GALEX photometry is in two bands, far- and near-ultraviolet (F and N), with $\lambda_{\rm eff} = 1528$ Å and 2271 Å. Figure 1 is a two-color diagram, with models of single and composite stars shown (synthetic photometry from Kurucz models). At the hot (upper left) end we show the observed colors of six known EHB stars (three of these are in binary systems, based on their 2MASS colors). We also found GALEX observations for a number of well-observed ($V \sim 9$) metal-poor single stars near $T_{\rm eff} = 6000$ K, and thus determined that the locus for such stars actually lies higher than the model line shows, by about 1–2 mag in F–N.

Of the 103 PG-rejects that were observed by GALEX, only twelve were detected in both FUV and NUV bands. We derived limits on F–N for the rest (assuming $F > F_{\rm lim} = 19.9$). We plot 24 limits in Figure 1; the other 67 systems have similar locations in the figure and are omitted to reduce confusion. Only three of the 103 stars show far-UV flux consistent with the presence of a hot star; the rest are consistent, given the errors and limits, with single cool stars. All of the "hot" detections have red J–K_s colors from 2MASS, so these stars are composite. (One of the three "hot" cases, at N–$V \approx 5.1$ and F–$N = 3.0$ is not an EHB+MS binary but can be modeled as a $T_{\rm eff} \approx 30$ kK WD+dG system.)

6. SUMMARY

A few objects ($\sim 3\%$) in our sample of PG-reject stars may plausibly be binary systems that include a hot subdwarf star as a member. The vast majority of the PG-reject stars, however, are sufficiently modeled as single stars, consistent with their being the metal-poor sdF and sdG contaminants that GSL86 were guarding against. The color-color sequences of sdB + cool (MS) star binaries are well separated from the observed colors of the PG-reject stars in both the optical vs.infrared plane and the optical vs. ultraviolet plane. There is no compelling evidence for large numbers of additional hot subdwarf stars hiding in binaries that were rejected from the PG catalog.

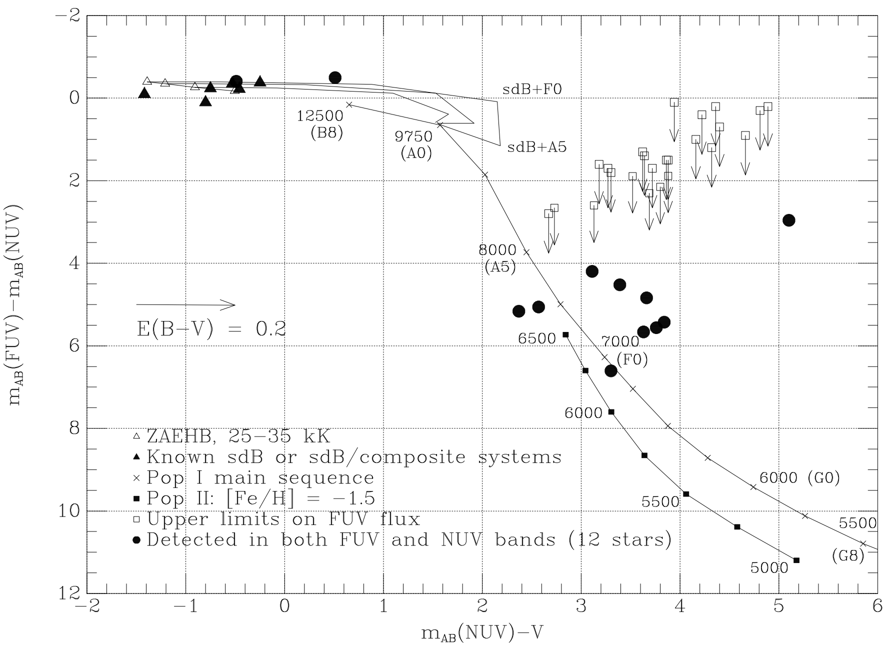

Fig. 1. GALEX and visible two-color diagram.

ACKNOWLEDGMENTS. We made use of SDSS Data Release 2, the 2MASS, GALEX Data Release 1, the USNO-A2 catalog, and SIMBAD. Supported in part by Sigma Xi, NASA grants NAG5-9586 and NGT5-50399, and the Pennsylvania Space Grant Consortium.

REFERENCES

Caloi V. 1972, A&A, 20, 357

Girardi L. et al. 2002, A&A, 391, 195

Girardi L, Grebel E. K., Odenkirchen M., Chiosi C. 2004, A&A, 422, 205

Green R. F., Schmidt M., Liebert J. 1986, ApJS, 61, 305 (GSL86)

Han Z., Podsiadlowski Ph., Maxted P. F. L., Marsh T. R., Ivanova N. 2002, MNRAS, 336, 448

Han Z., Podsiadlowski Ph., Maxted P. F. L., Marsh T. R. 2004, MNRAS, 341, 669

Reed M. D., Stiening R. 2004, PASP, 116, 506

Stark M. A., Wade R. A. 2003, AJ, 126, 1455

Baltic Astronomy, vol. 15, 85–90, 2006.

THE SUBDWARF DATABASE: RELEASED

R. H. Østensen
Isaac Newton Group, Apartado 321, E-38700 Santa Cruz de La Palma, Spain

Received 2005 August 15

Abstract. The work on the Subdwarf Database, presented at the previous meeting, has been completed, and the tool is now publicly available. The first release contains data from close to 240 different literature sources, but more still awaits entry. The database interface includes advanced search capabilities in coordinate, magnitude and color space. Output tables can be generated in HTML with hyperlinks to automatically generated finding charts, the Aladin viewer and a detailed data sheet that displays all registered data for each target, including physical data such as temperature, gravity and helium abundance, together with a finding chart. Search results can be visualized automatically as interactive position, magnitude or color diagrams.

Key words: stars: hot subdwarfs – catalogs – surveys

1. INTRODUCTION

As presented at the last subdwarf meeting (Østensen 2004) a database has been designed and implemented based on the data in The Catalogue of Spectroscopically Identified Hot Subdwarf Stars (or the Subdwarf Catalogue, for short: Kilkenny et al. 1988) and its updates. This list contains more than 2300 unique hot subdwarf stars.

The database runs under MySQL[1] with interfaces in Perl for uploading and linking together the database entries. The WWW interface uses HTML forms and PHP[2].

2. WHAT'S NEW

In the past year the whole database has been completely redesigned. The first implementation was merely a searchable version of the original electronic table, but it soon became evident that there was a major problem with this simple solution. For instance, the table allows space for a small number of different classifications and several photometry entries, but there was no way to distinguish between the quality of two measurements of the same object. This applies both to photometric data, classifications and physical data.

---

[1] MySQL (`www.mysql.com`) is an open source database.

[2] PHP (`www.php.net`) is a script language can produce HTML documents. The PHP code is interpreted when a page is requested, allowing the server to generate HTML in real time.

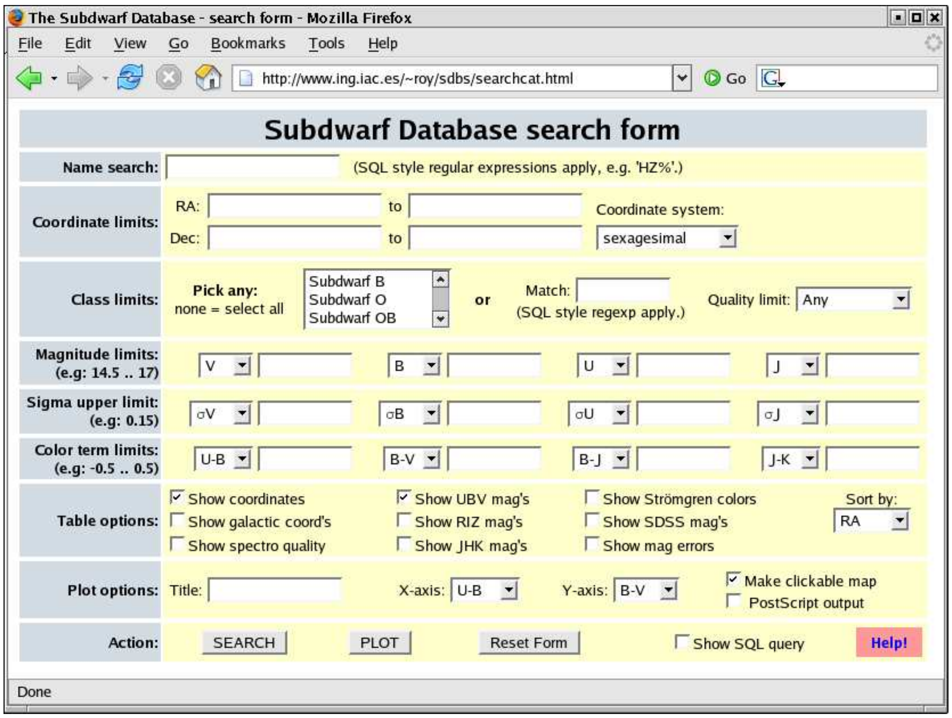

Fig. 1. The Subdwarf Database Search Form.

Obviously, if a particular object is observed and classified by several different authors, the reliability of the respective classifications will depend on the quality of the observations. If a classification entry was accompanied by a quality indicator, the system would be able to automatically adopt the classification with the highest quality flag, and thus vastly improve the reliability of the entries in the database. Thus, a scheme was implemented where a quality indicator of 1 signifies a photometric classification, a 2 signifies a classification based on a low resolution photographic spectrum, a 3 signifies a low to intermediate resolution spectrum (3–15 Å) – typically a photoelectric scan, a 4 signifies an intermediate resolution spectrum (1–3 Å) – typically a CCD observation in the blue part, and so on.

With this scheme in place it is easy to distinguish between reliably classified objects, and objects with dubious classifications. Also, for the photometric data in the database, it was decided that all entries must be accompanied by an error bar – either a one sigma error estimate provided by the observer, or at the very least a crude estimate based on the technique applied. Furthermore, the system is now able to convert magnitudes from photometric systems like the *Strömgren* system or *SDSS* magnitudes to Johnson *UVBRIZ* with reasonable precision and while maintaining realistic error estimates. It will then load the *UBVRIZ* magnitudes with the lowest error estimates available into the searchable database, regardless if this is an observed or derived magnitude. The database also contains *Strömgren, SDSS* and 2MASS *JHK* magnitudes, but these are never derived by conversion.

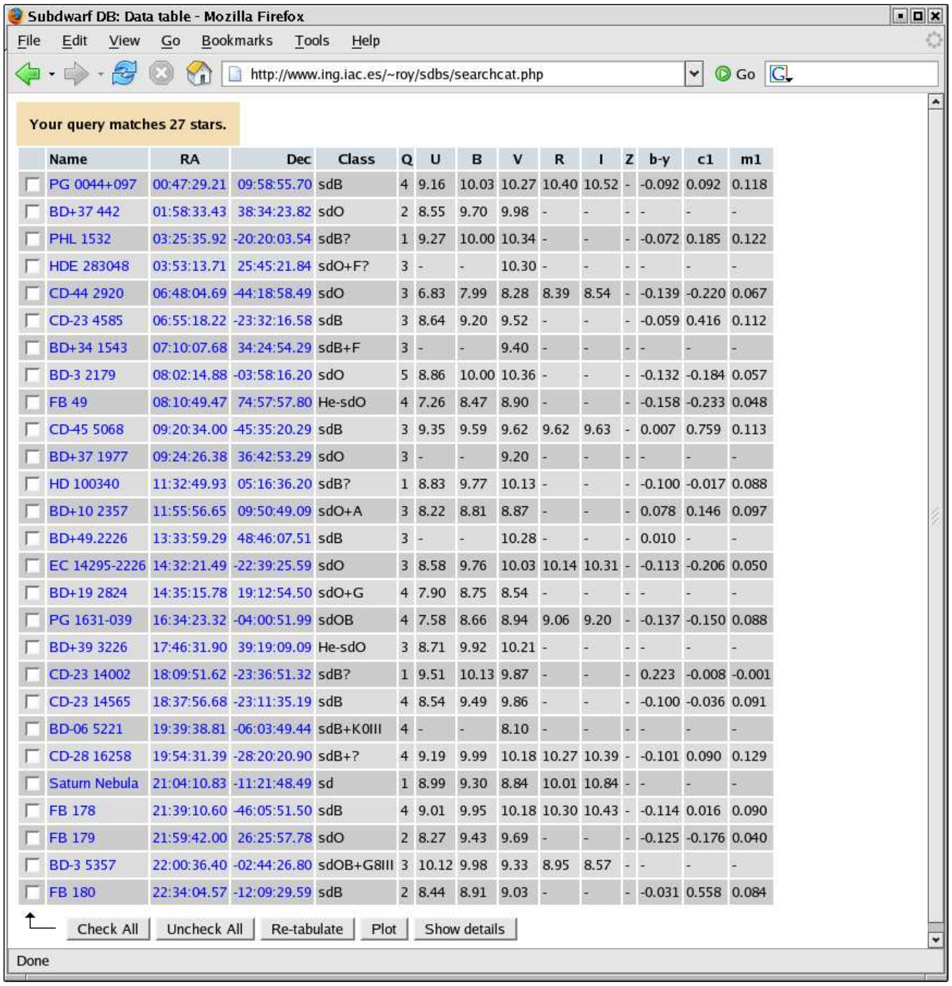

Subdwarf DB: Data table - Mozilla Firefox

File Edit View Go Bookmarks Tools Help

http://www.ing.iac.es/~roy/sdbs/searchcat.php

Your query matches 27 stars.

Name	RA	Dec	Class	Q	U	B	V	R	I	Z	b-y	c1	m1
PG 0044+097	00:47:29.21	09:58:55.70	sdB	4	9.16	10.03	10.27	10.40	10.52	-	-0.092	0.092	0.118
BD+37 442	01:58:33.43	38:34:23.82	sdO	2	8.55	9.70	9.98	-	-	-	-	-	-
PHL 1532	03:25:35.92	-20:20:03.54	sdB?	1	9.27	10.00	10.34	-	-	-	-0.072	0.185	0.122
HDE 283048	03:53:13.71	25:45:21.84	sdO+F?	3	-	-	10.30	-	-	-	-	-	-
CD-44 2920	06:48:04.69	-44:18:58.49	sdO	3	6.83	7.99	8.28	8.39	8.54	-	-0.139	-0.220	0.067
CD-23 4585	06:55:18.22	-23:32:16.58	sdB	3	8.64	9.20	9.52	-	-	-	-0.059	0.416	0.112
BD+34 1543	07:10:07.68	34:24:54.29	sdB+F	3	-	-	9.40	-	-	-	-	-	-
BD-3 2179	08:02:14.88	-03:58:16.20	sdO	5	8.86	10.00	10.36	-	-	-	-0.132	-0.184	0.057
FB 49	08:10:49.47	74:57:57.80	He-sdO	4	7.26	8.47	8.90	-	-	-	-0.158	-0.233	0.048
CD-45 5068	09:20:34.00	-45:35:20.29	sdB	3	9.35	9.59	9.62	9.62	9.63	-	0.007	0.759	0.113
BD+37 1977	09:24:26.38	36:42:53.29	sdO	3	-	-	9.20	-	-	-	-	-	-
HD 100340	11:32:49.93	05:16:36.20	sdB?	1	8.83	9.77	10.13	-	-	-	-0.100	-0.017	0.088
BD+10 2357	11:55:56.65	09:50:49.09	sdO+A	3	8.22	8.81	8.87	-	-	-	0.078	0.146	0.097
BD+49.2226	13:33:59.29	48:46:07.51	sdB	3	-	-	10.28	-	-	-	0.010	-	-
EC 14295-2226	14:32:21.49	-22:39:25.59	sdO	3	8.58	9.76	10.03	10.14	10.31	-	-0.113	-0.206	0.050
BD+19 2824	14:35:15.78	19:12:54.50	sdO+G	4	7.90	8.75	8.54	-	-	-	-	-	-
PG 1631-039	16:34:23.32	-04:00:51.99	sdOB	4	7.58	8.66	8.94	9.06	9.20	-	-0.137	-0.150	0.088
BD+39 3226	17:46:31.90	39:19:09.09	He-sdO	3	8.71	9.92	10.21	-	-	-	-	-	-
CD-23 14002	18:09:51.62	-23:36:51.32	sdB?	1	9.51	10.13	9.87	-	-	-	0.223	-0.008	-0.001
CD-23 14565	18:37:56.68	-23:11:35.19	sdB	4	8.54	9.49	9.86	-	-	-	-0.100	-0.036	0.091
BD-06 5221	19:39:38.81	-06:03:49.44	sdB+K0III	4	-	-	8.10	-	-	-	-	-	-
CD-28 16258	19:54:31.39	-28:20:20.90	sdB+?	4	9.19	9.99	10.18	10.27	10.39	-	-0.101	0.090	0.129
Saturn Nebula	21:04:10.83	-11:21:48.49	sd	1	8.99	9.30	8.84	10.01	10.84	-	-	-	-
FB 178	21:39:10.60	-46:05:51.50	sdB	4	9.01	9.95	10.18	10.30	10.43	-	-0.114	0.016	0.090
FB 179	21:59:42.00	26:25:57.78	sdO	2	8.27	9.43	9.69	-	-	-	-0.125	-0.176	0.040
BD-3 5357	22:00:36.40	-02:44:26.80	sdOB+G8III	3	10.12	9.98	9.33	8.95	8.57	-	-	-	-
FB 180	22:34:04.57	-12:09:29.59	sdB	2	8.44	8.91	9.03	-	-	-	-0.031	0.558	0.084

Check All Uncheck All Re-tabulate Plot Show details

Done

Fig. 2. Sample output from a magnitude limited search in the Subdwarf Database.

3. A FLEXIBLE INPUT FORMAT

Instead of the old system where the database merely reflected the entries in an electronic table with a fixed number of columns, the new system allows free format tables. Each data file under the new scheme contains information from one (or a related set of) publications with standardized tags to identify authors, title and a reference code. After a valid reference is given, each line contains data on one object in a format that specifies a list of names identifying the object followed by a colon and a list of data entries. The data entries are given in the form of a comma separated list of tag-value associations. Errors or quality flags are provided either on a separate line for all entries in the file, or as a number in brackets after each data value.

When the database is initialized, each data file is parsed and the data loaded

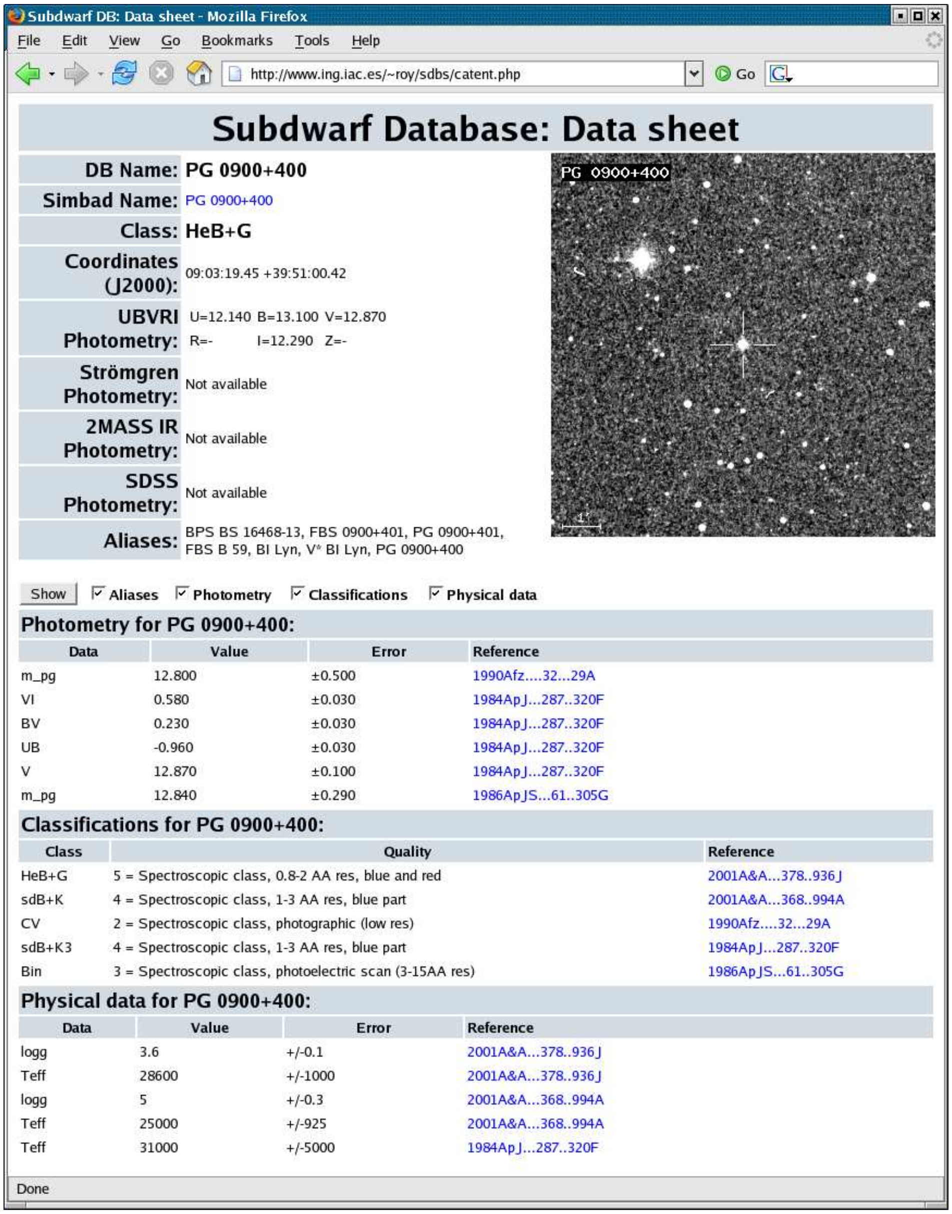

Fig. 3. Sample data sheet from the Subdwarf Database. Different observers have given many different classifications for this composite system.

into a number of database tables. The list of object names are loaded into one table, and coordinates, classifications, references and physical data are loaded into separate tables. Each entry is associated with its reference code, and there is no longer any limit on the number of entries for the same object.

After all available data files have been loaded into the set of database tables,

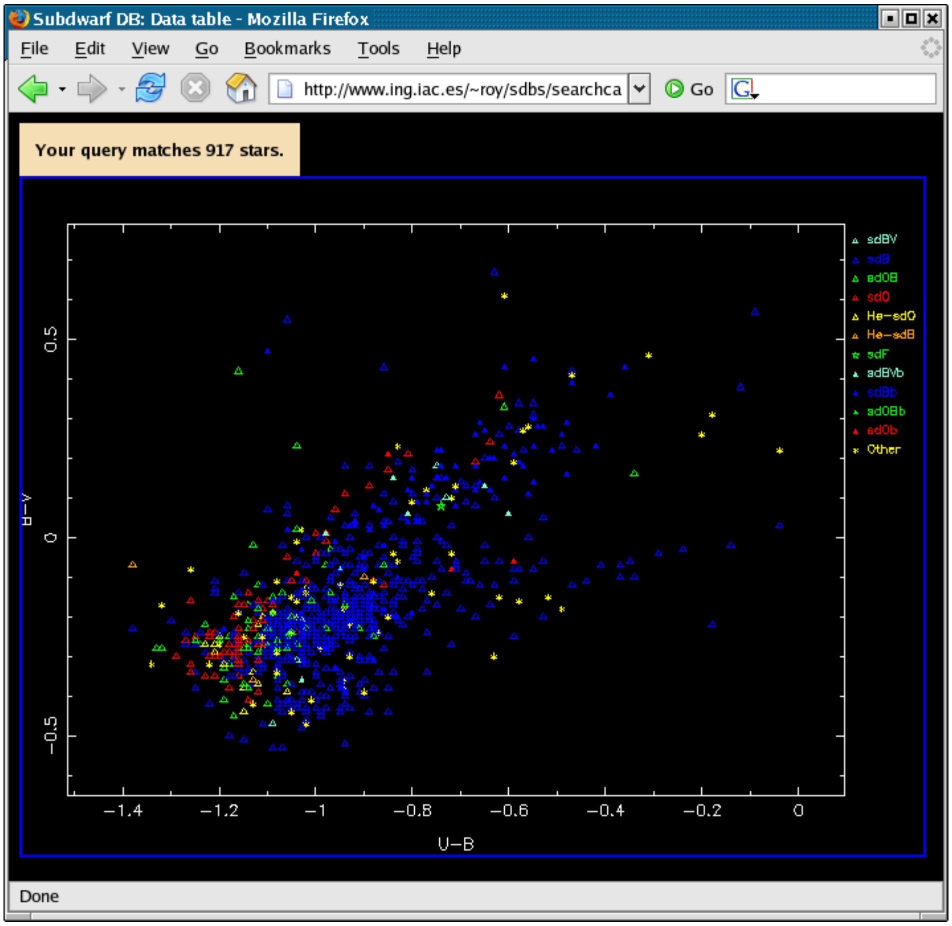

Fig. 4. A color-color plot auto-generated from the database with set limits on photometric quality. The plot is interactive in the sense that moving the pointer over a symbol will show the name of the star, and clicking on a symbol will produce the data sheet for that object.

a table containing compiled data is constructed. The script that does this job searches the table of classifications for entries of hot subdwarf stars. This list is then cross-checked so that each entry has a pair of valid coordinates associated with it. For each entry, all classifications and photometric data are loaded from the respective tables, derived magnitudes are computed, and only the best values are loaded into the compiled database. The entry that is created may actually not be that of a subdwarf star. All stars that have at one time been classified as a hot subdwarf star will be registered in the database, but the classification recognized is the one with the highest quality flag (e.g., Figure 3).

4. TO DO

The released database contains all the 146 references from the original Subdwarf Catalogue, with the exception of a few references that I have not been able to access. About 100 additional sources have been added to this collection, but this is still far away from exhausting the available sources. Many more papers still need to be recognized, and their data must be entered into tables. This is a work that can hardly ever be completed, and in order for the situation to improve, I will have to rely on people sending me notifications of old papers that have been missed as well as new papers being released. It would also be a great help if authors could provide electronic tables of their data that I can convert to the database format, thereby avoiding introducing further typing errors to the collection of discrepancies that already exist. If you spot any, please let me know.

The database is currently hosted at `http://www.ing.iac.es/~roy/sdbs/`. A more permanent home is being sought.

REFERENCES

Kilkenny D., Heber U., Drilling J. S. 1988, SAAOC, 12, 1, with updated electronic edition (1992)

Østensen R. H. 2004, Ap&SS, 291, 263